

Monsoons, ITCZs and the Concept of the Global Monsoon

Ruth Geen¹, Simona Bordoni^{2,3}, David S. Battisti⁴, Katrina Hui³

¹College of Engineering, Mathematics and Physical Sciences, University of Exeter, Exeter, UK.

²Department of Civil, Environmental and Mechanical Engineering, University of Trento, Trento, Italy.

³California Institute of Technology, Pasadena, CA, USA.

⁴Dept. of Atmospheric Sciences, University of Washington, Seattle, WA, USA.

Key Points:

- Theoretical understanding of the dynamics of Hadley cells, monsoons and ITCZs is developing rapidly
- Some aspects of observed monsoons and their variability can now be understood through theory
- Parallel theories should be reconciled and extended to account for zonal asymmetries and transients

Corresponding author: Ruth Geen, rg419@exeter.ac.uk

Abstract

Earth’s tropical and subtropical rainbands, such as Intertropical Convergence Zones (ITCZs) and monsoons, are complex systems, governed by both large-scale constraints on the atmospheric general circulation and regional interactions with continents and orography, and coupled to the ocean. Monsoons have historically been considered as regional large-scale sea breeze circulations, driven by land-sea contrast. More recently, a perspective has emerged of a Global Monsoon, a global-scale solstitial mode that dominates the annual variation of tropical and subtropical precipitation. This results from the seasonal variation of the global tropical atmospheric overturning and migration of the associated convergence zone. Regional subsystems are embedded in this global monsoon, localized by surface boundary conditions. Parallel with this, much theoretical progress has been made on the fundamental dynamics of the seasonal Hadley cells and convergence zones via the use of hierarchical modeling approaches, including aquaplanets. Here we review the theoretical progress made, and explore the extent to which these advances can help synthesize theory with observations to better understand differing characteristics of regional monsoons and their responses to certain forcings. After summarizing the dynamical and energetic balances that distinguish an ITCZ from a monsoon, we show that this theoretical framework provides strong support for the migrating convergence zone picture and allows constraints on the circulation to be identified via the momentum and energy budgets. Limitations of current theories are discussed, including the need for a better understanding of the influence of zonal asymmetries and transients on the large-scale tropical circulation.

Plain Language Summary

The monsoons are the moist summer circulations that provide most of the annual rainfall to many countries in the tropics and subtropics, influencing over one third of the world’s population. Monsoons in different regions have historically been viewed as separate continent-scale ‘sea breezes’, where land heats faster than ocean in the summer, causing warm air to rise over the continent and moist air to be drawn over land from the ocean. Here we show that recent theoretical advances and observational analyses support a novel view of monsoons as localized seasonal migrations of the *tropical convergence zone*: the band of converging air and rainfall in the tropics embedded within the tropical atmospheric overturning circulation. This updated perspective distinguishes the dynamics of low-latitude ($\sim 10\text{--}25^\circ$ poleward) ‘Intertropical Convergence Zones’ (ITCZs) from that of monsoons ($\sim 0\text{--}10^\circ$ poleward), explains commonalities and differences in behavior between the regional ITCZs and monsoons, and may help to understand year-to-year variability in these systems, and how the global monsoon might change in future. We end by discussing features that are not yet included in this new picture: the influence of mountains and continent shapes on the circulation and the relationship of the convergence zones with shorter lived weather systems.

1 Introduction

Monsoons are a dominant feature of the tropical and subtropical climate in many regions of the world, characterized by rainy summer and drier winter seasons, and accompanied by a seasonal reversal of the prevailing winds: Fig. 1a shows the difference in precipitation (GPCP; Huffman et al., 2001) and 850-hPa wind velocity (JRA-55; Kobayashi et al., 2015) between June-September and December-March, based on a climatology from 1979-2016. The magenta contour marks regions where local summer minus winter precipitation exceeds 2 mm/day and summer accounts for at least 55% of the annual total precipitation and thus identifies the various monsoon regions around the globe (cf. B. Wang & Ding, 2008; P. X. Wang et al., 2014).

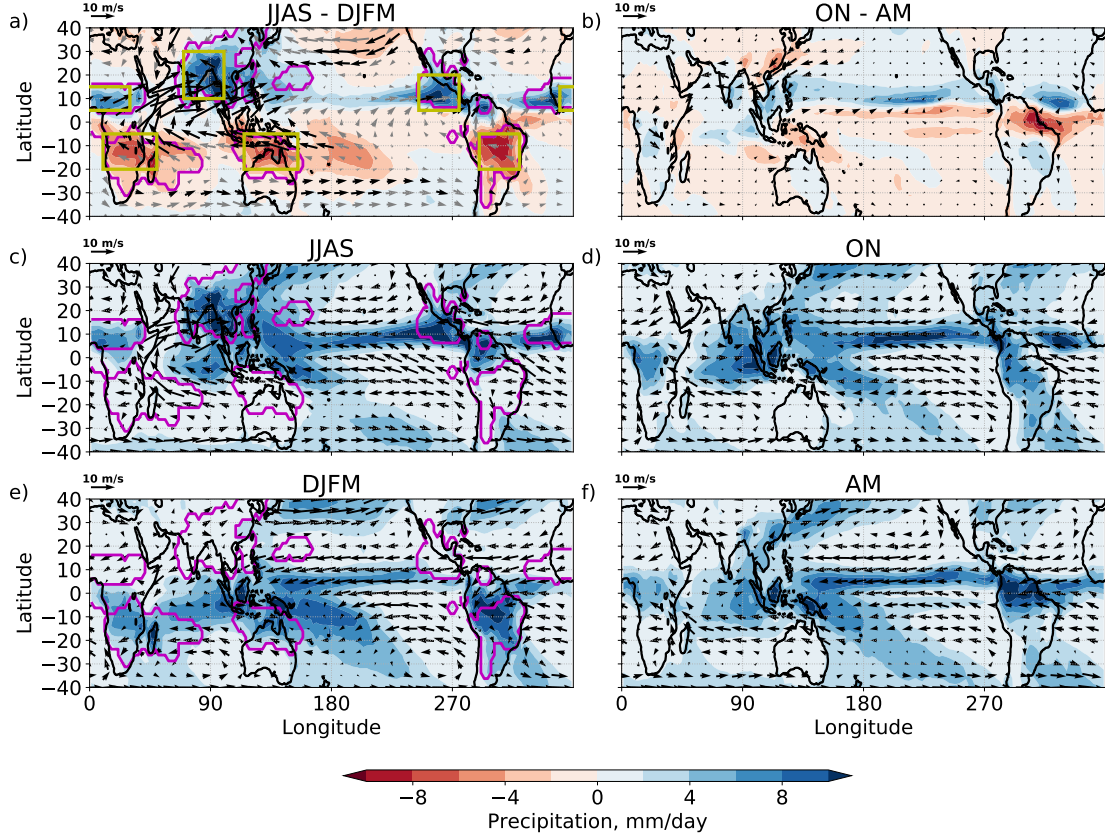


Figure 1. (a) Difference in precipitation (colors, mm/day) and 850-hPa wind speed (arrows, m/s) between Northern Hemisphere summer (defined as June-September) and Southern Hemisphere summer (defined as December-March). (c) and (e) show Northern and Southern Hemisphere summer precipitation and wind respectively. (b), (d) & (f) are as (a), (c) & (e) but for shoulder seasons defined as October & November and April & May. Black arrows in (a) indicate where the wind direction changes seasonally by more than 90° , where this criteria is not met arrows are gray. The magenta contour in (a), (c) & (e) indicates regions where local summer minus winter precipitation exceeds 2 mm/day and summer accounts for at least 55% of the annual total precipitation (cf. B. Wang & Ding, 2008; P. X. Wang et al., 2014). The extent of these regions does not change critically if these criteria are varied. Yellow boxes in (a) approximate these regions for use in Fig. 3.

For practical purposes, such as agriculture, it has generally been of interest to explore the controls on seasonal rainfall at a regional scale. However, empirical orthogonal function (EOF) analyses of the annual cycle of the global divergent circulation (Trenberth, Stepaniak, & Caron, 2000) and of precipitation and lower-level winds (e.g., Fig. 2) reveal a dominant, global-scale solstitial mode, driven by the annual cycle of insolation: the Global Monsoon. On interdecadal to intraseasonal timescales, the local monsoons appear to behave largely as distinct systems, albeit with some degree of coordination via teleconnections to ENSO (B. Wang, Liu, Kim, Webster, & Yim, 2012; Yim, Wang, Liu, & Wu, 2014). For example, interannual variability in precipitation shows weak

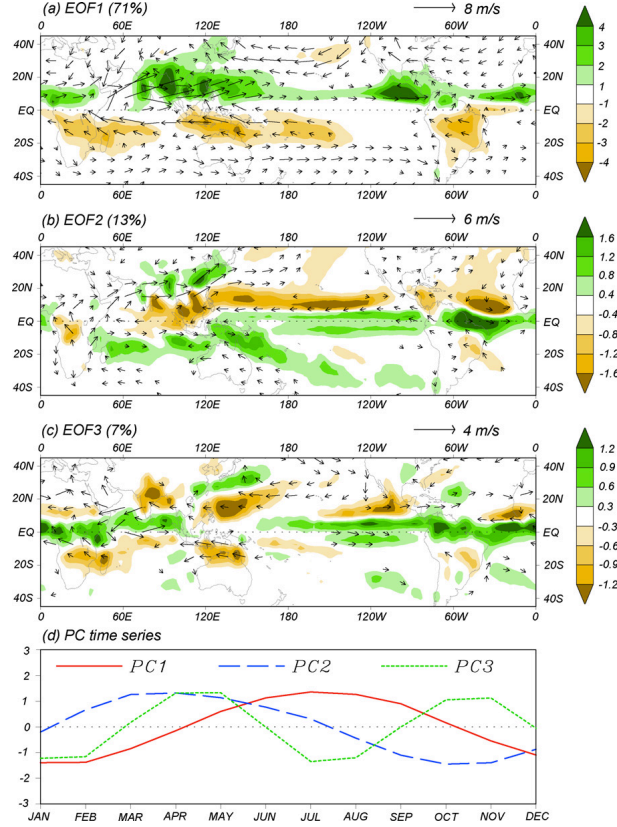


Figure 2. (a–c) The spatial patterns of the first three multi-variable empirical orthogonal functions of the climatological monthly mean precipitation (colors, mm/day) and winds (arrows, m/s) at 850 hPa, and (d) their corresponding normalized principal components. Winds with speed less than 1 m/s are omitted. From B. Wang and Ding (2008). ©Elsevier. Used with permission.

correlation between regions (Fig. 3).¹ As paleoclimate proxy datasets have become more comprehensive and reliable, it has become possible to investigate monsoon variability on longer timescales. For example, Fig. 4 shows that there were coherent millennial-scale abrupt changes in precipitation throughout the tropics and subtropics associated with Heinrich events and Dansgaard-Oeschger (D–O) cycles.² Modeling studies reproduce these hydrologic changes and demonstrate they are due to sudden changes in sea ice extent in the North Atlantic (see Pausata, Battisti, Nisancioglu, & Bitz, 2011; Atwood, Donohoe, Battisti, Liu, & Pausata, 2020 and references therein). On longer timescales (~23–26 kyr), the isotopic composition of the aragonite forming stalagmites throughout the tropics is strongly related to orbitally induced changes in insolation (see, e.g., Fig. 5).

¹ Note that even within an individual region, the dominant mode of interannual variability may have spatial structure, so that precipitation does not vary coherently across the domain (e.g., Goswami & Ajaya Mohan, 2001).

² Heinrich events are sudden discharges of ice from the Laurentide ice sheet that flood the North Atlantic with freshwater (Heinrich, 1988; Hemming, 2004). D–O cycles are a mode of natural variability that is manifest during (at least) the last ice age. A millennial-scale D–O cycle includes abrupt changes in North Atlantic sea ice extent (see Dansgaard et al., 1993; Dokken, Nisancioglu, Li, Battisti, & Kissel, 2013, and references therein).

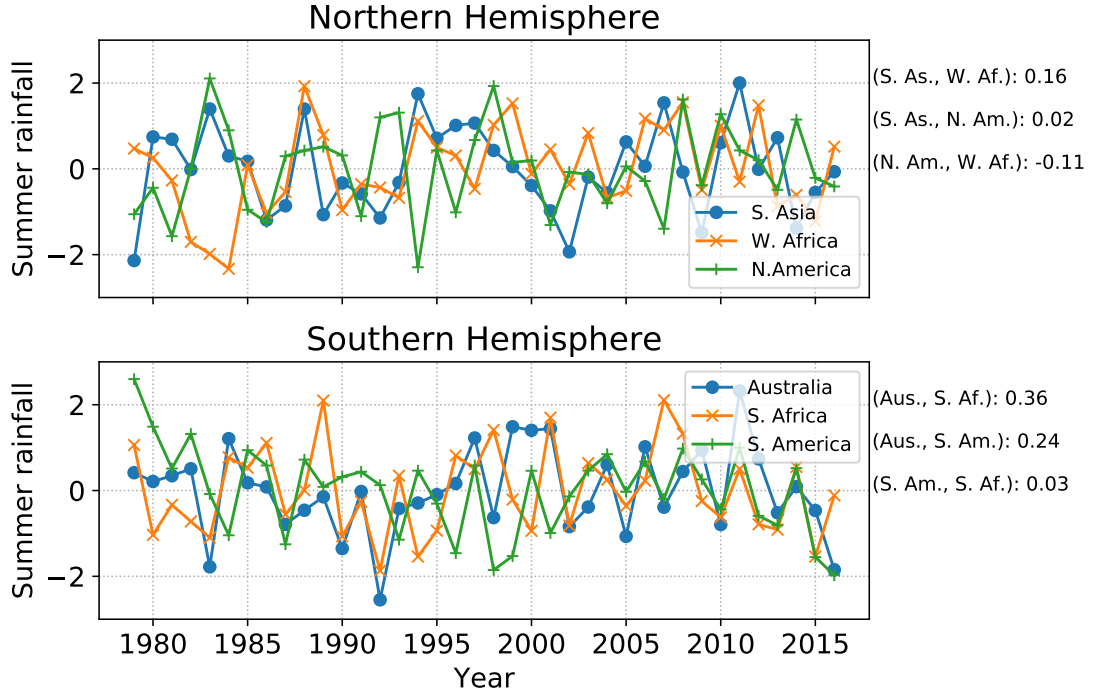


Figure 3. Timeseries of summer-time (June-September mean in the Northern Hemisphere and December-March mean in the Southern Hemisphere) rainfall averaged over the yellow boxes marked in Fig. 1, which are used as approximations to the monsoon regions defined by the magenta contour. For ease of comparison, the timeseries are standardized by subtracting the mean and dividing by the standard deviation. Pearson correlation coefficients are given to the right of the figure; except for the correlation between Australian and Southern African rainfall, correlations are not significantly different from zero ($p=0.10$). Data are taken from the Global Precipitation Climatology Project (GPCP; Huffman et al., 2001) over 1979-2016.

Simulations using isotope-enabled climate models reproduce these proxy data and demonstrate that precession causes coordinated, pan-tropical changes in the strength of the monsoons (accentuated in times of high orbital eccentricity) (Battisti, Ding, & Roe, 2014; Liu, Battisti, & Donohoe, 2017).

The evidence for coherent global-scale monsoons raises questions about our physical understanding of the systems. Historically, the localization of summertime tropical rainfall around land led to the intuitive interpretation of monsoons as a large-scale sea breeze, with moist air drawn over the continent in the local summer season, when the land is warm relative to the ocean, resulting in convective rainfall over land (Halley, 1686). Traditionally, monsoons were considered distinct phenomena to the Intertropical Convergence Zone (ITCZ), with the latter coincident with the ascending branch of the Hadley circulation and generally being defined as the location where the trade winds of the Northern and Southern Hemispheres converge. This perspective of monsoons as a sea breeze has been pervasive, despite the fact that land-sea temperature contrast has long been known to be greatest prior to monsoon onset over India (Simpson, 1921), and that drought years are accompanied by higher land surface temperatures (Kothawale & Kumar, 2002). However, consistent with the picture of the dominant global monsoon mode (Trenberth et al., 2000; B. Wang & Ding, 2008), more recent work suggests a perspective of the regional monsoons as localized and more extreme migrations of the tropical convergence

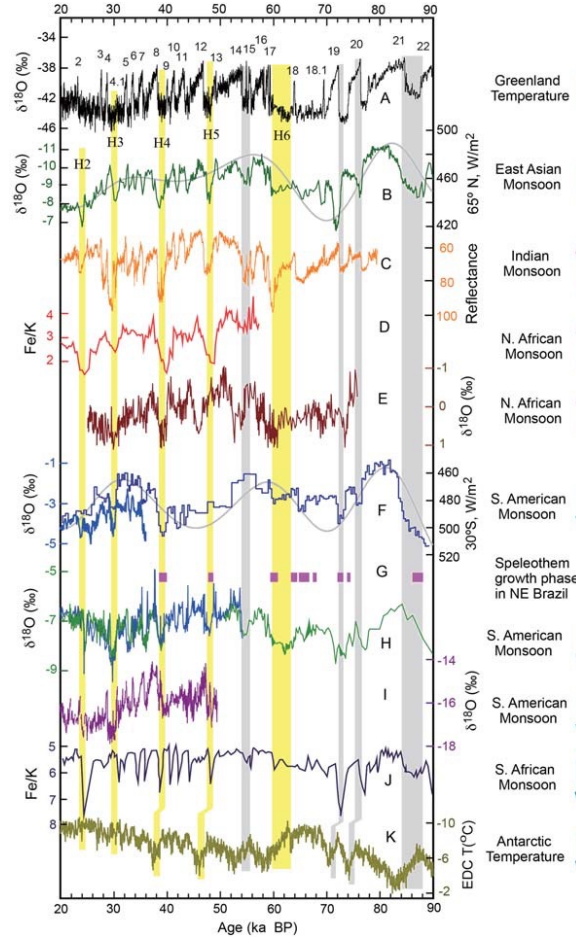


Figure 4. Paleoclimate proxy records from over the past 90,000 years. (a) Greenland ice core $\delta^{18}\text{O}$ record (Svensson et al., 2008, NGRIP). (b) East Asian monsoon record composited by using the Hulu and Sanbao records (H. Cheng et al., 2009). (c) Indian monsoon record inferred from Arabian Sea sediment total reflectance from core SO130-289KL (Deplazes et al., 2013). (d) Bulk Fe/K ratios from core GeoB9508-5 indicate arid (low) and humid (high) conditions in the North African monsoon region (Mulitza et al., 2008). (e) The North African monsoon proxy record based on the age model tuning to the GISP2 chronology (Weldeab, 2012). (f) South American monsoon records from Botuvera Cave (X. Wang et al., 2006, 2007). (g) Northeastern Brazil speleothem growth (wet) periods (X. Wang et al., 2004). (h) South American monsoon record from northern Peru (H. Cheng et al., 2013). (i) South American monsoon record from Pacupahuain Cave (Kanner et al., 2012). (j) Fe/K record (marine sediment core CD154-17-17K) from the southern African monsoon region (Ziegler et al., 2014). (k) Antarctic ice core temperature record (Jouzel et al., 2007, EDC). Numbers indicate Greenland warm phases of D-O cycles. Vertical yellow bars denote Heinrich events (H2-H6), and gray bars indicate correlations between northeastern Brazil wet periods, strong South American events and cold Greenland weak Asian monsoon events. Summer insolation (gray curves) at (b) 65°N (JJA) and (f) 30°S (DJF) (Berger, 1978) is plotted for comparison. Arrows on the right side depict anti-phased changes of monsoons between the two hemispheres. From P. X. Wang et al. (2014). ©Author(s) 2014. CC Attribution 3.0 License.

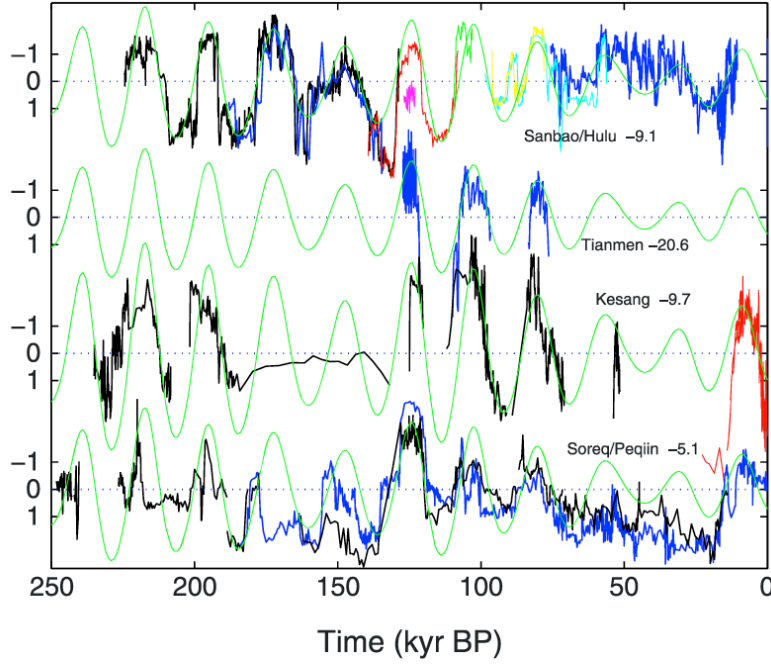


Figure 5. Time series of the oxygen isotopic composition of aragonite $\delta^{18}\text{O}$ (‰) in stalagmites across Asia that are sufficiently long to resolve orbital time scales. For each speleothem, the time average $\delta^{18}\text{O}$ is noted (e.g., Tianmen=−20.6‰) and removed before plotting. Superposed on each record is the summer (JJA) insolation at 30°N (green). For ease of viewing, the insolation has been multiplied by −1 and scaled so the standard deviation of insolation is identical to the standard deviation of the $\delta^{18}\text{O}$ for the respective cave record. From Battisti et al. (2014).

zone, which may sit near the Equator forming an ITCZ, or be pulled poleward over the continent as a monsoon (see Gadgil, 2018, and references therein).

Simultaneously, a significant body of work investigating the fundamental dynamics of the monsoon has been undertaken via hierarchical modeling approaches, ranging from dry axisymmetric models (e.g., Bordoni & Schneider, 2010; Hill, Bordoni, & Mitchell, 2019; Schneider & Bordoni, 2008), to cloudless moist models (e.g., Bordoni & Schneider, 2008; Faulk, Mitchell, & Bordoni, 2017; Geen, Lambert, & Vallis, 2018, 2019; Privé & Plumb, 2007a), to more comprehensive models including full physics and realistic orography (e.g., Boos & Kuang, 2010; Chen & Bordoni, 2014). This hierarchy has allowed a wide range of factors controlling the structure of tropical precipitation to be explored. Findings from these studies strongly support the view of monsoons as local expressions of the global tropical convergence zone, and provide valuable, theoretically grounded insights into the controls on the tropical circulation and precipitation.

In this review, we attempt to synthesize the results of studies on the observed characteristics of Earth’s monsoon systems with recent theoretical advances that provide constraints on the large-scale dynamics of ITCZs and monsoons, with the aim of taking stock of the progress achieved and identifying avenues for future work. Note that throughout the review, ‘monsoon’ refers to the local summer, as opposed to winter, monsoon. Specifically, as we will motivate through discussion of theoretical work, for the remainder of the paper we reserve the term ‘*monsoon*’ to describe precipitation associated with overturning circulations with ascending branches located well poleward of $\sim 10^\circ$ latitude. We will show that, unlike the ITCZs, monsoons are characterized by angular momen-

tum conserving circulations, whose strength is largely determined by energetic constraints. The term ‘**ITCZ**’ is reserved to describe the zonally oriented precipitation bands that remain within $\sim 10^\circ$ of the Equator and whose dynamics are much more strongly influenced by momentum fluxes associated with large-scale transient eddies. The term **convergence zone** will be used to refer to the location of both monsoonal and ITCZ precipitation because, regardless of their governing dynamics, precipitation in both types of circulation is associated with ascending branches of overturning cells. The zonal and annual mean tropical convergence zone is referred to as the **ITCZ**.

The goals of this article are:

1. To assess the relevance of theoretical advances (which stem from studies using idealized models) to the real-world monsoons and ITCZs;
2. To help to motivate relevant simulations from the modeling community to answer open questions on the dynamics governing tropical convergence zones;
3. To provide an introduction to both of these aspects for readers new to the field.

With these aims in mind, Section 2 discusses theoretical results derived from idealized models, particularly aquaplanets with symmetric boundary conditions and heating perturbations. Section 3 discusses the features of the observed regional convergence zones, their combined role in the global monsoon, and the applicability of the dynamical processes identified in idealized models to the various systems. Section 4 explores the roles of asymmetries in the boundary conditions and transient activity in the monsoons and ITCZs. These factors are sometimes overlooked in formulating theories in idealized models. In Section 5 we summarize the successes and limitations of this synthesis of theory and observations, and propose some areas on which to focus future research.

2 Idealized modeling of tropical and subtropical convergence zones

Reanalyses, observations, and state-of-the-art global circulation models (GCMs) give our best estimates of Earth’s climate. However, when viewed as a whole, the Earth system is dizzyingly complex, and identifying the processes controlling the various elements of climate is hugely challenging. Idealized models provide a valuable tool for breaking down some of this complexity, and for proposing mechanisms whose relevance can then be investigated in more realistic contexts.³ In this section, we review the use of idealized models in understanding the dynamics of the monsoons and ITCZs.

Some key insights into the controls on tropical rainfall and monsoons have come from a perhaps unexpected source: aquaplanets. Despite lacking zonal asymmetries such as land-sea contrast, which localize regional monsoons, these models have been shown to capture the basic elements of a monsoon. For example, in aquaplanets with moist physics and a low thermal inertia slab ocean, the convergence zone migrates rapidly and far away from the Equator into the summer hemisphere during the warm season (Bordoni & Schneider, 2008). This migration is associated with a rapid reversal of the upper- and lower-level wind in the summer hemisphere, and the onset of intense off-equatorial precipitation, similar to the behaviors seen in Earth’s monsoons (e.g., Fig. 6). Thus, in so far as the rapid development of an off-equatorial convergence zone accompanied by similarly rapid circulation changes can be interpreted as a monsoon, aquaplanets provide a simple tool for exploring the lowest-order processes at work. This represents a significant change in perspective from the classical view of monsoon wind reversal as driven by land-sea thermal contrast (Halley, 1686), towards a view of monsoons as local and seasonal manifestations of the meridional overturning circulation.

³ For further discussion of the use of idealized models and the model hierarchy see (Held, 2005; Jeevanjee, Hassanzadeh, Hill, & Sheshadri, 2017; Levins, 1966; Maher et al., 2019)

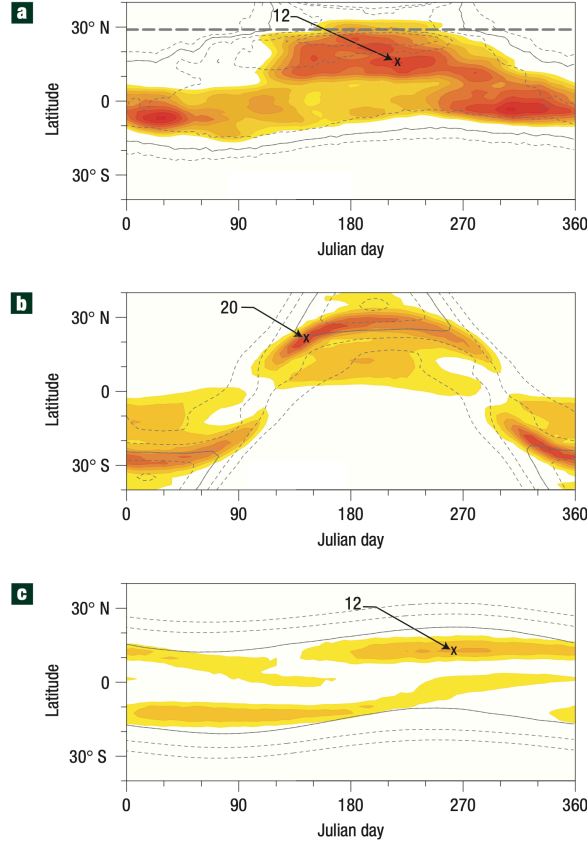


Figure 6. Seasonal cycle of zonal- and pentad-mean precipitation (color contours, data from GPCP 1999-2005) and sea-level air temperature (gray contours, data from the ERA-40 reanalysis (Uppala et al., 2005)) for (a) observations in the Asian monsoon sector (70-100°E), and for aquaplanet simulations with ocean mixed-layer heat capacity equivalent to (b) 0.5m and (c) 50m of water.¹ The precipitation contour interval is 1 mm/day in (a) and 2 mm/day in (b) and (c), and maxima are indicated by crosses. For sea-level air temperature, the contour interval is 2°C in all panels, and the solid gray line indicates the 24°C isoline. The thick dashed line in (a) shows the latitude at which the zonal-mean topography in the Asian monsoon sector rises above 3 km. From Bordoni and Schneider (2008). NB. Mixed layer depths here are corrected from Bordoni and Schneider (2008), (S. Bordoni, pers. com., 2020).

Different theoretical approaches have been used to interpret the results from these idealized simulations, primarily using large-scale budgets of energy and angular momentum. The momentum budget gives insight into the drivers and regimes of the overturning circulation, and how these relate to monsoon onset. The energy budget provides a framework for understanding the controls on the latitude of the zonally averaged convergence zone, and its meridional migration. In a real-world context, this is useful in interpreting the latitude of tropical rainfall bands, and the meridional extent of Earth's monsoons. These complementary approaches are discussed in Sections 2.1 and 2.2, respectively.

2.1 Dynamical constraints

One important constraint on the atmospheric circulation is conservation of angular momentum. Recent results from aquaplanet simulations suggest that this can help to explain controls on the latitude of the convergence zone, the extent of the Hadley circulation, and the rapidity of monsoon onset.

The axial component of the angular momentum associated with the atmospheric circulation is

$$M = \Omega a^2 \cos^2 \phi + ua \cos \phi, \quad (1)$$

where Ω and a are Earth's rotation rate and radius, u is the zonal wind speed, and ϕ is latitude. Eq. 1 states that the atmosphere's angular momentum comprises a planetary contribution from Earth's rotation, and a contribution from the zonal wind relative to this. In the absence of torques (e.g., from friction, zonal pressure gradients or orography; see Egger, Weickmann, & Hoinka, 2007), M is conserved by an air parcel as it moves meridionally. Above orography, in the zonal mean we can approximate

$$\frac{DM}{Dt} = 0. \quad (2)$$

In the absence of stationary eddies, as is the case in an aquaplanet, substituting Eq. 1 into Eq. 2, linearising about the zonal and time mean state, and considering upper-level flow where viscous damping is weak and can be neglected gives

$$\bar{v} \left(f - \frac{1}{a \cos \phi} \frac{\partial(\bar{u} \cos \phi)}{\partial \phi} \right) - \bar{\omega} \frac{\partial \bar{u}}{\partial p} = \frac{1}{a \cos^2 \phi} \frac{\partial(\overline{u'v'} \cos^2 \phi)}{\partial \phi} + \frac{\partial \overline{u'\omega'}}{\partial p}, \quad (3)$$

where f is the Coriolis parameter, and v and ω are the meridional and vertical wind components, respectively. Overbars indicate the time and zonal mean, and primes deviations from the time mean. Terms relating to the mean flow have been grouped on the left hand side, while terms relating to the transient eddy fluxes of momentum are grouped on the right. In the upper branch of the Hadley circulation, where meridional streamlines are approximately horizontal (e.g., Fig. 13), the vertical advection term on the left hand side can be neglected. Additionally, meridional eddy momentum flux convergence is generally much larger than the vertical eddy momentum flux convergence outside of the boundary layer (e.g., Schneider & Bordoni, 2008). Utilising the definition of relative vorticity, $\zeta = \hat{\mathbf{k}} \cdot \nabla \times \mathbf{u}$, the leading order balance in Eq. 3 can be expressed in terms of a local Rossby number, $Ro = -\bar{\zeta}/f$, (cf. Schneider & Bordoni, 2008) as

$$f(1 - Ro)\bar{v} = \frac{1}{a \cos^2 \phi} \frac{\partial(\overline{u'v'} \cos^2 \phi)}{\partial \phi}. \quad (4)$$

Ro is a non-dimensional metric of how far (small Ro) or close ($Ro = 1$) the circulation is to conservation of angular momentum.

2.1.1 The axisymmetric case

Considering first the case of an axisymmetric atmosphere, in which there are no eddies, Eq. 4 has two classes of solution. Firstly, the zonal averaged meridional and (by continuity) vertical velocities may be zero everywhere. This corresponds to a radiative-convective equilibrium (RCE) solution. Alternatively, Ro may be equal to 1 and an axisymmetric circulation may exist, so that the zonal and time mean flow conserves angular momentum. Plumb and Hou (1992) and Emanuel (1995) explored the conditions under which either of these cases might occur in dry and moist atmospheres, respectively. Importantly, the RCE solution is not viable if the resulting zonal wind in thermal wind balance with the RCE temperatures violates Hide's theorem (Hide, 1969) by giving rise to a local extremum in angular momentum. Plumb and Hou (1992) demonstrate that

for an off-equatorial forcing, this implies the existence of a threshold curvature of the depth-averaged RCE temperature, above which the RCE solution cannot exist and an overturning circulation will develop. They also speculate that this threshold behavior in the axisymmetric model might be related to the rapid onset of Earth’s monsoons. The overall argument is as follows.

Taking the RCE case, in which \bar{v} and $\bar{\omega}$ vanish, gradient wind and hydrostatic balance can be expressed in pressure coordinates as

$$\frac{\partial}{\partial p} \left[f \bar{u}_e + \frac{\bar{u}_e^2 \tan \phi}{a} \right] = \frac{1}{a} \left(\frac{\partial \bar{\alpha}}{\partial \phi} \right)_p, \quad (5)$$

where $\bar{\alpha}$ is specific volume and \bar{u}_e is a RCE zonal wind profile. Note that in the axisymmetric case, overbars denote only the time mean, as by construction there are no zonal variations. Assuming the zonal wind speed at the surface is zero, the above can be integrated down to the surface for a given upper-level wind profile to give an associated RCE depth-averaged temperature distribution (cf. Lindzen & Hou, 1988; Plumb & Hou, 1992).

In modeling Earth’s atmosphere, moist processes must also be accounted for. In the tropics, frequent, intense moist convection means that in the time mean, the lapse rate is approximately moist adiabatic, so that the saturation moist entropy of the free atmosphere is nearly equal to the subcloud moist entropy, s_b (the b denoting subcloud values) (e.g., Arakawa & Schubert, 1974; Emanuel, Neelin, & Bretherton, 1994). This is known as *convective quasi-equilibrium* (CQE).⁴ Assuming the tropical atmosphere to be in CQE, Emanuel (1995) uses Eq. 5 to derive a relation between the angular momentum at the tropopause, M_t , and subcloud equivalent potential temperature, θ_{eb} :

$$c_p(\bar{T}_s - \bar{T}_t) \frac{\partial \ln \theta_{eb}}{\partial \phi} = -\frac{1}{a^2} \frac{\tan \phi}{\cos^2 \phi} (\bar{M}_t - \Omega^2 a^4 \cos^4 \phi), \quad (6)$$

where T_s and T_t are the RCE temperatures at the surface and tropopause respectively, c_p is the heat capacity of dry air at constant pressure and θ_{eb} is related to moist entropy as $s_b = c_p \ln \theta_{eb}$. The condition that no local maximum in angular momentum exist gives a critical curvature of θ_{eb} :

$$-\left[\frac{\partial}{\partial \phi} \left(\frac{\cos^2 \phi}{\tan \phi} c_p(\bar{T}_s - \bar{T}_t) \frac{\partial \ln \theta_{eb}}{\partial \phi} \right) \right]_{crit} = 4\Omega^2 a^2 \cos^3 \phi \sin \phi. \quad (7)$$

In an axisymmetric atmosphere, if the left hand side of Eq. 7 is less than the right hand side, the RCE solution is viable and there is no meridional overturning cell. If this condition is violated, so that the profile of θ_{eb} is supercritical, the RCE solution is not viable and a meridional flow must exist (cf. Emanuel, 1995; Hill et al., 2019; Plumb & Hou, 1992). This condition is illustrated graphically in Fig. 7, which shows the profiles of RCE zonal wind, angular momentum, and absolute vorticity (proportional to the meridional gradient of angular momentum) that result from a range of forcings with a local subtropical maximum (Fig. 7a).⁵ For weak forcing (blue lines), no extrema of \bar{M}_t are produced, illustrated by the fact that absolute vorticity (Fig. 7d) is positive everywhere. At the critical forcing profile (gray lines) a saddle point in \bar{M}_t is produced (Fig. 7c), where absolute vorticity is 0. Beyond this point, the profiles of \bar{u} that are in gradient wind balance with the forcing are such as to produce extrema in \bar{M}_t , and are in violation of Hide’s theorem (Hide, 1969) so that a Hadley circulation must develop.

⁴ NB. One important assumption in CQE is that it holds for large spatial and temporal scales compared to the convective scales, so that convection can be assumed to be in quasi-equilibrium with its large-scale environment. On exactly what scales this breaks down is an open question.

⁵ This figure, taken from Hill et al. (2019), corresponds to a dry atmosphere, (cf. Plumb & Hou, 1992), but the behavior is equivalent to that for Eq. 7.

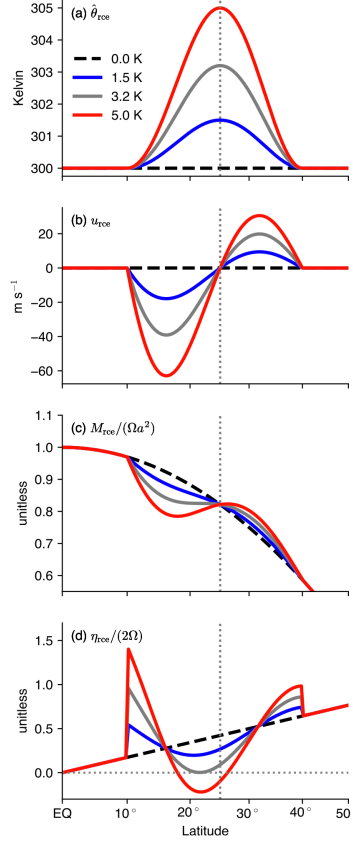


Figure 7. Illustration of the effects of a subcritical (blue lines), critical (gray lines) or supercritical (red lines) RCE potential temperature profile. Forcing profiles, shown in (a), are based on those used by Plumb and Hou (1992). The remaining panels show (b) zonal wind (m s^{-1}), (c) absolute angular momentum, normalized by the planetary angular momentum at the Equator, (d) absolute vorticity, normalized by twice the planetary rotation rate. From Hill et al. (2019). ©American Meteorological Society. Used with permission.

The above arguments assess the conditions under which a Hadley circulation will exist in an axisymmetric atmosphere. Privé and Plumb (2007a) further showed that this framework can give some insight into the controls on the latitude of the convergence zone. They noted that, if the overturning circulation conserves angular momentum in the free troposphere, the circulation boundary for a vertical streamline must be located in a region of zero vertical wind shear. Where CQE applies, so that free tropospheric temperatures are coupled to lower-level θ_{eb} , this implies that the zero streamfunction contour must occur in a region of zero horizontal gradient of θ_{eb} (i.e. where θ_{eb} maximizes). Most of the ascent in the circulation ascending branch, and consequently the precipitation, will occur just equatorward of this maximum. They additionally noted that either the maximum in θ_{eb} or the maximum in moist static energy (MSE), h , could also be used to estimate the latitude of the convergence zone (see their Section 5)⁶, as the two variables

⁶ θ_e is useful due to its relationship to moist entropy, which for example allows the substitution of a Maxwell relation into Eq. 5 (Emanuel, 1995). However, MSE is a linear quantity that is straightforward to calculate, and so is more widely used.

are related by

$$\partial\theta_{eb} \approx \frac{1}{T_b} \partial h_b, \quad (8)$$

$$h = c_p T + L_v q + g z. \quad (9)$$

In the above, T is temperature, q is specific humidity, z is height, L_v is the latent heat of vaporisation of water, c_p is the specific heat capacity and g is gravitational acceleration.

2.1.2 Eddy-permitting solutions

Conservation of angular momentum provides important constraints on the existence and extent of axisymmetric overturning circulations. However, it is now well known that extratropical eddies generated in midlatitude baroclinic zones propagate into the subtropics where they break, and have non-negligible impact on the Hadley circulation (e.g., Becker, Schmitz, & Geprägs, 1997; C. C. Walker & Schneider, 2006). In particular, as transport of angular momentum by large-scale eddies becomes non-negligible, the associated eddy momentum flux convergence in Eq. 4 can no longer be neglected. In the limit of small Ro , the advection of zonal momentum by the zonal mean meridional flow is negligible, and the dominant balance is between the Coriolis effect on the zonal mean meridional flow and the eddy momentum flux divergence. This regime is linear, in that the mean advection term is negligible, and eddy driven, in that the strength of the overturning circulation is strongly constrained by the eddy momentum fluxes. As Ro approaches 1, eddy effects become negligible, advection of zonal relative momentum by the mean meridional circulation is dominant and the circulation approaches conservation of angular momentum. In reality, cases intermediate between these two limits, with $Ro \sim 0.5$, are also observed, where both nonlinear zonal mean advection and eddy terms are important (Schneider, O’Gorman, & Levine, 2010).

Transitions from regimes with small Ro to regimes with Ro approaching unity have been connected to the rapid changes in the tropical circulation that occur during monsoon onset. Examining the upper-level momentum budget in aquaplanet simulations with shallow slab oceans (e.g., ~ 1 m) and a seasonal cycle, Bordoni and Schneider (2008) found that around the equinoxes, the Hadley cells in the two hemispheres are roughly symmetric and the associated convergence zone is near the Equator, $Ro \lesssim 0.5$ and the circulation strength is governed by eddies (e.g., Fig. 8a). As the insolation maximum starts moving into the summer hemisphere, the winter Hadley cell starts becoming cross equatorial. The zonal mean ascent and precipitation move to a subtropical location in the summer hemisphere (e.g., Fig. 6), and upper-level tropical easterlies develop. The latter limit the ability of eddies from the winter hemisphere to propagate into the low latitudes, and the circulation shifts quickly towards the $Ro \sim 1$ angular momentum conserving flow regime, at the same time strengthening and expanding rapidly (e.g., Fig. 8b). As the cross-equatorial circulation approaches conservation of angular momentum, the dominant balance becomes between the terms on the left hand side of Eq. 3, with the eddy terms a small residual. Once in this regime, the circulation strength is no longer constrained by the zonal momentum budget, which becomes a trivial balance, but is instead constrained by the energy budget, and so responds strongly to the thermal forcing.

The rapid meridional migrations of the convergence zone in the aquaplanet are a result of a positive feedback relating to advection of cooler and drier air up the MSE gradient in the lower branch of the winter Hadley cell (Bordoni & Schneider, 2008; Schneider & Bordoni, 2008). As summer begins the summer hemisphere warms via diabatic fluxes of MSE into the air column. This pulls the lower-level peak in MSE and, in accordance with the arguments of Privé and Plumb (2007a), pulls the ITCZ off of the Equator. Simultaneously, the winter Hadley circulation begins to redistribute MSE, advect-

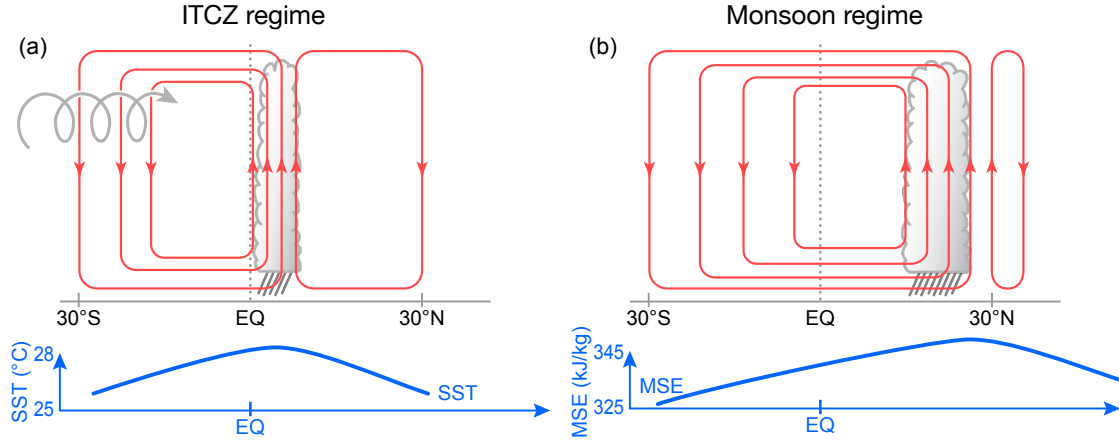


Figure 8. Schematic illustration of the two regimes of the meridional overturning circulation identified in aquaplanets (Bordoni & Schneider, 2008; Schneider & Bordoni, 2008). The gray cloud denotes clouds and precipitation, red contours denote streamfunction. (a) Convergence zone is an ITCZ located near to the Equator, and approximately co-located with the peak SST. Hadley cells are significantly eddy driven, as indicated by the helical arrow. (b) Convergence zone is monsoon-like, located farther from the Equator, with the mid-tropospheric zero contour of the streamfunction aligned with the MSE maximum (Privé & Plumb, 2007b) and precipitation falling just equatorward of this. The winter Hadley cell crosses the Equator and is near angular-momentum conserving, with eddies only weakly influencing the overturning strength. The summer Hadley cell is comparatively weak, if present at all. Known physics of these regimes is summarized in Table 1. Illustration by Beth Tully.

ing cooler and drier air up the MSE gradient. This pushes the lower-level MSE maximum farther off the equator. The overturning circulation strengthens, further increasing the lower-level advection of cool air, and expanding the upper-level easterlies, allowing the circulation to become further shielded from the eddies and amplifying its response to the thermal forcing. It is important to note that in this view land is necessary for monsoon development only insofar as it provides a lower boundary with low enough thermal inertia for the MSE to adjust rapidly and allows the feedbacks described above to act on intraseasonal timescales. Behavior consistent with these feedbacks has been observed in Earth’s monsoons, and will be discussed in more detail in Section 3.

2.1.3 Hadley cell regimes and cell extent

The idealized modeling work discussed above indicates that the Hadley cells in an aquaplanet change their circulation regime over the course of the year, shifting rapidly between an eddy-driven ‘ITCZ’ regime and a near angular momentum conserving ‘monsoon’ regime. In addition, that the cross-equatorial Hadley cell approaches angular momentum conservation suggests that axisymmetric theories (e.g., Eq. 7) might not be applicable to the understanding of the zonal and annual mean Hadley cell, but might provide important constraints on monsoonal circulations, which do approach an angular momentum conserving state. The relationship between these two regimes and the latitude of the convergence zone raises further questions: How far into the summer hemisphere must the Hadley cell extend for the regime transition, and associated rapid shift in convergence zone latitude, to occur? Does the latitude at which the convergence zone shifts from being governed by ‘ITCZ’ to ‘monsoon’ dynamics in aquaplanets relate to the ob-

served latitudes of the ITCZs and monsoons? If the upward branch of the Hadley cell follows the peak in MSE (Privé & Plumb, 2007a), what governs the extent of the cross-equatorial cell, e.g., is a pole-to-pole cell possible?

Geen et al. (2019) investigate the first of the above questions. By running aquaplanet simulations under a wide range of conditions, including different slab ocean depths, year lengths, and rotation rates, they investigated how the convergence zone latitude and migration rate were related, and how these factors varied over the year. They found that, at Earth's rotation rate, the convergence zone appeared least stable (migrated poleward fastest) at a latitude of 7° , suggesting that, in an aquaplanet, this may be the poleward limit of the rising branch of an eddy-driven overturning circulation; i.e., the poleward limit of an ITCZ. Beyond this latitude there is a rapid transition to a monsoon circulation characterized by an overturning circulation with a rising branch far off the Equator and weak eddy momentum transports. In their simulations, this 'transition latitude' does not vary significantly with surface heat capacity or year length, but it does increase with decreasing planetary rotation rate. Although the mechanism setting the transition latitude is not yet fully understood, they suggest that this 7° threshold might give a guideline for where the tropical precipitation is dynamically associated with a near-equatorial 'ITCZ' vs. a monsoon system.

Consistent with these results, simulations introducing zonally symmetric continents in the Northern Hemisphere with southern boundaries at various latitudes suggest that monsoon circulations extending into the subtropics only develop if the continent extends equatorward of 20° latitude, into tropical latitudes. For continents with more poleward southern boundaries, the main precipitation zone remains close to the Equator and moves more gradually into the summer hemisphere. The absence of regions of low thermal inertia at tropical latitudes in this second case prevents the establishment of a reversed meridional MSE gradient and, with it, the rapid poleward displacement of the circulation ascending branch and convergence zone; i.e., it prevents a monsoon circulation (Hui & Bordoni, submitted.). Table 1 summarizes the characteristics and dynamics of the overturning (Hadley Cells) associated with the ITCZ and monsoon regimes.

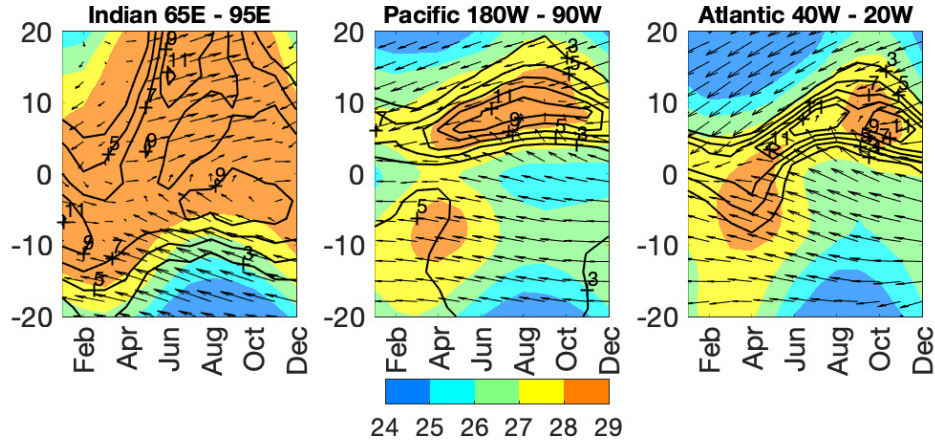


Figure 9. Hovmöller diagram of the climatological SST and 10m wind averaged across the (left) Indian, (center) eastern half of the Pacific and (right) Atlantic basin. SST is shaded (in $^\circ\text{C}$) and precipitation is contoured (contour interval 2 mm/day). The wind vectors are relative to the maximum in each panel. Precipitation data are from CMAP 1979-2017 (Xie & Arkin, 1997a), SST data are from HADISST 1870-2017 (Rayner et al., 2003), and wind data are from ERA-Interim 1979-2017 (Dee et al., 2011). From Battisti et al. (2019). ©American Meteorological Society. Used with permission.

Table 1. Characteristics of Hadley cell regimes associated with the limits of Eq. 4. The transition between the two regimes is determined by the criteria in Eq. 7.

Property	Regime	
	ITCZ	Monsoon
Position of convergence zone	Within $\sim 10^\circ$ of the Equator	Subtropics, up to $\sim 30^\circ\text{N/S}$
Physics setting convergence zone position	Under development	Under development
Strength of overturning cell/precipitation	Eddy momentum fluxes	Energetic controls (still under development)

In contrast with the idealized model results of Geen et al. (2019), the observed ITCZs over the Atlantic and Pacific migrate as far poleward as 10° from the Equator over the year (see Figs. 1 and 9). There is considerable evidence that the latitude of these ITCZs is a result of a symmetric instability in the boundary layer flow (Levy & Battisti, 1995; Stevens, 1983; Tomas & Webster, 1997). Symmetric instability is a two-dimensional (latitude-height) instability that results from the joint criteria of conservation of angular momentum and potential temperature (potential vorticity).⁷ The instability in the boundary layer flow is set up by cross-equatorial pressure gradients, driven by equatorially asymmetric boundary layer heating. In the case of the Pacific and Atlantic ITCZs, the instability results from the low-latitude, meridionally-asymmetric sea surface temperature (SST) distribution that is set up by the Andes and from meridionally asymmetric land heating over Africa respectively (see Section 4.1.3). The result of the instability is a band of divergence in the boundary layer that lies between the Equator and the latitude of neutral stability, flanked by a narrow zone of convergence that lies just poleward and provides the moisture convergence that fuels the ITCZ convection (Tomas & Webster, 1997). Monsoon flows have also been observed to be symmetrically unstable (e.g., Tomas & Webster, 1997), with the instability in this case generated by the seasonally varying meridional pressure gradient set up by the insolation.

2.1.4 Extratropical limit to monsoons

The application of the theoretical concepts discussed in Sections 2.1.1 and 2.1.2 to Hadley cell extent has been addressed in recent work by Faulk et al. (2017), Hilgenbrink and Hartmann (2018), Hill et al. (2019) and Singh (2019). Faulk et al. (2017) performed a series of simulations using an eddy-permitting aquaplanet model in which they varied rotation rate under seasonally varying insolation. They found that, at Earth's rotation, the MSE maximized at the summer pole, but the convergence zone did not migrate poleward of $\sim 25^\circ$ from the Equator even in perpetual solstice simulations, contrary to expectations from Privé and Plumb (2007a). The influence of eddies on the cross-equatorial circulation was found to be weak, consistent with the suppression of eddies by upper-level easterlies (Bordoni & Schneider, 2008; Schneider & Bordoni, 2008) and justifying the use of axisymmetric based considerations as a starting point for understanding the cell extent. Faulk et al. (2017) found that a Hadley circulation existed over the latitudes where the curvature of θ_{eb} was supercritical (see Eq. 7), with the curvature subcritical in the extratropics.

⁷ For motion on a constant potential temperature (angular momentum) surface, the criteria reduces to the criteria for inertial (convective) instability (Emanuel, 1988; Tomas & Webster, 1997).

While these studies have provided novel insight into important features of cross-equatorial Hadley cells, prognostic theories for their poleward boundary (the zero streamfunction contour) in the summer hemisphere have yet to emerge. Singh (2019) investigated the limitations of CQE-based predictions based on the lower-level MSE maximum. The vertical instability addressed by CQE is not the only form of convective instability in the atmosphere. If vertical wind shear is strong, CQE predicts an unstable state in which potential energy is released when saturated parcels move along slantwise paths, along angular momentum surfaces (Emanuel, 1983a, 1983b). Singh (2019) showed that the extent of the perpetual solstitial overturning cell can be accurately estimated by assuming that the large-scale circulation adjusts the atmosphere towards a state that is neutral to this slantwise convection. When the peak in subcloud moist entropy is relatively close to the Equator, the cell boundary is near vertical and the atmosphere is near CQE, and this reduces to the condition of Privé and Plumb (2007a).

Notably, this developing body of literature indicates that the planetary rotation rate determines the latitudinal extent of the Hadley cell, potentially limiting the maximum latitudinal extent of a monsoon circulation. This might provide a guideline for distinguishing a monsoon associated with a cross-equatorial Hadley cell and governed by eddy-less, angular momentum conserving dynamics, where the convergence zone is located in the subtropics ($\sim 20-25^\circ$ latitude, e.g., South Asia) from a monsoon that is strongly influenced by extratropical processes, where summer rainfall is observed at even higher latitudes (e.g., 35° in East Asia).

2.2 Energetic constraints

The regional monsoons are an integral part of the tropical convergence zone. As such, theories that have recently emerged to explore controls on the location of the zonally and annually averaged convergence zone ($\overline{\text{ITCZ}}$) might prove useful to the understanding of monsoon dynamics. For example, the $\overline{\text{ITCZ}}$ is located in the Northern Hemisphere, at 1.7°N if estimated by the precipitation centroid; (Donohoe, Marshall, Ferreira, & Mcgee, 2013), or $\sim 6^\circ\text{N}$ if judged by the precipitation maximum; (e.g., Gruber, Su, Kanamitsu, & Schemm, 2000). While it is usually the case that the $\overline{\text{ITCZ}}$ is co-located with SST maxima, both paleoclimate proxies (e.g., Figs. 4 & 5; Arbuszewski, Demenocal, Cléroux, Bradtmiller, & Mix, 2013; Lea, Pak, Peterson, & Hughen, 2003; McGee, Donohoe, Marshall, & Ferreira, 2014) and model simulations (Broccoli, Dahl, & Stouffer, 2006; Chiang & Bitz, 2005; Kang, 2020; Kang, Shin, & Xie, 2018; R. Zhang & Delworth, 2005) indicate that the location of the $\overline{\text{ITCZ}}$ responds to extratropical forcing, that is, to forcing remote from its location. Analysis of the atmospheric and oceanic energy budget has helped to explain these behaviors.

Not surprisingly, aquaplanet simulations have been used to examine systematically controls on the $\overline{\text{ITCZ}}$ latitude by imposing a prescribed hemispherically asymmetric forcing in the extratropics and varying its strength. Kang, Held, Frierson, and Zhao (2008) found that the atmospheric energy transport associated with the Hadley cell largely compensates for changes in hemispherically asymmetric extratropical surface heating. The Hadley cell diverges energy away from its ascending branch, i.e. away from the $\overline{\text{ITCZ}}$, and generally transports energy in the direction of the upper-level meridional flow. Hence a hemispherically asymmetric atmospheric heating will cause the $\overline{\text{ITCZ}}$ to shift towards the hemisphere with the greater heating, as illustrated in Fig. 10. Kang et al. (2008) further noted that the $\overline{\text{ITCZ}}$ latitude was approximately colocated with the ‘Energy Flux Equator’ (EFE), the latitude at which the vertically integrated MSE flux is zero, and that it varied proportionally to the strength of the asymmetric forcing. Anticorrelation between the $\overline{\text{ITCZ}}$ latitude and the cross-equatorial atmospheric energy transport in the tropics has since been observed in aquaplanet models with different physical parameterizations (Kang et al., 2009), and in models with realistic continental configurations under global warming and paleoclimate scenarios (Donohoe et al., 2013; D. M. W. Frier-

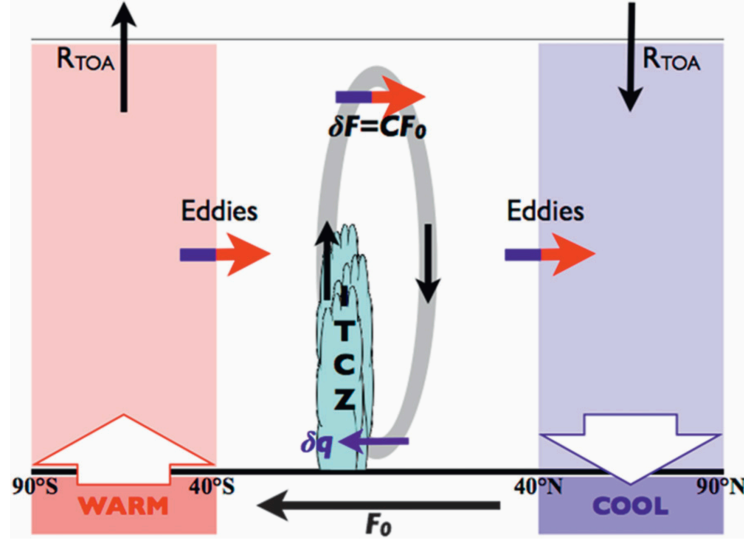


Figure 10. Schematic illustrating the energetics framework to determine the tropical response to extratropical thermal forcing (Kang et al., 2009). Warming is applied to the southern extratropical slab ocean, giving an implied ocean heat transport anomaly F_o . The atmosphere compensates for the additional warming by altering the top-of-atmosphere net radiative flux (R_{TOA}) and horizontal energy transports by the atmosphere. In the tropics, the gray oval indicates the anomalous Hadley circulation response, the direction of which is represented by black arrows. The blue (red) part of the colored arrow indicates regions where energy transports act to (anomalously) cool (warm) the atmosphere. These energy transports are due to midlatitude eddies and the Hadley circulation. The clockwise anomalous Hadley circulation transports energy northward to cool (warm) the southern (northern) subtropics and largely compensates the warming (cooling) by eddies. From Kang et al. (2009). ©American Meteorological Society. Used with permission.

son & Hwang, 2012). However, the degree of compensation between the imposed heating and the atmospheric energy transport is sensitive to the parameterizations of convection, clouds, and ice (D. M. W. Frierson & Hwang, 2012; Kang et al., 2009, 2008); to the nature of the forcing applied; to whether the response is dominated by the zonal mean circulation or stationary and transient eddies (Roberts, Valdes, & Singarayer, 2017); and to changes in energy transport by the ocean, which has been shown to play a significant role in the energy transport response to an imposed perturbation (Green & Marshall, 2017; Hawcroft et al., 2017; Kang, 2020; Kang et al., 2018; Kay et al., 2016; Levine & Schneider, 2011; Schneider, 2017).

The relationship between the \overline{ITCZ} , EFE, and tropical atmospheric energy transport can be understood more quantitatively using the steady state, zonally averaged, vertically integrated energy budget,

$$\overline{S} - \overline{\mathcal{L}} - \overline{\mathcal{O}} = \frac{\partial \langle v\overline{h} \rangle}{\partial y}. \quad (10)$$

In the above, \overline{S} is the net downward top-of-atmosphere shortwave radiation, $\overline{\mathcal{L}}$ the outgoing longwave radiation and $\overline{\mathcal{O}}$ represents any net energy uptake at the surface. Angular brackets denote a vertical integral, and overbars a time and zonal mean. Eq. 10 states that net energy input into the atmospheric column through top-of-atmosphere ra-

diative fluxes and surface energy fluxes must be in balance with meridional convergence or divergence of MSE into the atmospheric column. For small meridional displacements, δ , this equation can be Taylor expanded around the Equator to 3rd order as (Bischoff & Schneider, 2014, 2016)

$$\langle \overline{vh} \rangle_\delta = \langle \overline{vh} \rangle_0 + a \partial_y \langle \overline{vh} \rangle_0 \delta + \frac{1}{2} a^2 \partial_{yy} \langle \overline{vh} \rangle_0 \delta^2 + \frac{1}{6} a^3 \partial_{yyy} \langle \overline{vh} \rangle_0 \delta^3, \quad (11)$$

where the $_0$ subscript denotes quantities evaluated at the Equator. At the EFE, by definition, the vertically integrated, zonal mean MSE flux, $\langle \overline{vh} \rangle$, is zero. Taking δ as the latitude of the EFE, and substituting in from Eq. 10, gives

$$0 = \langle \overline{vh} \rangle_0 + a(\overline{S} - \overline{L} - \overline{O})_0 \delta + \frac{1}{2} a^2 \partial_y (\overline{S} - \overline{L} - \overline{O})_0 \delta^2 + \frac{1}{6} a^3 \partial_{yy} (\overline{S} - \overline{L} - \overline{O})_0 \delta^3. \quad (12)$$

The net energy input $(\overline{S} - \overline{L} - \overline{O})$ is approximately symmetric about the Equator, so the quadratic term is small relative to the other terms (Bischoff & Schneider, 2016), and can be neglected. Hence, to a good approximation, Eq. 12 can be written as

$$\delta = - \frac{\langle \overline{vh} \rangle_0}{a(\overline{S} - \overline{L} - \overline{O})_0}. \quad (13)$$

Eq. 13 has been shown to give a good estimate of the EFE latitude under a range of warming scenarios in aquaplanets (Bischoff & Schneider, 2014), and over the annual cycle in reanalysis (Adam, Bischoff, & Schneider, 2016b). The EFE in turn acts as an indicator of the \overline{ITCZ} latitude. More broadly, (Bischoff & Schneider, 2016) found that the first order approximation is adequate when the net energy input at the Equator is large and positive, but that the cubic term is needed when it is small or negative. Notably the negative case corresponds to a double convergence zone.

Unfortunately, the convergence zone and EFE latitudes do not covary on all timescales. In particular these can deviate from one another significantly over the seasonal cycle (e.g., Adam et al., 2016b; Wei & Bordoni, 2018). While the EFE denotes the latitude at which the meridional MSE flux changes sign, the convergence zone is associated with the ascending branch of the tropical meridional overturning circulation, which is close to the latitude where the mass flux changes sign. The energy flux and overturning circulation are related via the gross moist stability (GMS, defined here following e.g., D. M. W. Frierson, 2007; Hill, Ming, & Held, 2015; Wei & Bordoni, 2018, 2020):

$$GMS = \frac{\langle \overline{vh} \rangle}{\Psi_{max}} = \frac{\langle \overline{vh} \rangle}{g^{-1} \int_0^{p_m} \overline{v} dp}. \quad (14)$$

In the above, Ψ_{max} is the maximum of the overturning streamfunction, corresponding to the mass flux by the Hadley cell, and p_m is the pressure level at which this maximum occurs. Considering Eq. 14 at the Equator, and combining with Eq. 13, we see that the strength of the Hadley circulation (and hence the position of the convergence zone) will therefore covary with the EFE provided that the efficiency with which the Hadley cell transports energy, as captured by GMS, remains approximately constant. However, recent aquaplanet simulations indicate that over the seasonal cycle GMS varies significantly, and in fact at times becomes negative, allowing the EFE and convergence zone to sit in opposite hemispheres (Wei & Bordoni, 2018). GMS has also been observed to vary significantly under changes to orbital precession and increased CO_2 in aquaplanet simulations (Biasutti & Voigt, 2020; Merlis, Schneider, Bordoni, & Eisenman, 2013). It is also worth noting that, in addition to variations in GMS, the zonal mean energy flux compensating an energetic forcing may be achieved by transient or stationary eddies, rather than by changes to the zonal mean overturning circulation (Roberts et al., 2017; Xiang, Zhao, Ming, Yu, & Kang, 2018). When these factors do not play a significant role, changes in hemispheric asymmetry in surface energy flux appear to exert a tighter control than changes in SST on the latitudinal location of tropical precipitation (Kang & Held, 2012).

However, recent analysis of the TRACMIP model ensemble (Voigt et al., 2016) indicates that the significant changes in GMS which occur both over the seasonal cycle and in the response to increased CO₂ mean that in these cases the convergence zone latitude is more closely related to changes in SST than to energy flux changes (Biasutti & Voigt, 2020).

Despite these limitations, the energetic framework has been a major advance, and has given insight into variations in tropical rainfall over both the observational and paleo record (see reviews by Kang, 2020; Kang et al., 2018; Schneider, Bischoff, & Haug, 2014, and references therein). One attractive feature of this perspective is that it provides a simple explanation for why, in the annual and zonal mean, the ITCZ sits in the Northern Hemisphere (Donohoe et al., 2013; Gruber et al., 2000). The energetic framework neatly shows that the ITCZ latitude can be understood as a result of the net flux of energy into the Northern Hemisphere by the ocean, in particular due to asymmetry introduced by the Drake passage (D. M. Frierson et al., 2013; Fučkar, Xie, Farneti, Maroon, & Frierson, 2013; Marshall, Donohoe, Ferreira, & McGee, 2014). Efforts to extend this framework to account for zonal asymmetry in the boundary conditions (the ‘Energy Flux Prime Meridian’ Boos & Korty, 2016) are discussed in Section 3.2.

3 Interpreting observations and modeled response to forcings

In parallel with the theoretical developments described in Section 2, observational and reanalysis datasets have allowed more detailed analysis of the behavior of Earth’s monsoons. As discussed in Section 1, one major step has been moving from a perspective of monsoons as individual, unrelated systems, to a perspective of a global monsoon manifesting itself into several regional systems (B. Wang & Ding, 2008). In this section, we look at the insight into the dynamics of Earth’s monsoons gained from observations and Earth System models, and at how it connects to the theoretical ideas developed using idealized model simulations discussed in Section 2. First, we give an overview of the characteristics of Earth’s regional monsoons, ITCZs and the global monsoon. We then discuss the extent to which theory, particularly that from aquaplanet models, may help us understand the behavior of these systems.

3.1 The global and regional monsoons

The magenta line in Fig. 1a-c marks out the regional monsoons, indicating areas where the local difference between summer and winter precipitation exceeds 2 mm/day, and where summer precipitation accounts for the majority of the annual total. Six regions can be identified: Asia, West Africa, Southern Africa, South America, North America and Australia (cf. S. Zhang & Wang, 2008). The Asian monsoon is the most intense and largest in scale of these, and is often further divided into three subregions: the South Asian, East Asian, and Western North Pacific monsoons, as shown in Fig. 11. (B. Wang & LinHo, 2002).

3.1.1 Regional monsoon and ITCZ characteristics

South Asian Monsoon

The South Asian monsoon features a wind reversal from winter easterlies to summer westerlies at lower levels (e.g., B. Wang & LinHo, 2002). Onset spreads from the south to the north, with the earliest onset of the system over the Southern Bay of Bengal, between late April and mid-May (Mao & Wu, 2007), reaching Kerala between mid-May and mid-June (Ananthakrishnan & Soman, 1988; J. M. Walker & Bordoni, 2016; B. Wang, Ding, & Joseph, 2009). Onset occurs over the South China Sea between early May and mid-June (B. Wang, LinHo, Zhang, & Lu, 2004).

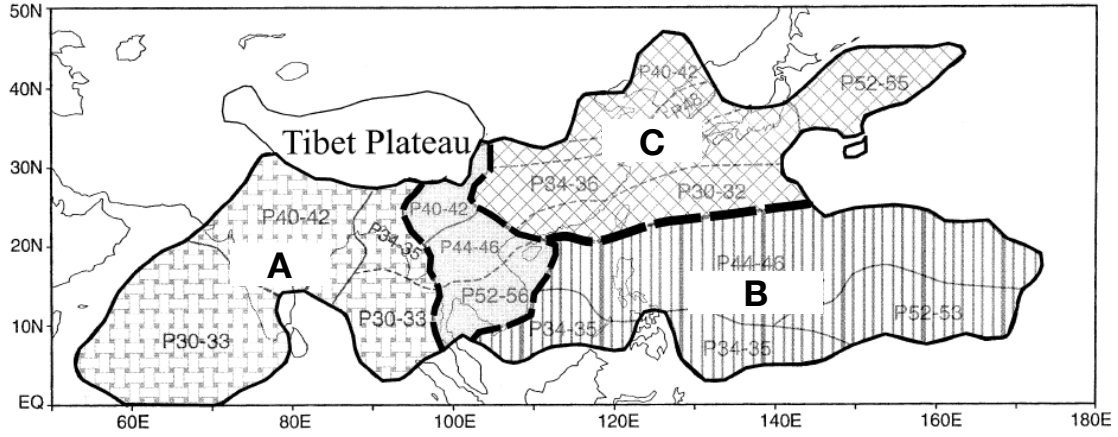


Figure 11. Map showing the division of the Asian monsoon into three subregions. The South Asian monsoon (A) and Western North Pacific monsoon (B) are tropical monsoon regions. A broad corridor in the Indochina Peninsula separates them. The East Asian monsoon (C) is an extratropical ‘monsoon’ (see Section 4.1.1). Numbers indicate the pentad range during which the peak monsoon rainfall occurs. Adapted from B. Wang and LinHo (2002). ©American Meteorological Society. Used with permission.

The wet season over India generally lasts from June to September, during which time about 78% of the total annual rain falls over India (Parthasarathy, Munot, & Kothawale, 1994). The rain band withdraws towards the Equator between late September and early November (B. Wang & LinHo, 2002).

East Asian ‘Monsoon’

While the South Asian monsoon is confined to be equatorward of $\sim 30^\circ\text{N}$, the East Asian monsoon extends north of this into the extratropics. Although the monsoon onset over the South China Sea has been considered a precursor to the East Asian monsoon onset (Martin et al., 2019; B. Wang et al., 2004), some authors (e.g., B. Wang & LinHo, 2002) consider it as an entirely subtropical system. A key element of the East Asian monsoon is an east-west oriented band of precipitation, known as Meiyu in China and Baiu in Japan, that is accompanied by a wind reversal from winter northerlies to summer southerlies. The Meiyu-Baiu front brings intense rainfall to the Yangtze River valley and Japan from mid-June to mid-July, after which it breaks down and allows rainfall to extend into northern China and Korea. Prior to the onset of the Meiyu-Baiu front, South China experiences periods of rainfall in the form of the South China spring rain, intensifying from mid-March to May (Linho, Huang, & Lau, 2008). A thorough review of the East Asian monsoon’s characteristics, including its onset and development, governing processes and teleconnections is given in Ding and Chan (2005); see also Section 4.1.1.

Western North Pacific Ocean Monsoon

Monsoon rains arrive later over the western subtropical North Pacific ocean (see Fig. 11) than the South and East Asian sectors, and last from July to October/November (B. Wang & LinHo, 2002). The monsoon advances from the south-west to north-east in a stepwise pattern associated with shifts in the Western North Pacific subtropical high (R. Wu & Wang, 2001), while withdrawal occurs from the north-west to south-east (S. Zhang & Wang, 2008). A predominantly zonally oriented change in wind direction is seen be-

tween winter and summer, associated with a weakening of the low-latitude easterly flow as the Western North Pacific subtropical high shifts eastward (e.g., Fig. 1).

Australian Monsoon

The Australian monsoon develops over Java in October-November, and progresses southeastward, reaching northern Australia in late December (Hendon & Liebmann, 1990; S. Zhang & Wang, 2008). During austral summer, the low-latitude easterlies over the western Maritime Continent reverse to a southwesterly flow, as seen in Fig. 1b and c. Monsoon withdrawal occurs over northern Australia and the southeastern Maritime Continent through March, with the wet season persisting into April over Java (S. Zhang & Wang, 2008).

West African Monsoon

The West African monsoon begins near the Equator, with intense rainfall over the Gulf of Guinea in April. This continues through to the end of June, with a second maximum developing near 10°N in late May. The peak precipitation is observed to jump rapidly to this second maximum in late June, accompanied by a reversal of the wind direction from north-easterly to south-westerly to the south of this maximum (Sultan & Janicot, 2003). Precipitation weakens from August to September and the peak rainfall migrates back towards the Equator. Over the Sahel, the monsoon precipitation accounts for 75-90% of the total annual rainfall (Lebel, 2003). Another notable feature in this region is the presence of a secondary shallow meridional circulation, with dry air converging and ascending over the Sahara, where sensible heating is strong, and a return flow at 500-750 hPa (Hagos & Cook, 2007; Shekhar & Boos, 2017; Trenberth et al., 2000; C. Zhang, Nolan, Thorncroft, & Nguyen, 2008). The precise seasonality of this shallow circulation was found to vary between the NCEP1, NCEP2 and ERA-40 reanalyses by C. Zhang et al. (2008). We find that in the JRA-55 data used here the seasonality is most consistent with that of ERA-40 in that study, with the return flow present year-round, but strengthening semi-annually in boreal winter from late November to late March and boreal summer from mid-May to mid-October (not shown).

Southern African Monsoon

The Southern African monsoon is offset longitudinally to the east of its Northern Hemisphere counterpart. The global monsoon onset metric of S. Zhang and Wang (2008) indicates that the rainy season begins in November over Angola and the southern DRC, and extends southeastward over the continent, progressing over southern Tanzania, Zambia and out over the ocean over northern Madagascar through December, and reaching Zimbabwe, Mozambique, and as far as the northeast of South Africa by January. The system extends out over the Southwestern Indian Ocean through January and February. Withdrawal occurs directed towards the north and west from February to April. In austral winter, the prevailing wind is southeasterly, but in summer this reverses to a weak northeasterly flow, with stronger northeasterly flow to the north of the region, over the Horn of Africa, as seen in Fig. 1c. Although, as we will show, the seasonality of both the circulation and precipitation in this region is consistent with monsoon dynamics, the summertime precipitation over this region is more often referred to as the ‘Southern African rainy season’, and it is only with the advent of the Global Monsoon perspective that this system is gaining more attention as a monsoon (e.g., S. Zhang & Wang, 2008).

North American Monsoon

The North American monsoon is observed as a marked increase in precipitation over Mexico and Central America, beginning in June-July, and withdrawing through September and October (Adams & Comrie, 1997; Barlow, Nigam, & Berbery, 1998; Ellis, Saffell, & Hawkins, 2004). S. Zhang and Wang (2008) observed that onset (withdrawal) over this area occurs in a northward (southward) moving band. There is no large-scale re-

versal of the winds in this region (see Figs. 1b and 1c). However, the northwesterly flow down the coast of California observed in boreal winter weakens in boreal summer, the southeasterly flow over the east coast of Mexico strengthens, and the low-latitude easterlies over the eastern Pacific weaken in the Northern Hemisphere (e.g., Fig. 7 of Barlow et al., 1998). In addition, at a smaller scale, the lower-level wind direction reverses over the Gulf of California from northerly to southerly flow (Bordoni, Ciesielski, Johnson, McNoldy, & Stevens, 2004).

South American Monsoon

The monsoon season in South America begins in October, with an abrupt shift of convection southward over the Amazon river basin (Marengo et al., 2012). The precipitation progresses southeastward through November and December (S. Zhang & Wang, 2008). Withdrawal occurs from March to May, with the rain-band returning northward. During austral winter, the prevailing 850-hPa winds over the continent are predominantly easterly between 10°S and 10°N, but in summer the flow becomes northeasterly and cross equatorial, and a northwesterly jet, the South American Low-Level jet, develops along the east side of the Andes (Marengo et al., 2012). An upper-level anticyclone is observed over Bolivia, and a lower-level cyclone develops over northern Argentina (Rao, Cavalcanti, & Hada, 1996). Central Brazil receives over 70% of its annual rainfall during the monsoon season, between September and February (Rao et al., 1996).

The Atlantic and Pacific ITCZs

The latitudinal position of the ITCZs in the Atlantic and Pacific also has a distinct seasonal cycle, as can be seen from the north-south dipole in the October/November-April/May precipitation difference, shown in Fig. 1b. Precipitation associated with the Atlantic and Pacific ITCZs reaches farthest north in October and farthest south (but still north of the Equator; see Section 4.1.3) in March about three months after the boreal and austral solstice, respectively (Fig. 9) due to the large heat capacity of the upper ocean that participates in the seasonal cycle.

3.1.2 The Global Monsoon

The regional monsoons exhibit a diverse range of behaviors, but some common features can be identified. From Fig. 1a, it can be seen that most monsoon regions feature anomalous westerly lower-level flow in their summer season, with a cross-equatorial component directed into the summer hemisphere. However, comparing Figs. 1b and c shows that these anomalies are not always sufficient to cause a local reversal of the wind direction. Onset generally occurs as a poleward advancement of rainfall off of the Equator, often with an eastward directed progression. Onset also sometimes features sudden jumps or steps in the latitude (poleward) and longitude of precipitation, as observed over South Asia, West Africa, the Western North Pacific, and South America.

These common features are particularly evident in EOF analyses of the annual cycle of the global divergent circulation (Trenberth et al., 2000) and of precipitation and lower-level winds (B. Wang & Ding, 2008). These reveal a global-scale solstitial mode, that accounts for 71% of the combined annual variance in precipitation and surface winds, and closely reflects the summer-winter differences in precipitation (compare Fig. 1a and Fig. 2a). B. Wang and Ding (2008) also identified a second major mode, an equinoctial asymmetric mode that reflects spring-fall asymmetry (compare Fig. 1b and Fig. 2b). This mode is particularly evident in the ITCZs, relating to their delayed seasonality. These dominant modes motivate a perspective of a global monsoon system that is driven by the annual cycle of insolation, and so can be expected to respond to orbital forcings in a coherent manner. The global monsoon might be interpreted as the seasonal migration of the convergence zone into the summer hemisphere throughout the year, with regional monsoons corresponding to locations where this migration is enhanced, and with cou-

pling between the zonal and meridional overturning circulations contributing to this localisation of rainfall (Trenberth et al., 2000; B. Wang & Ding, 2008; Webster et al., 1998).

This perspective is further supported by paleoclimate reconstructions, present-day observations, and model simulations, which have begun to elucidate how the regional monsoons and ITCZs vary under a range of external and internal forcings. Forcings that preferentially warm or cool one hemisphere relative to the other - such as Heinrich events, changes in Earth’s axial precession and high latitude volcanic eruptions - are found to intensify the monsoons of the warmer hemisphere, and to weaken the monsoons of the cooler hemisphere (e.g., An et al., 2015; Atwood et al., 2020; Battisti et al., 2014; H. Cheng, Sinha, Wang, Cruz, & Edwards, 2012; Eroglu et al., 2016; Liu & Battisti, 2015; Pausata et al., 2011; P. X. Wang et al., 2014, and see Figs. 4 and 5).

3.2 Aquaplanet-like monsoons

Aquaplanet-based theoretical work, as discussed in Section 2, has used symmetric boundary conditions to study the fundamental processes governing the zonal mean convergence zone, Hadley cells, and global monsoon. In contrast, the bulk of studies using observations, reanalysis, and Earth System models have tended to focus on the mechanisms controlling regional monsoons. While local factors are important in determining the seasonal evolution and the variability of the individual monsoon systems, we argue here that aquaplanet results can inform us of unanticipated commonalities in the dynamics of the monsoons, and help us interpret the behaviors observed. Of the two perspectives discussed in Section 2 the energetic approach has received more attention (Bisutti et al., 2018; Kang, 2020; Kang et al., 2018; Schneider et al., 2014), perhaps due to the relative ease with which the relevant diagnostics can be evaluated and the intuitive picture it presents (Fig. 10). In this section we explore where these approaches can provide insight into the dynamics of Earth’s monsoons. Section 4 discusses regions where zonal asymmetry limits the relevance of the aquaplanet theories.

3.2.1 *Insight from the momentum budget and CQE considerations*

For an aquaplanet, the momentum framework, combined with the assumption of CQE, indicates that:

1. Convergence associated with a cross-equatorial ‘monsoon’ meridional overturning circulation lies just equatorward of the peak in subcloud MSE or θ_{eb} (Emanuel, 1995; Privé & Plumb, 2007a, 2007b).
2. Meridional overturning cells associated with monsoons approach conservation of angular momentum more than cells associated with ITCZs, and consequently are more strongly coupled to meridional MSE gradients (Schneider & Bordoni, 2008).
3. Rapid transitions can occur between an ITCZ regime with two eddy-driven Hadley cells and an angular momentum conserving monsoon regime with one dominant cell that extends into the summer hemisphere (cf. Figs. 8a and 8b). These transitions are mediated by feedbacks relating to advection of MSE in the lower branch of the Hadley circulation, and suppression of eddies by upper-level easterlies (Bordoni & Schneider, 2008, 2010; Schneider & Bordoni, 2008).
4. At Earth’s rotation rate, the transition from the eddy-driven to angular momentum conserving Hadley cell regime appears to occur at $\sim 7^\circ$ latitude on an aquaplanet with zonally symmetric boundary conditions (Geen et al., 2019).
5. At Earth’s rotation rate, convergence zones within the ascending branches of monsoons appear to be unable to migrate farther than $\sim 25^\circ$ from the Equator (Faulk et al., 2017; Hill et al., 2019; Singh, 2019).

The above ideas were developed in a very idealized framework, but some consistent behavior has been observed on Earth. Nie, Boos, and Kuang (2010) investigated whether the CQE assumption was relevant locally in the regional monsoons. By analysing ERA-40 and Tropical Rainfall Measuring Mission (TRMM) data, they demonstrated that, in the South Asian, Australian, and African monsoons, maxima of θ_{eb} and free-troposphere saturation equivalent potential temperature, θ_e^* , are approximately colocated, and peak precipitation indeed lies just equatorward of the peak in subcloud MSE, consistent with CQE (Fig. 12). The picture in Northern Africa is slightly complicated by remote upper-tropospheric forcing due to the Rossby wave induced by the South Asian summer monsoon, but the ridge of θ_e^* nonetheless reflects the structure of θ_{eb} over the Sahel (Fig. 12b). In South Asia gradients of θ_{eb} are tightly set by topography and the maximum in upper-level temperature is not centered over the Tibetan Plateau (Fig. 12a). These findings led to re-interpretation of the role of topography in driving a strong monsoon in the region, with the elevated topography now recognized as a mechanical barrier to cold, dry air from the north that generates a strong θ_{eb} maximum, rather than influencing the monsoon primarily via elevated heating (Boos & Kuang, 2010, 2013).

CQE does not hold well in the Americas or East Asia. Over North America, maxima of θ_e^* and θ_{eb} occur at different latitudes; the reason for this is not clear but may relate to advective drying of the lower troposphere. In South America the θ_{eb} distribution has a broad maximum extending from the Equator to 20° S, while θ_e^* has a more localized peak at 20° S. In East Asia, a tropical peak of precipitation is found just equatorward of the peak in θ_{eb} , but the maximum of θ_e^* occurs farther north, just south of the precipitation associated with the Meiyu-Baiu front. The Atlantic ITCZ and the Pacific ITCZ (sufficiently west of North America) both approximately follow CQE in boreal summer (Figs. 12b & c), but in boreal winter the maxima of precipitation and θ_{eb} remain in the Northern Hemisphere, while the maxima of θ_e^* shift equatorward (Figs. 12e & f). Further discussion of these regions is given in Section 4.1.3. It is also worth noting that while CQE does not hold in all locations, tropical precipitation is generally located close to or just equatorward of the maximum θ_{eb} throughout the year (see Fig. 12). θ_{eb} appears a useful indicator of where precipitation will fall, even where this does not take the form of intense, deep convection in a monsoonal overturning circulation. Over ocean this is unsurprising, as θ_{eb} is strongly coupled to the SST. However, that this holds over land reinforces the emerging view of monsoon precipitation being governed by MSE, rather than surface temperature.

Also consistent with the idealized modeling work, seasonal changes in the character of the overturning circulation have been observed in the regional monsoons. The Hadley circulation over the South Asian monsoon region in particular has been highlighted as showing rapid transitions between an eddy-driven and an angular momentum conserving Hadley circulation that are similar to those seen in aquaplanet simulations. In this region, precipitation migrates rapidly off the Equator to $\sim 25^\circ$ and the summertime circulation is nearly angular momentum conserving (Bordoni & Schneider, 2008; Geen et al., 2018; J. M. Walker & Bordoni, 2016). To give an indication of other regions where angular momentum conservation may apply, Fig. 13 shows the local overturning circulation, defined using the divergent component of the meridional wind (e.g., Schwendike et al., 2014; G. Zhang & Wang, 2013) for each of the monsoon regions marked in Fig. 1. Angular momentum contours are plotted in gray. The upper-level summertime overturning circulation becomes roughly aligned with angular momentum contours in the deep tropics in the South Asian, West and Southern African monsoon regions. In contrast, the overturning circulations over Australia and the Americas are not angular momentum conserving, even very close to the Equator. The case of Australia highlights that regions where CQE applies may not reflect those where the circulation conserves angular momentum.

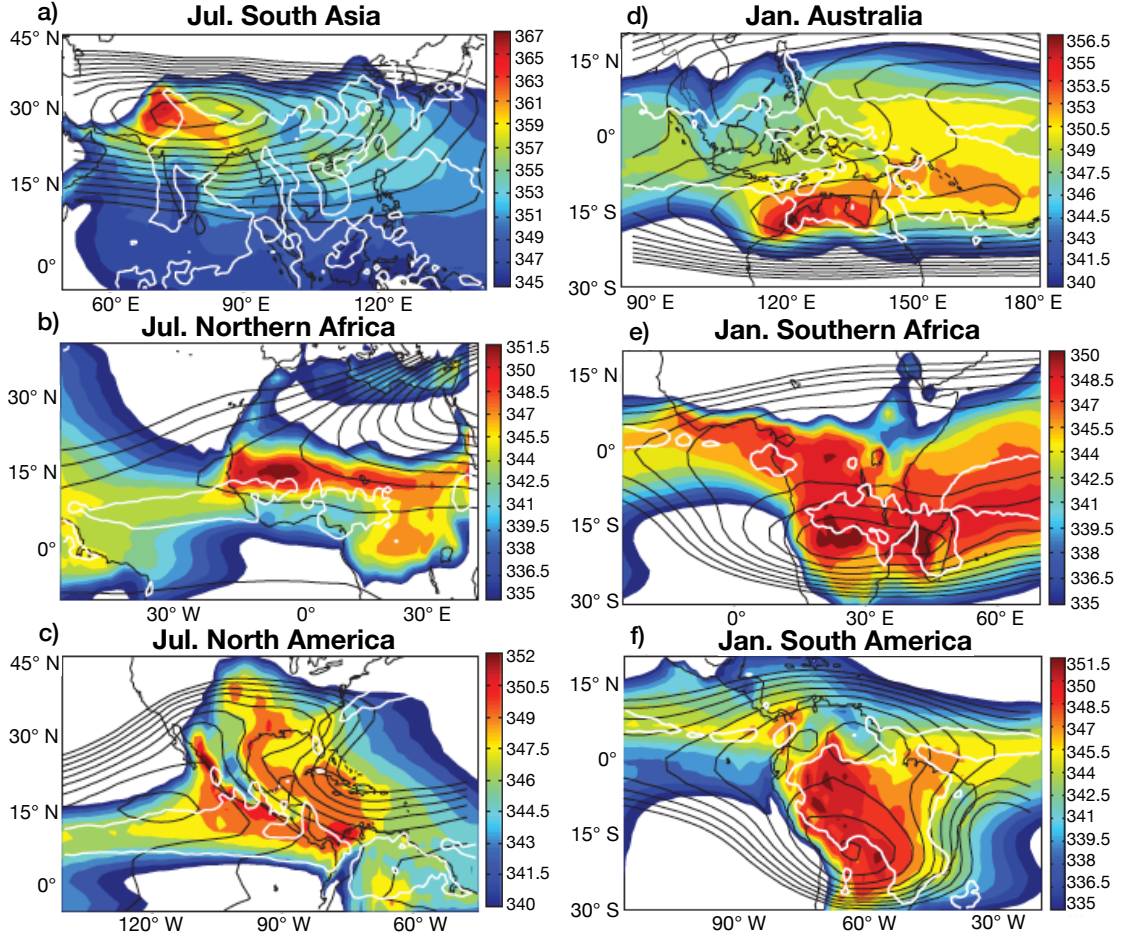


Figure 12. Evaluation of CQE for the (a) South Asia, (b) northern Africa, (c) North America, (d) Australia, (e) southern Africa and (f) South America monsoons. Colors show subcloud equivalent potential temperature, θ_{eb} . The black contour is the free-troposphere saturation equivalent potential temperature, θ_e^* , averaged from 200 to 400 hPa. The white contour indicates the region that has precipitation greater than 6 mm day^{-1} . The θ_e^* contours start from (a) 345 K, (b) 340 K, (c) 340 K, (d-f) 341 K and the respective interval is (a) 1 K, (b) 1 K, and (c-f) 0.5 K. Adapted from Nie et al. (2010). ©American Meteorological Society. Used with permission.

Findings from aquaplanets show consistency with climatological behavior of some regional monsoons, although it is clear that there is still more to be learned. Awareness of the relevance of the lower-level MSE and upper-level wind structures to the meridional overturning circulation may additionally help in understanding present day variability of the monsoons and model projections of future climate. For example, Hurley and Boos (2013) used reanalysis and observational datasets to explore whether variability in monsoon precipitation could be connected to variability in θ_{eb} , as expected theoretically in a monsoon circulation. Even removing the signal of variability linked to ENSO, they found that positive precipitation anomalies in the American, African, South Asian and Australian monsoons were associated with enhanced θ_{eb} , consistent with previous findings over West Africa (Eltahir & Gong, 1996). In addition, variability in θ_{eb} was found to be due primarily to variability in moisture rather than in temperature, with strong monsoon years associated with enhanced specific humidity near the climatological θ_{eb} maximum, with temperature anomalies of the opposite sign (see also J. M. Walker, Bor-

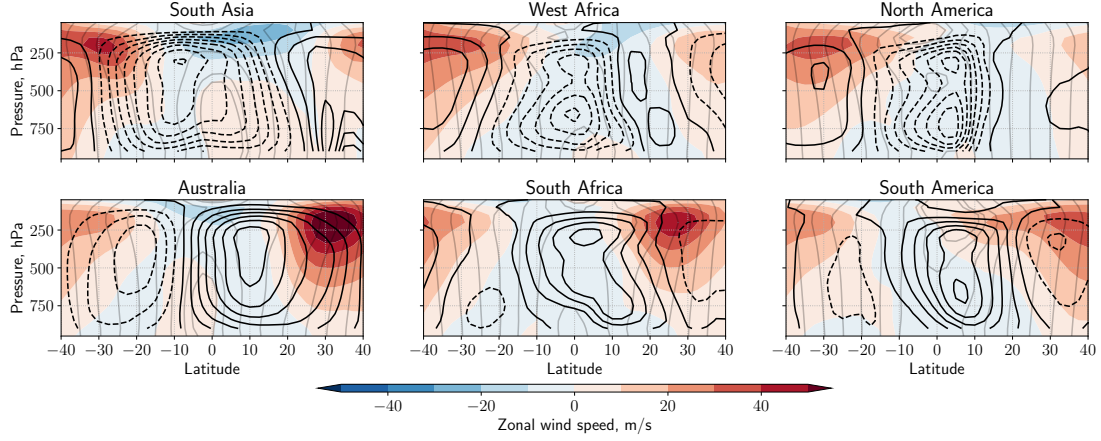


Figure 13. Black contours show local summer (June-September or December-March) meridional overturning circulations for: South Asia (70-100°E), West Africa (10°W-30°E), North America (85-115°W), Australia (115-155°E), South Africa (10-50°E), South America (40-70°W). This is computed by vertically integrating the divergent component of the meridional wind, averaged in longitude, from the top of the atmosphere to the surface (cf. Schwendike et al., 2014; G. Zhang & Wang, 2013). Shading shows zonal wind. Light gray contours indicate absolute angular momentum per unit mass, with contours at $\Omega a^2 \cos^2 \phi_i$ ($\phi_i = 0^\circ, \pm 5^\circ \pm 10^\circ, \dots$).

doni, & Schneider, 2015). This clearly contradicts the classical sea-breeze view of the monsoons, but is consistent with the CQE perspective. Shaw and Voigt (2015) showed that the CQE perspective can help to explain the weak response of the Asian monsoons to global warming seen in climate model projections. Using data from the Atmospheric Model Intercomparison Project (AMIP) experiments, they compared the circulation response to a quadrupling of CO₂ with fixed SSTs (AMIP4xCO₂) with the response to a uniform 4K increase in SST (expected due to a 4x increase in CO₂), but with no CO₂ increase (AMIP4K). They found that the CO₂ forcing led to θ_{eb} changes that supported a more intense monsoon, but the SST forcing led to opposite θ_{eb} changes which, they argued, led to a weak net response to an increase in CO₂.

The tight, albeit diagnostic, relationship between lower-level MSE and precipitation (Fig. 12) makes assessment of the influence of forcings or teleconnections on the MSE budget (e.g., via advection, enhanced evaporation etc.) an intuitive focus for research into monsoon variability and future change. The connection to the upper-level momentum budget and Hadley cell regimes has not yet been so comprehensively investigated. However, it has been observed that anomalous upper-level easterlies and westerlies are associated with anomalous upper-level divergence and convergence in monsoon regions in a sense that is consistent with the aquaplanet regimes. For example, on intraseasonal and interannual timescales over South Asia and West Africa, anomalously wet conditions are associated with easterly upper-level zonal wind anomalies, westerly lower-level zonal wind anomalies, and expansion and strengthening of the meridional overturning, with the opposite applying in dry phases (Goswami & Ajaya Mohan, 2001; Sultan & Janicot, 2003; J. M. Walker et al., 2015). However, these circulations are zonally confined, and terms in the momentum budget that are trivially zero in an aquaplanet might play a more dominant role. More work is needed to understand the leading order momentum budget in the different monsoon regions and if and to what extent conservation of angular momentum is approached even at the regional scale.

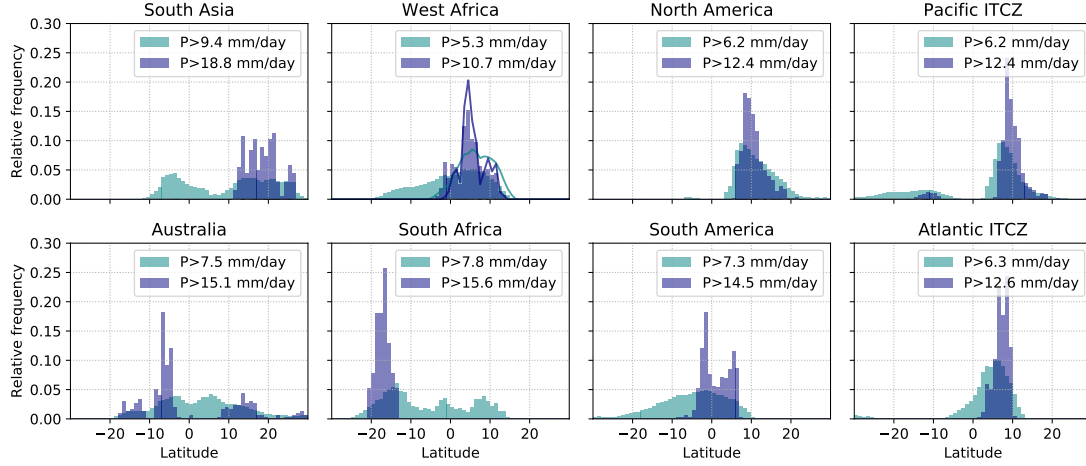


Figure 14. Relative frequency distributions of latitudes where the strongest precipitation falls in the regional monsoons and ITCZs. Monsoon regions are defined as in Fig. 1, and ITCZs as in Fig. 4.1.3. For West Africa, lines show the distribution for -10 to 10°E . Data are from a linearly detrended pentad-mean climatology of GPCP precipitation data spanning 1997–2014.

The recent findings summarized in points (4) and (5) above suggest that planetary rotation constrains the latitude at which the overturning circulation tends to transition from an eddy-driven to an angular momentum conserving regime, and the maximum latitude that the convergence zone can reach. The implications for Earth’s tropical circulations remain to be explored. However, one could imagine that these latitudinal bounds might provide information on what circulation regime we expect to be associated with ascending air and precipitation at a given latitude. Fig. 14 shows the relative frequency distribution of precipitation that exceeds some threshold (see legends) in each monsoon region and ITCZ.⁸ In the South Asian, Australian and Southern African monsoon regions, the distribution suggests multiple preferred locations for strong precipitation to fall. Over South Asia and South Africa, the strongest precipitation (dark blue) is located in monsoon convergence zones, poleward of 10° . Over the Australian sector, intense precipitation appears to occur most often nearer the Equator, though smaller peaks are found poleward of 10° in both hemispheres. In the Northern Hemisphere a small peak is also seen poleward of 25° ; these peaks reflect rainfall in the Western North Pacific and East Asian monsoons. Looking at the West Africa region as defined in Fig. 1 (-10 – 30°E), a broad peak is seen. Limiting the region to -10 – 10°E (as studied by e.g., Sultan & Janicot, 2003) two peaks emerge: a larger peak at $\sim 5^\circ$ and a second peak at $\sim 10^\circ$. In the other monsoon regions and ITCZs a single peak is seen, suggesting no change in precipitation regime over the year.⁹

Fig. 15 shows the mass flux associated with meridional and zonal overturning circulations for May to September and November to March (cf. Schwendike et al., 2014).

⁸ Specifically the procedure followed is as follows: (1) Weight precipitation to account for decrease in grid box size with latitude. (2) Find the maximum value of (weighted) precipitation within the region. (3) Calculate thresholds as $1/3$ and $2/3$ of this maximum, this allows for different rainfall intensities between regions. (4) For each threshold, count gridboxes in the region (over longitude and time) where the threshold is exceeded and sum the counts zonally to give a frequency distribution. (5) Normalize the total counts at each location by the domain total counts to obtain the relative frequency.

⁹ The distributions over South America and the Pacific ITCZ show some hint of secondary peaks, likely from the Atlantic ITCZ and South Pacific Convergence Zone respectively (cf. Fig. 1).

Gray shading indicates the region between 10–25° from the Equator. Consistent with the findings of Faulk et al. (2017) for the aquaplanet circulation, the upward mass fluxes associated with the Hadley cell are confined to within 25° of the Equator. One might further speculate that circulations for which the upward mass flux and intense rain are concentrated between 10–25° from the Equator (Asia, Southern Africa) might bear similarities to the aquaplanet angular momentum conserving regime, while those where ascent and precipitation largely remain equatorward of 10° (Australia and South America) might behave more like the aquaplanet eddy-driven regime. Figs. 13 and 15 suggest this idea shows promise, with, for example, the summer overturning circulation over Australia remaining in an eddy-driven regime, while the circulation over areas such as South Asia and Southern Africa becomes more aligned with angular momentum contours. These categorisations of the various flow regimes associated with tropical rainfall could be of use in interpreting the responses of different regions to external forcings. We note that while Fig. 14 supports the idea of multiple preferred precipitation regimes at a given longitude, both Figs. 14 and 15 indicate that the critical latitude for delineating the ITCZ and monsoon regimes is $\sim 12\text{--}15^\circ$ rather than the $\sim 7^\circ$ threshold found in aquaplanets. It remains to be explored if and how asymmetric boundary conditions and/or other processes and feedbacks that are absent in the aquaplanets might give rise to quantitative differences in regional critical latitudes.

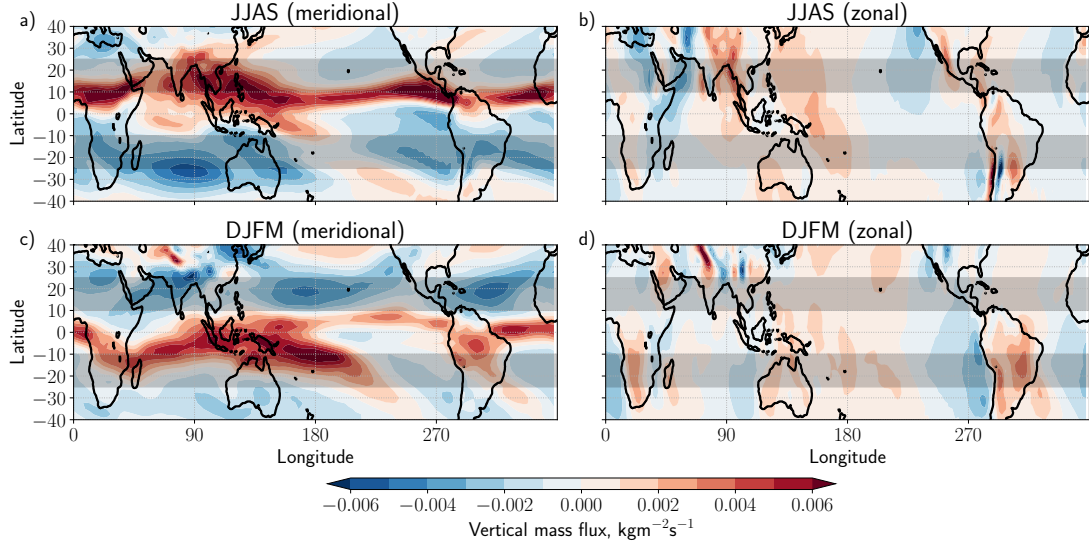


Figure 15. Vertical mass flux at 500 hPa, calculated from JRA-55, associated with (a) the divergent meridional circulation and (b) the divergent zonal circulation (cf. Schwendike et al., 2014) in boreal summer, defined as in Fig. 13. (c) and (d) are as (a) and (b) but for austral summer. Gray shading highlights the regions between 10 and 25°N/S, see discussion in text.

While the aquaplanet results provide a common framework for interpreting regional monsoons and their variability, some caveats must be remembered. The regional monsoons are local systems with overturning associated with both meridional and zonal flows (e.g., Fig. 15). Simple symmetric theories do not necessarily extend straightforwardly to these cases, with stationary waves modifying the momentum and energy budgets (Shaw, 2014). Also, in addition to the deep, moist convective overturning circulation, the West and Southern African and Australian monsoons feature a shallow, dry circulation whose ascent is colocated with the peak in potential temperature (e.g., Hagos & Cook, 2007; Nie et al., 2010; Trenberth et al., 2000; C. Zhang et al., 2008); advective drying by this shallow circulation appears to suppress monsoon precipitation (Shekhar & Boos, 2017;

Zhai & Boos, 2017). Shekhar and Boos (2016) used idealized model simulations to explore whether the CQE and energetic perspectives could still characterize the ITCZ latitude in the presence of a shallow circulation. In such cases the ITCZ was no longer well-characterized by the maximum subcloud MSE, but the maximum of a weighted average of lower tropospheric MSE, from 20 hPa above the surface to 500 hPa, was more consistently located close to the ITCZ. They suggest this weighted average accounts for the entrainment of low-MSE air into deep convective updrafts.

3.2.2 Applications of the EFE framework

As reviewed in Section 2.2., the vertically integrated atmospheric energy budget provides a complementary approach to understanding constraints on tropical rainfall. An elegant finding from applying this in aquaplanets is that the convergence zone approximately follows the EFE, so that changes in zonal mean convergence zone latitude can be linked to changes in net forcing not only in the tropics, but also at higher latitudes (see Section 2.2 and e.g., Bischoff & Schneider, 2014; Kang et al., 2008). Additionally, the MSE budget allows for a more mechanistic understanding of the local response to such changes. Recent reviews have discussed the energetic perspective of the convergence zone (Kang, 2020; Kang et al., 2018; Schneider et al., 2014) and its application to Earth’s monsoons (Biasutti et al., 2018), and so only a brief discussion is given here.

The latitude of the zonally averaged convergence zone is strongly anticorrelated with the zonally averaged meridional atmospheric energy transport at the Equator, and correlated with the EFE latitude. This relation holds in both observations and under a range of modeled forcing scenarios (although it breaks down where the convergence zone shifts far from the Equator over the seasonal cycle; Adam et al., 2016b; Bischoff & Schneider, 2014; Donohoe et al., 2013). This relationship helps to explain why the $\overline{\text{ITCZ}}$ is north of the Equator (Marshall et al., 2014).

Extending this framework to local cases has proved more challenging. Boos and Korty (2016) used the longitudes where the zonally divergent column integrated MSE flux vanishes, and has positive zonal gradient, to define ‘Energy Flux Prime Meridians’ (EFPMs). Two EFPMs can be identified in each season: over the Bay of Bengal and Gulf of Mexico/Caribbean Sea in boreal summer, and over the Western Pacific and South America in austral summer. They showed that this extended theory gives some basic insight into how localized shifts in precipitation with ENSO relate to anomalous energy transports. Adam, Bischoff, and Schneider (2016a) defined the zonally varying EFE as the latitude at which the meridionally divergent column integrated MSE flux vanishes and has positive meridional gradient. This was found to approximate the seasonal cycle of convergence zone migrations over Africa, Asia and the Atlantic. However, the influence of the Walker cell limited the local EFE’s usefulness over the Pacific, and the EFE deviates from the convergence zone in the solstitial seasons that are particularly relevant to the monsoons.

As with the momentum budget framework, while the EFE framework is valuable in explaining some features of the overturning circulation, limitations must be remembered. Relating changes in the latitude of the convergence zone to that of the zonally averaged EFE assumes that the response to forcing is via changes to the meridional overturning circulation, and neglects changes to the GMS. Such changes have been shown to be non-negligible both over the seasonal cycle and in the response to orbital and greenhouse gas forcings (Merlis et al., 2013; Seo, Kang, & Merlis, 2017; Smyth, Hill, & Ming, 2018; Wei & Bordoni, 2018). In addition, Biasutti et al. (2018) noted that while the EFE predicts changes to the convergence zone latitude once the net energy imbalance is known, changes in ocean energy transport, and feedbacks internal to the atmosphere, can result in a net imbalance different to that expected from an imposed external forcing, including orbital forcing (Liu et al., 2017). More generally, even when the energy budget frame-

work correctly places the location of the zonal mean convergence zone, the latter can represent an average over zonally asymmetric contributions that are much greater than the zonal average (Atwood et al., 2020).

3.2.3 *Reconciling the momentum budget/CQE and EFE perspectives*

The two perspectives discussed so far in this review have emerged via separate consideration of the momentum and energy budgets, and a unified theory for monsoon circulations remains an outstanding challenge (e.g., Biasutti et al., 2018; Hill, 2019). Common to both pictures is consideration of processes that can alter the distribution of MSE either in the boundary layer or in a vertically integrated sense, and this might provide a bridge to fill the gaps between these two frameworks.

The local, vertically integrated MSE budget has long been used to diagnose the distribution of tropical precipitation. Chou and Neelin (2001) and Chou and Neelin (2003) analysed the column integrated MSE budget in the South American and North American, Asian and African monsoon regions respectively. They identified three key processes governing the MSE distribution and thus determining the extent of tropical rainfall over land: advection of high or low MSE air into the region, soil-moisture feedbacks, and the interaction between the convergence zone and the Rossby wave induced subsidence, which occurs to the west of monsoon heating (the interactive Rodwell-Hoskins mechanism; see Rodwell and Hoskins (2001)). The column integrated MSE budget has also allowed investigation of the mechanisms determining the differing responses of models to intuitively similar forcing scenarios (e.g. D’Agostino, Bader, Bordoni, Ferreira, & Jungclaus, 2019), and the different responses of model variants to the same forcing (e.g Hill, Ming, Held, & Zhao, 2017; Hill, Ming, & Zhao, 2018).

Provided CQE holds, so that the tropical atmosphere is near a moist neutral state, the horizontal distribution of column integrated moist static energy will be strongly tied to the distribution of subcloud moist static energy. This may allow connections to be made between the constraints arising from the momentum and energetic frameworks, at least in the zonal mean. Precipitation appears to track subcloud MSE throughout the year whether CQE holds or not, and there is likely more to explore about how the boundary layer dynamics and large-scale overturning circulation interact (e.g., Adames & Wallace, 2017; Biasutti & Voigt, 2020; Chiang, Zebiak, & Cane, 2001; Duffy, O’Gorman, & Back, 2020).

4 Beyond the aquaplanet perspective

The theories that have emerged from the aquaplanet perspective have begun to prove useful in interpreting the climatology and variability of the tropical monsoon systems on both regional and global scales, particularly where their dynamics show similarities to that of the convergence zone in an aquaplanet. Synthesising idealized modeling work with observational and realistic modeling studies suggests a picture that is consistent with a view of the monsoons and ITCZs as local migrations of the tropical convergence zone:

1. In the zonal mean, the latitude of the convergence zone is set by energetic constraints (Fig. 10).
2. Locally and seasonally, the convergence zone location appears governed by the MSE distribution, which can be understood via the regional MSE budget (Fig. 12).
3. When the convergence zone is near the Equator (i.e., is an ITCZ), the overturning circulation is strongly influenced by extratropical eddies (Fig. 8a). Once it is far from the Equator, the cross-equatorial (winter) Hadley cell may approach an angular momentum conserving monsoon regime (Figs. 8b & 13).

4. Some regional variability in monsoon precipitation on interannual timescales (and perhaps subseasonal timescales) appears related to local variations in MSE which, where CQE applies, is connected to variations in the Hadley circulation.
5. Global variability in the latitude of the zonal mean convergence zone on interdecadal and longer timescales is driven by variations in the hemispheric energy budgets, with consequences for regional monsoon rainfall.

However, there are important influences on the regional monsoons and ITCZs that are not well accounted for by the above, in particular, the role of the continental configuration and geometry; these are discussed in Section 4.1. The interplay of the two convergence zone regimes with the transients that comprise the climatological precipitation are discussed in Section 4.2.

4.1 Asymmetries in the boundary conditions

Zonal asymmetries, such as land-sea contrast, orography, and the ocean circulation, introduce complications unaccounted for by the simple aquaplanet framework. Regional convergence that cannot be captured by the symmetric picture includes the Meiyu-Baiu frontal zone, the South Pacific Convergence Zone (SPCZ), the South Atlantic Convergence Zone (SACZ), and the South Indian Convergence Zone, which extends off the southeast coast of Southern Africa (Cook, 2000; Kodama, 1992). In particular, the East Asian and South American ‘monsoons’ require us to step beyond the perspective of angular momentum conserving monsoons and eddy-driven ITCZs. In addition, the seasonality of the Atlantic and Pacific ITCZs is strongly influenced by localized atmosphere-ocean feedbacks.

4.1.1 East Asia - a frontal monsoon

While the South Asian monsoon fits well with the theoretical paradigm emerging from idealized work, the circulation over East Asia behaves very differently. Here, wind reversal is predominantly meridional, and monsoon precipitation extends north into the subtropics (zone B in Fig. 11). Summer precipitation is concentrated in a zonal band at $\sim 35^\circ$ known as the Meiyu-Baiu front, which forms north of the high MSE air mass centered over South Asia and the Bay of Bengal (Ding & Chan, 2005, and references therein). This front migrates northward in steps over the summer season, as detailed in Section 3.1.

Unlike in tropical monsoon regions, in the Meiyu-Baiu region the net energy input into the atmospheric column is negative. Vertical upward motion and convection in the front (with associated energy export) require MSE convergence, which is provided by horizontal advection, with interactions between the Tibetan Plateau and the westerly jet playing a key role (Chen & Bordoni, 2014; Chiang, Kong, Wu, & Battisti, 2020; Molnar, Boos, & Battisti, 2010; Sampe & Xie, 2010). Comparing the monsoon season precipitation in this region in numerical experiments with and without the Tibetan Plateau indicates that, when the plateau is removed, precipitation is weakened and is no longer focused into the front (Chen & Bordoni, 2014; Chiang et al., 2020). Analysis of the MSE budget of these simulations suggests that the Plateau chiefly reinforces convergence into the Meiyu-Baiu region by strengthening the southerly stationary wave downstream. The westerly jet off the eastern flank of the Plateau additionally appears to act as an anchor for transient precipitating weather systems, focusing precipitation along the front (Molnar et al., 2010; Sampe & Xie, 2010).

Over the summer season, the East Asian Summer monsoon features two abrupt northward jumps of the precipitation, with three stationary periods (Ding & Chan, 2005). This intraseasonal evolution of the monsoon has also been suggested to relate to interactions between the Plateau and westerly jet, with the migration of westerlies from the south

of the Plateau to the north causing the first abrupt jump and the development of the Meiyu-Baiu front, and the northward migration of westerlies away from the Plateau causing the second (Kong & Chiang, 2020; Molnar et al., 2010). A series of recent papers has examined implications of this interaction for interpretation of changes to the East Asian summer monsoon over the paleoclimate record (Chiang et al., 2015) and the Holocene (Kong, Swenson, & Chiang, 2017), and for interannual variability of the East Asian summer monsoon (Chiang, Swenson, & Kong, 2017), with the hypothesis appearing able to explain all cases.

4.1.2 *South America - a zonal monsoon*

Similarities have been noted between the South American and East Asian monsoons; however, studies indicate that diabatic heating over land is most important in generating the upper-level monsoon anticyclone over South America (Lenters & Cook, 1997). One important difference is that the Andes form a narrow, meridionally oriented barrier from the tropics to subtropics. This acts to divert the easterly flow from the Atlantic to the south, concentrating it into the South American Low-Level Jet (Byerle & Paegle, 2002; Campetella & Vera, 2002) and inducing adiabatic ascent (Rodwell & Hoskins, 2001). In austral summer, the result is a zonally convergent mass flux of similar magnitude to the meridionally convergent component (Fig. 15), which extends the summer precipitation southward.

4.1.3 *The Atlantic and Pacific ITCZs and the North American monsoon*

Except for in the far western tropical Atlantic where the ITCZ dips slightly south of the Equator in March and April, the ITCZ is north of the Equator year-round in the Atlantic and Pacific (Fig. 9). One important factor for the off-equatorial location of the Atlantic ITCZ appears to be the land monsoon heating and the geometrical asymmetry in tropical Africa (Rodwell & Hoskins, 2001). Specifically, the austral summer monsoon in southern Africa forces subsidence to the west and causes a subtropical high to build over the southern subtropical Atlantic, increasing the southeasterly trade winds which act to cool the ocean by enhanced turbulent energy fluxes. Together, the subsidence and cool water suppress convection south of the Equator in the austral summer and fall. In addition, in boreal summer the west African monsoon forces a strong local Hadley circulation that also causes subsidence in the sub-tropical south Atlantic that supports the formation of stratus clouds which further cool the ocean during austral winter. Hence, the ITCZ does not transit into the Southern Hemisphere in austral summer.

The ITCZ in the eastern half of the Pacific is also north of the Equator year-round, and there is subsidence and cooling in the south-east subtropics. Modeling studies indicate that this descent can be attributed to several factors. SSTs over the western coast of South America are cooler due to coastal upwelling (e.g., Takahashi, 2005), but this cooling is largely confined to within 100km of the coast. In response to summer heating over the Amazon (Rodwell & Hoskins, 2001), air descends adiabatically over the south-east Pacific and flows equatorward. Simulations with and without the Andes suggest orography plays a dominant role. Throughout the year, the extratropical mid-level westerlies incident on the Andes are diverted equatorward, contributing to descent and evaporative cooling of the ocean by the dry subsiding air (e.g., Fig. 9; Rodwell & Hoskins, 2001; Takahashi & Battisti, 2007). The large-scale descent forced by the Andes causes an inversion to form that allows for the development of large-scale stratus clouds that cool the ocean for thousands of kilometers offshore (to the Date Line) and suppress convection over the eastern Pacific, particularly in austral summer. Combined with the atmosphere-ocean feedbacks described in the next paragraph, this descent causes the Pacific ITCZ to be located exceptionally far north of the Equator throughout the year (Maroon, Frier-

son, & Battisti, 2015; Takahashi & Battisti, 2007).¹⁰ The forcing by the Andes also causes a convergence zone to form that is located and oriented in a fashion similar to the observed SPCZ (Takahashi & Battisti, 2007). It may also partially account for the large seasonal contrast in precipitation in the North American monsoon, which involves an eastward extension of the Pacific ITCZ (Figs. 1 and 15). We note that three other hypotheses have been proposed for why the Pacific ITCZ is north of the Equator all year round (Chang & Philander, 1994; B. Wang & Wang, 1999; Xie & Philander, 1994). However, model experiments that serve as tests of these hypotheses (e.g., Battisti et al., 2014; Philander et al., 1996; Shi, Lohmann, Sidorenko, & Yang, 2020) do not support them. In contrast, the studies that we are aware of that include the Andes in atmospheric GCMs coupled to either a slab or dynamic ocean all produce a single ITCZ in the Northern Hemisphere that is in a very similar position and orientation to the observed ITCZ in the Pacific, and does not transit into the Southern Hemisphere at any time during the calendar year, consistent with observations.

Atmosphere-ocean feedbacks are important for the seasonal cycle in the latitude of the Atlantic and Pacific ITCZs. For example, with the onset of summer in the Northern Hemisphere, water in the Northern Hemisphere subtropics is warmed by increasing insolation (moving the ITCZ northward) which in turn warms the air in the boundary layer above and causes the sea level pressure (SLP) to drop (a hydrostatic response; see Lindzen & Nigam, 1987). The drop in SLP to the north of the Equator increases the cross-equatorial SLP gradient and thus increases the speed of the southeasterly trade winds south of (and along) the Equator, causing more air to converge into the ITCZ. South of the Equator, the strengthened trade winds increase evaporation and thus cools the ocean and the air in the boundary layer above. As a consequence, the meridional pressure gradient is further strengthened, the southerlies flowing across the Equator into the ITCZ are enhanced and the ITCZ is intensified and moves farther north. This positive feedback is known as the wind-evaporation feedback (Chang & Philander, 1994; Xie & Philander, 1994). Although ocean dynamics is not essential to explain the annual cycle in the latitude of the ITCZ (it is reproduced in slab ocean models coupled to atmospheric GCMs), it also plays a role (Mitchell & Wallace, 1992; B. Wang & Wang, 1999).

4.2 The role of transients

Even in an aquaplanet, tropical rainfall does not occur in a zonally uniform, continuously raining band. For simplicity, theoretical studies like those discussed in Section 2 tend to consider time and zonal averages and neglect transient activity except for its contribution to the momentum and energy budgets via eddy fluxes from the extratropics. While the climatological monsoons and ITCZs result from large-scale dynamics acting over a season and longer, the phenomena responsible for the accompanying precipitation are transient and generally of smaller spatial and temporal scales.

Many types of transient activity occur in the tropics. Wheeler and Kiladis (1999) produced wavenumber-frequency spectra of tropical outgoing longwave radiation (OLR), which is used as a proxy for deep convection, and showed that the spectral peaks that emerge are similar to wave modes of the shallow water equations on the beta plane (Matsuno, 1966), providing clear evidence for a strong influence of convectively coupled waves on tropical precipitation. Fig. 16 shows a Wheeler-Kiladis wavenumber-frequency spectrum for Northern Hemisphere summer (Kiladis et al., 2006). In this season, the spectrum of the symmetric component of tropical OLR exhibits three dominant peaks: eastward propagating Kelvin waves, westward propagating waves classed as tropical depres-

¹⁰ In the annual mean, the ITCZ in the Eastern Pacific is found at $\sim 10^\circ\text{N}$, whereas the maximum precipitation in the zonal average $\overline{\text{ITCZ}}$ is at $\sim 6^\circ\text{N}$.

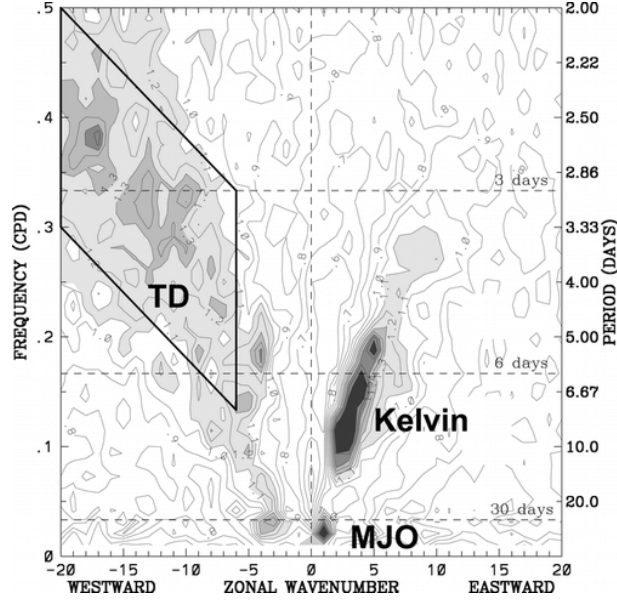


Figure 16. Wavenumber-frequency power spectrum of the symmetric component of OLR for June-August 1979-2003, averaged from 15°N to 15°S , plotted as the ratio of the raw OLR spectrum against a smooth red noise background (see Wheeler & Kiladis, 1999, for details). Contour interval is 0.1. Shading begins at 1.1, where the signal is statistically significant at approximately the 95% level. Peaks associated with the MJO, tropical depressions, and Kelvin waves are identified. From Kiladis et al. (2006). ©American Meteorological Society. Used with permission.

sions, and a low frequency eastward propagating signal associated with the Madden-Julian Oscillation (MJO).¹¹

Here we focus first on the synoptic phenomena that both contribute significantly to the seasonally averaged precipitation *and* owe their existence to the large-scale circulation regime discussed in previous sections. This is followed by a discussion of slower, larger-scale intraseasonal oscillations, such as the MJO, that interact with the monsoons and ITCZs, but do not appear as directly governed by the large-scale background flow as the smaller, shorter-lived transients.

4.2.1 Monsoon transients

Regional monsoon precipitation has long been observed to be organized by westward propagating synoptic-scale low-pressure systems, including monsoon depressions, observed in the Indian and Australian monsoon regions (e.g., Godbole, 1977; Mooley, 1973; D. Sikka, 1978), and African Easterly Waves, observed over West Africa (e.g., Burpee, 1974; Reed, Norquist, & Recker, 1977). Hurley and Boos (2015) produced a global climatology of monsoon lows. They found that the behavior over India, the western Pacific and northern Australia showed strong similarities, with a deep warm-over-cold core (e.g., Fig. 17a). A second class of systems was seen over West Africa and western Aus-

¹¹ A more detailed discussion of equatorial waves can be found in Roundy and Frank (2004), who develop a climatology, and in a review of the subject by Kiladis, Wheeler, Haertel, Straub, and Roundy (2009).

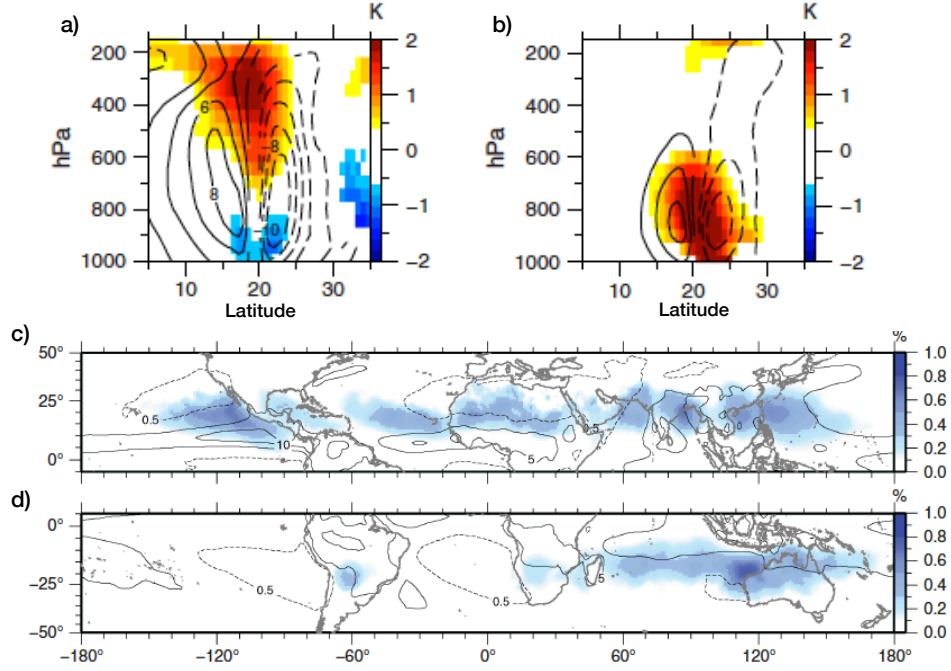


Figure 17. Northern Hemisphere summer (May-September) regional composites of monsoon depressions from ERA-Interim (1979-2012). Composite vertical sections through the storm center of potential temperature (K, shading) and zonal wind (ms^{-1} , contours) anomalies are shown for (a) India and (b) West Africa. Dashed contours are negative. Values are shaded or contoured where a t-test indicates significance at the 5% level. (c) and (d) show the fraction (shading) of total summer precipitation that can be attributed to monsoon lows and monsoon depressions in May-September and November-March respectively. Shading indicates the ratio of the summed precipitation within 500 km of all tracked lows and depressions to the total summer precipitation. Contours reflect the summer climatological precipitation rate. Dashed contours surround dry regions, where precipitation is on average less than 0.5 mm/day. Solid contours indicate wet regions, where precipitation is greater than 5mm/day (5 mm/day contour interval). Adapted from Figs. 9 and 12 of Hurley and Boos (2015). ©2014 Royal Meteorological Society. Used with permission.

tralia, with a shallower warm core (e.g., Fig. 17b). They estimated that organized low-pressure systems are responsible for at least 40% of precipitation in monsoon regions (Fig. 17c,d).

While many questions about their dynamics remain open, recent work indicates that monsoon depressions form over South Asia from moist barotropic instability due to the meridional shear of the monsoon trough, and are intensified by latent heating (Diaz & Boos, 2019a, 2019b). The background monsoonal flow hence is the source of instability for these propagating disturbances and can modulate their variability. For example, ENSO causes large-scale changes in the summertime environment that have a modest statistical effect on the strength of synoptic scale tropical depressions that propagate from the Bay of Bengal to the northwest over India (Hunt, Turner, Inness, Parker, & Levine, 2016), with La Niña (El Niño) conditions favoring tropical depressions with enhanced (weakened) precipitation.

Over Africa and the Atlantic, strong surface heating of the Sahara in summer forces a monsoon circulation that is barotropically and baroclinically unstable (Burpee, 1972; M.-L. C. Wu, Reale, Schubert, Suarez, & Thorncroft, 2012, and references therein), giving rise to African Easterly Waves. While the precise dynamics governing the amplification, propagation and variability of these waves remain unclear, the dynamics of these transients is clearly a result of the background large-scale monsoonal flow. Seasons with strong African Easterly Wave activity have been found to be associated with a strong upper-level easterly jet (Nicholson, Barcilon, Challa, & Baum, 2007) and an enhancement of other equatorial waves, specifically Rossby and westward-moving mixed Rossby-gravity wave modes (Y.-M. Cheng, Thorncroft, & Kiladis, 2019; Yang, Methven, Woolnough, Hodges, & Hoskins, 2018).

4.2.2 *Atlantic and Pacific ITCZ transients*

In the tropical Atlantic and Pacific ITCZs, precipitation is strongly modulated by easterly waves and other organized synoptic disturbances. African Easterly Waves borne from the monsoonal circulation over the Sahel propagate westward into the Atlantic Ocean and are the primary precursors of tropical cyclones in the Atlantic. The associated rainfall contributes to the summer precipitation in the Atlantic ITCZ. Easterly waves are also found in the tropical east and central Pacific, although the dynamics of these systems is different from their Atlantic counterparts. Many easterly waves in the Pacific are Mixed Rossby-Gravity waves: antisymmetric equatorially trapped waves with low pressure centered on 5–10° latitude (Kiladis et al., 2009; Matsuno, 1966). Friction acts to cause convergence in the low pressure centers and in the Northern Hemisphere this leads to moisture convergence and precipitation (Holton, Wallace, & Young, 1971; Liebmann & Hendon, 1990) (the low pressure center in the Southern Hemisphere does not feature precipitation because the water is cold and there is strong subsidence). Other convectively coupled equatorial waves that contribute to the ITCZ in the central Pacific include Kelvin waves (in which convection is not symmetric about the Equator) and inertio-gravity waves (Kiladis et al., 2009).

An upper bound on the contribution by transients to ITCZ precipitation can be estimated by assuming that all precipitation events lasting more than 24 hours are related to organized synoptic disturbances, in which case the fraction of the total precipitation in the Atlantic and Pacific ITCZs that is due to large-scale organized waves is about 40% (White, Battisti, & Skok, 2017). In addition to synoptic scale systems, about half of the total precipitation in these ITCZs is in the form of stratiform precipitation (Schumacher & Houze Jr, 2003), which is overwhelmingly in the form of long-lived mesoscale convective systems (Houze Jr, 2018).

4.2.3 *Other modes of tropical intraseasonal variability*

The above transients appear to be caused by instabilities associated with shear in the large-scale circulation, and can be interpreted as a product of the overturning regime and local boundary conditions. In addition to these convectively coupled waves generated by the large-scale environment, slower, larger-scale disturbances are also observed in the tropics. Fig. 16 shows intense activity associated with low wavenumbers and a period of 30–60 days. This has been shown to correspond to the MJO; a convectively coupled, large-scale equatorially trapped wave that propagates slowly eastward from the east coast of Africa to the western-central Pacific, whereafter it continues eastward as a Kelvin wave (Madden & Julian, 1971, 1972; C. Zhang, 2005, and references therein). The oscillation has strong influences on tropical rainfall, particularly in the Indo-Pacific region (see examples below), but the precise mechanism responsible remains a topic of extensive ongoing research.

The Madden Julian Oscillation and the tropical Indian Ocean ‘ITCZ’

Precipitation in the Indian Ocean sector in austral summer is found between 10°N and 15°S, but is concentrated slightly south of the Equator. It can be seen from Fig. 9 that, unlike the Atlantic and Pacific ITCZs, precipitation in the Indian Ocean is not organized into a narrow zonal band due to different physics than is described in Section 2.1.3 (the zonal asymmetry in SST is insufficient to drive a symmetrically unstable flow). Indeed, estimates show that between 30 and 40% of the annual precipitation in the Indian Ocean and Maritime continent (10°N and 10°S, 70°E and 150°E) is associated with the MJO (Kerns & Chen, 2020).

Intraseasonal variability in the Indo-Pacific

In the Indo-Pacific region, the MJO features trailing Rossby waves with enhanced shear zones that angle polewards and westwards from the precipitation center near the Equator and support precipitation. Hence, along a fixed longitude, bands of precipitation appear to propagate poleward from the Equator to about 20°N over India as the MJO propagates eastward over the maritime continent (Hartmann & Michelsen, 1989).

In boreal summer, in addition to the MJO, the climate in this region appears to be modulated by propagating ‘Boreal Summer Intraseasonal Oscillations’ (BSISO), observed to have dominant timescales of 10-20 and 30-60 days, and to propagate northward over the continent (Annamalai & Slingo, 2001; Goswami & Ajaya Mohan, 2001; Hartmann & Michelsen, 1989; Lee et al., 2013). These oscillations modulate the active and break phases of the Indian monsoon, with the tropical convergence zone and associated Hadley circulation oscillating between an off-equatorial ‘monsoon’ location, and a near equatorial ‘ITCZ’ location (e.g., Annamalai & Slingo, 2001; Goswami & Ajaya Mohan, 2001; D. R. Sikka & Gadgil, 1980). Like the MJO, the propagation mechanism and precise drivers of the BSISOs remain unclear, and are the subject of ongoing research. Some authors argue that the BSISOs are distinct from the MJO (e.g. Lee et al., 2013; B. Wang & Xie, 1997), while others identify them as associated with the MJO (e.g., Hartmann & Michelsen, 1989; Jiang, Adames, Zhao, Waliser, & Maloney, 2018).

5 Conclusions and outlook

In this article, we have reviewed the theory of monsoons that has resulted in large part from idealized models and discussed the behavior of Earth’s monsoons in light of the theory. While the regional monsoons have a diverse range of individual features, they also have much in common, including enhancement of cross-equatorial and westerly flow in the summer season, rapid onset, and development in an off-equatorial direction. In addition, regional monsoons often covary as components of a global monsoon, under both changes to orbital forcing and internal variations. The theoretical considerations outlined in Section 2 are starting to provide explanations for these behaviors, as presented in Section 3, but many open questions remain in how to connect theoretical ideas to observations (Section 4). We conclude the review by first discussing these successes and challenges, before proposing more specific directions for future research.

5.1 Successes

Insight from theory has caused a shift in the understanding of monsoon dynamics – from that of primarily land-sea contrast driven, sea-breeze-like circulations, to localized variations of the tropical overturning circulation and associated convergence zones, strongly governed by the momentum and energy budgets.

The momentum budget, Eq. 4, indicates three classes of solution for the Hadley circulation: a ‘radiative-convective equilibrium’ regime, $\bar{v} = \bar{\omega} = 0$; an ‘angular momentum conserving’ regime, in which the Rossby number Ro approaches 1 and eddies

Table 2. Suggested classifications of tropical and subtropical convergence zones. Regions are defined as in Fig. 1 & 14. Wind reversal is assessed based on Fig. 1, and the presence of multiple preferred latitudes for rainfall is based on Fig. 14. P_{0-10° , P_{10-25° and P_{25-35° are the area-weighted fractions of precipitation (mm/day) falling in each monsoon/ITCZ region between the indicated latitudes (bounded in longitude by the boxes in Fig. 1), relative to the total evaluated from $0-35^\circ$. Conclusions are not sensitive to small variations in the latitude bounds used; the use of 10° rather than 7° (cf. Geen et al., 2019) here is motivated by discussion in Section 3.2.1. $\phi(\theta_{eb})$ and $\phi(P_{max})$ are the latitudes of maximum season-mean subcloud equivalent potential temperature and precipitation respectively. Precipitation fractions and maxima are calculated using GPCP data and θ_{eb} is calculated using JRA-55 reanalysis, with 1979–2016 used in both cases. Season means over June–Sept are used for Northern Hemisphere monsoons, Dec–March for Southern Hemisphere monsoons, and all months for the Atlantic and Pacific ITCZs.

System	Type	Wind reversal?	Multiple preferred latitudes?	P_{0-10° (%)	P_{10-25° (%)	P_{25-35° (%)	$\phi(\theta_{eb})$ ($^\circ$)	$\phi(P_{max})$ ($^\circ$)
S. Asia	Monsoon	yes	yes	24	57	19	25	21.25
Australia	Hybrid	yes	yes	48	44	8	-7.5	-6.25
W. Africa	Hybrid	yes	yes	58	40	2	12.5	8.75
S. Africa	Monsoon	yes	yes	33	54	13	-12.5	-13.75
N. America	ITCZ extension	no	no	32	55	13	10.	8.75
S. America	Neither	no	yes	41	43	16	-12.5	-6.25
Atlantic	ITCZ	no	no	69	19	12	2.5	6.25
E. Pacific	ITCZ	no	no	50	35	15	7.5	8.75

have a negligible effect; and an ‘eddy-driven’ regime, where Ro is much less than 1 and eddies strongly influence the overturning circulation. Our understanding of monsoon dynamics has been greatly advanced by considering the transitions between these regimes, and the controls on the latitude of the ascending branch of the circulation.

Constraints on the zonal mean convergence zone latitude have been identified by considering the energetics of the circulation, in addition to the momentum budget. If the atmosphere is in CQE then, for an angular momentum conserving overturning circulation, the convergence zone is expected to lie just equatorward of the peak in sub-cloud moist static energy (see Privé & Plumb, 2007a, 2007b, and Section 2.1). The sub-cloud distribution of MSE therefore strongly constrains the circulation.¹² A related energetic constraint is obtained from considering the vertically integrated MSE budget (Eq. 10). The latitude of the EFE has been found to be approximately colocated with the convergence zone latitude, allowing the zonal mean convergence zone location to be related to the meridional cross-equatorial energy flux and net energy input at the Equator (e.g., Bischoff & Schneider, 2016; Kang, 2020; Kang et al., 2018).

The latitude of the convergence zone is also strongly related to the dynamics that govern the Hadley circulation. In aquaplanet simulations when the convergence zone is on or near the Equator the circulation is more eddy driven (i.e., an ITCZ), while when the convergence zone is far from the Equator the circulation is near angular momentum conserving and the strength of the circulation is determined mainly by energetics (Bordoni & Schneider, 2008, 2010; Schneider & Bordoni, 2008). These ‘ITCZ’ and ‘monsoon’ regimes are illustrated schematically in Fig. 8a and b respectively. When the slab ocean in these aquaplanets is thin, and hence the surface thermal inertia low, similar to land, a fast transition between these two regimes is observed over the course of the seasonal cycle, with the zonal mean convergence zone rapidly moving away from the Equator into the summer hemisphere at the start of the summer season. This fast transition is mediated by two feedbacks. Firstly, as the convergence zone shifts off the Equator and the Hadley circulation becomes cross equatorial, the lower branch of the Hadley cell advects cooler, drier air up the meridional MSE gradient. Combined with the continued diabatic warming of the summer hemisphere by the insolation, this has the effect of pushing the MSE peak poleward and so shifting the convergence zone farther off the Equator. Secondly, as a result of angular momentum conservation, the equatorward upper-level meridional flow gives rise to upper-level easterlies. These easterlies suppress propagation of extratropical eddies into the low latitudes (Charney & Drazin, 1961) and help to kick the Hadley cell into the angular momentum conserving regime, so that the meridional overturning is strongly responsive to the thermal forcing and strengthens and broadens further.

Recent results suggest that in an aquaplanet, the transition between an eddy-driven and angular momentum conserving Hadley circulation occurs when the convergence zone migrates beyond $\sim 7^\circ$, regardless of slab ocean characteristics (Geen et al., 2019). In this review, we have argued that the former regime is relevant to the dynamics of the observed ITCZs, while the latter is appropriate for understanding the monsoon circulations. Another recent strand of research has explored the maximum limits on the migrations of the convergence zone away from the Equator: in aquaplanets, the convergence zone does not migrate more than 25° away from the equator, even when the MSE maximum is at the poles (Faulk et al., 2017). Current work (Hill et al., 2019; Singh, 2019) is exploring this poleward limit of monsoons using constraints relating the Hadley circulation regime to the curvature of the subcloud equivalent potential temperature.

¹² Although it is important to remember that the MSE distribution is itself set partially by the circulation, and interactions between the MSE and circulation must be considered.

Analysis of observations has demonstrated that the South Asian, Australian and African monsoons show behavior similar to that described by the above theoretical work. In these monsoons, the peak precipitation is located just equatorward of the peak in sub-cloud MSE (Nie et al., 2010) and the convergence zones migrate in line with the EFE (Adam et al., 2016a; Boos & Korty, 2016). In monsoons where the ascending branch migrates far from the Equator, such as the South Asian and Southern African monsoons, the summertime overturning circulation becomes aligned with angular momentum contours, suggesting a strongly thermally driven cross-equatorial flow regime (e.g., Bordoni & Schneider, 2008; J. M. Walker & Bordoni, 2016). In addition, Figs. 14 & 15 suggest the threshold distinguishing an eddy-driven (‘ITCZ’) from an angular momentum conserving (‘monsoon’) overturning regime is $\sim 10^\circ$ latitude, which is qualitatively similar to that seen in aquaplanet simulations. Consistent with modeling results in which rotation rate is varied, the observed overturning circulations are confined to be within $\sim 25^\circ$ of the Equator (Faulk et al., 2017).

Based on the aquaplanet frameworks, we suggest the regional systems might be classified into either an ITCZ or monsoon circulation regime based on the following criteria: the latitude at which precipitation falls; the occurrence of wind reversal; and the presence of multiple preferred latitudes for precipitation, which gives some indication of where abrupt onset of precipitation might occur when the convergence zone shifts between these locations. With these criteria in mind, Table 2 summarizes which systems the authors feel fit the dynamics-based categories of monsoon, ITCZ or a hybrid with characteristics of both regimes. In South America and East Asia orography results in dynamics that does not seem to fit these descriptions. Note that the East Asian region encompasses both the the tropical South China Sea monsoon and the orographically controlled Meiyu-Baiu front (Section 3.1), and so is not included in the table.

Awareness of these mechanisms can help motivate work investigating sources of interannual variability, and the response to external forcings, with one clear goal being a better mechanistic understanding of model projections forced by future warming scenarios. On this front, some success has already been achieved. For example, interannual variability in monsoon precipitation has been found to be correlated to variability in sub-cloud MSE (Hurley & Boos, 2013). Migrations of the zonal mean convergence zone under historical forcings have been examined in relation to migrations of the EFE (Donohoe et al., 2013). The weak changes to the Asian monsoon in simulations of future climate appear to be explained by opposing responses to increased CO_2 levels and surface warming (Shaw & Voigt, 2015). Further exploration of the observations, informed by theory, could prove fruitful for improved understanding of model biases, or for identifying sources of seasonal predictability.

5.2 Challenges

The theoretical frameworks discussed in Section 2 each have significant known limitations. The EFE framework appears most directly predictive. However, even in an aquaplanet, uncertainties in changes in GMS and column fluxes, for example due to cloud feedbacks, limit the predictive power of energetic diagnostics, such as the EFE and the cross-equatorial energy transport, to the understanding of tropical and subtropical precipitation changes (e.g., Biasutti & Voigt, 2020). The momentum framework is conceptually useful for understanding seasonal changes in the Hadley cell dynamics (Bordoni & Schneider, 2008; Geen et al., 2018), but implications for the response of monsoons and ITCZs to variability on different time scales remain to be explored.

Despite these limitations, constraints on the zonal and time mean convergence zone and overturning circulation are beginning to emerge from theory and have now been successfully applied to aquaplanets and to some features of the observations. This represents a significant step in our understanding of the tropical circulation. However, asym-

metries that arise from land-sea contrast and orography introduce a zoo of additional complications that these simple theories do not account for, and some care must therefore be taken in applying aquaplanet theories to reality. For example, while the monsoon circulation in an aquaplanet is characterized by an angular momentum conserving Hadley circulation, stationary waves can be important when zonal asymmetries are included in the boundary conditions (Shaw, 2014). However, as we show here in Fig. 13, in individual monsoon sectors (South Asia, Africa and Australia) advection of momentum by the mean circulation appears to be non-negligible, suggesting that even in the presence of zonal asymmetries some monsoons do approach an angular momentum conserving regime.

As discussed in Section 4, the pattern of precipitation in the South American monsoon and the intensity of the East Asian monsoon in particular are strongly influenced by orography. The interaction of the westerly jet with the orography of Tibet generates a stationary wave downstream over East Asia that gives rise to the Meiyu-Baiu front and governs the duration of the stages of the East Asian summer ‘monsoon’. In South America, the Andes divert the tropical easterly and subtropical westerly flow, resulting in strong equatorward descending flow to the west of the mountains, and poleward ascending flow to the east. In austral summer, the South American Low-Level jet develops to the east of the Andes and extends the South American monsoon flow southward. This results in precipitation that is displaced far from the Equator, but without the formation of an angular momentum conserving Hadley cell of the kind seen in aquaplanets. The descending flow to the west of the Andes suppresses precipitation year-round off the coast of South and Central America, over the East Pacific and helps to push the convergence zone north of the Equator year round. Overall, we conclude that aquaplanet theories do not appear applicable to the systems seen in the Americas or East Asia.

Last, transients make a non-negligible contribution to precipitation in the regional monsoons and ITCZs. These phenomena are not accounted for in the theoretical framework reviewed in Section 2. Whether they feedback onto the large-scale circulation, or are simply organized by it, remains to be determined.

5.3 Outlook

Based on the challenges above we suggest the following focus areas for future research, including both idealized modeling and study of the new experiments available in the Coupled Model Intercomparison Project Phase 6 (CMIP6).

5.3.1 *Address limitations of theory and connect frameworks within aquaplanets*

The issues discussed above limit the application of theory to problems such as climate change. One focus of future idealized modeling work should be to try to resolve known issues with theory that arise even in aquaplanets. For example TRACMIP has proved useful in exploring elements of theory that do and do not make successful predictions across aquaplanet simulations with different climate models (Biasutti & Voigt, 2020; Harrop, Lu, & Leung, 2019; Voigt et al., 2016). Radiation-locking simulations could tease apart the importance of cloud feedbacks (Byrne & Zanna, 2020, in press). The EFE and momentum frameworks both consider the large-scale overturning circulation, but are generally applied separately. A first step to connecting these is to examine both the MSE and momentum budgets in parallel when studying tropical convergence zones. It would also be interesting to examine whether dynamics of the overturning circulation cell has implications for the cell’s response to forcings. For example, might the underlying dynamics of the cell determine the strength of the precipitation response to forcing? Will the response to forcing a system with more ITCZ-like characteristics, e.g., the

Australian or West African monsoons, be different to that of the South Asian or Southern African monsoons?

5.3.2 *Build beyond the aquaplanets*

While aquaplanets are a valuable tool for studying the circulation in a simple context, it is clear from Section 4 that the application of theory developed in these settings is limited. New terms enter both the momentum and energy budgets when zonal asymmetries are included, and zonal mean changes in inter-hemispheric energy imbalances can be achieved via regional changes.

Hierarchical modeling work, where complexity is introduced in a progressive way, is a clear path forward to begin to specialize theory to individual monsoon systems, as well as identifying commonalities between systems. Initial steps on this hierarchy are already being taken, by introducing heating (Shaw, 2014) or continents into idealized models (e.g., TRACMIP, and Chiang et al., 2020; Geen et al., 2018; Hui & Bordoni, submitted.; W. Zhou & Xie, 2018), or removing orography from more complete models (Baldwin, Vecchi, & Bordoni, 2019; Boos & Kuang, 2010; Wei & Bordoni, 2016). Idealized modeling frameworks such as Isca (Vallis et al., 2018) have been developed with such problems in mind, allowing boundary conditions (e.g., land and orography) and physical parameterizations (e.g., convection, radiation and land hydrology) to be trivially modified. The Global Monsoon Model Intercomparison Project (GMMIP) is ongoing under CMIP6, and includes plans for simulations in which features of orography are removed and/or surface fluxes are modified (T. Zhou et al., 2016).

In terms of developing theory further, the additional terms entering the budgets make this challenging, though some regional approximations to the EFE have been derived (Adam et al., 2016a; Boos & Korty, 2016). The definition of the local Hadley and Walker cells are useful for visualising the regional characteristics of the overturning circulation (Schwendike et al., 2014). Decomposition of the momentum and energy budgets into rotational and divergent components in this way, and consideration of the both zonal and meridional balances, may help in extending theoretical frameworks further, if simple balances can be identified. It is worth noting that these budgets are difficult to compute and close offline; we recommend that where possible all terms be computed online and saved as output.

5.3.3 *Investigate the dynamics of variability and transients*

As well as exploring how theory can be extended to regional scales, we suggest looking at possible connections to shorter temporal scales. For example, on what timescales does CQE cease to hold? Can changes in the leading order momentum balance explain variability on shorter timescales? Can theory provide new insights into the processes responsible for variability on interdecadal, interannual or intraseasonal timescales? Does the nature of the transient convective systems in which rain falls influence the large-scale circulation?

In some cases, theory of monsoon circulations might prove to be commensurate with observations that suggest a more causal role for the transients. For example, as discussed in Section 4, monsoon onset over South Asia and the South China Sea has been suggested to relate to the arrival of the moist phase of a transient Intraseasonal Oscillation (ISO), with active and break phases throughout the season then arising due to further ISOs and shifts in the convergence zone (e.g., Lee et al., 2013; Webster et al., 1998). Aquaplanet based modeling work has instead led to development of a zonal- and climatological-mean view of monsoon onset as a regime change of the Hadley circulation (see Section 2.1 and Bordoni & Schneider, 2008; Schneider & Bordoni, 2008). These ideas appear tantalizingly reconcilable; for example the arrival of an ISO might act as the trigger for the regime

change of the circulation, or perhaps active and break phases of the Indian monsoon might be connected to intraseasonal changes in the strength of the Hadley cell. The MSE budget has been used to investigate the propagation of the MJO (Andersen & Kuang, 2012; Jiang et al., 2018; Sobel & Maloney, 2013), and may provide a way to bridge these two perspectives.

On interannual timescales, enhanced upper-level tropical easterlies accompany more intense precipitation over West Africa via enhancement of upper-level divergence and meridional overturning (Nicholson, 2009). This variability in the meridional overturning again occurs in a sense consistent with the aquaplanet regimes, although in this case the circulation has significant zonal asymmetry. Modulation of the monsoons by anomalous upper-level flow may help in understanding teleconnections influencing regional monsoons, although more work is needed to explore the mechanisms involved and to ascertain the direction of causality between anomalous upper- and lower-level circulations and precipitation.

5.3.4 *Look at how theory can be tested in CMIP6*

Perhaps the greatest challenge for theory and modeling is to determine how the monsoon systems will change in future climates. The current consensus from models is that the precipitation in the global monsoon is likely to increase under anthropogenic forcings, though the monsoon circulation is likely to weaken (Christensen et al., 2013). However, there is a significant spread in model projections (e.g., Seth et al., 2019, and references therein), and models show varying degrees of skill in capturing the present-day climatology of the monsoon and its variability (e.g. Jourdain et al., 2013; Roehrig, Bouniol, Guichard, Hourdin, & Redelsperger, 2013; Sperber et al., 2013). Future changes in regional tropical precipitation are strongly influenced by changes in the circulation, which are not well constrained (Chadwick, Boutle, & Martin, 2013).

As discussed in Section 3.2, future predictability depends on direct and indirect responses to radiative forcing, which may oppose one another (Shaw & Voigt, 2015). Phase 3 of the Cloud Feedback Model Intercomparison Project is built into CMIP6 (Webb et al., 2017). This includes both simulations studying the radiative effects of clouds, and also ‘timeslice’ simulations in which models are forced with SSTs from the climatology of either pre-industrial control or abrupt-4xCO₂ runs. In a hierarchy of simulations, physics schemes for radiation, sea ice and plant physiology are progressively permitted to respond to CO₂ forcing, building up the components of the full model response (cf. Chadwick, Douville, & Skinner, 2017). Applying theoretical ideas in these simulations may help to identify how the dynamics of the monsoons is influenced by the various forcings and feedbacks that build up the response to climate change. Although current theories for the ITCZ and monsoon circulations are more diagnostic than predictive, developing and applying these to understanding model bias and climate changes is a clear priority.

Glossary

AMIP Atmospheric Model Intercomparison Project. A project comparing the behaviors of atmospheric general circulation models forced by realistic sea surface temperatures and sea ice.

BSISO Boreal Summer Intraseasonal Oscillation. Describes the dominant modes of tropical intraseasonal variability over Asia during boreal summer.

CMIP6 The Coupled Model Intercomparison Project, Phase 6. An intercomparison of the results of state-of-the-art climate models under a range of consistent experimental protocols.

CQE Convective Quasi-Equilibrium. A theoretical framework for the tropical atmosphere that assumes the atmospheric lapse rate is maintained close to a moist adiabat

- 1492 due to the occurrence of frequent, intense moist convection. See discussion in Sec-
 1493 tion 2.1.
- 1494 **Dansgaard–Oeschger (D–O) Cycles** Millennial-scale oscillations during the last glacial
 1495 period that are nearly global in extent and feature an abrupt transition.
- 1496 **Earth System model** A comprehensive model of the Earth System, simulating the
 1497 fluid motions and thermodynamics of the atmosphere and ocean, as well as inter-
 1498 actions with ice, the land surface and vegetation, and ocean biogeochemistry.
- 1499 **EFE** Energy Flux Equator. The latitude at which the vertically integrated MSE flux
 1500 by the atmospheric circulation is zero.
- 1501 **EFPM** Energy Flux Prime Meridian. Defined as the longitudes at which the zonally
 1502 divergent column integrated MSE flux vanishes and has positive zonal gradient.
- 1503 **ENSO** The El Niño–Southern Oscillation. A recurring climate pattern involving changes
 1504 to the temperature of the waters in the Pacific Ocean. El Niño (La Niña) phases
 1505 are associated with warmer (cooler) than usual SSTs in the central and eastern
 1506 tropical Pacific Ocean.
- 1507 **GCM** Global Circulation Model. A numerical model for the circulation of the atmo-
 1508 sphere and/or ocean.
- 1509 **GMS** Gross Moist Stability. A measure of how efficiently the large scale circulation ex-
 1510 ports MSE. Various definitions are used in the literature, here we define GMS by
 1511 Eq. 14.
- 1512 **Heinrich event** A natural phenomenon featuring the collapse of Northern Hemisphere
 1513 ice shelves and consequently the release of large numbers of icebergs.
- 1514 **Idealized model** A model in which only some elements of the Earth System are in-
 1515 cluded to allow testing of theories in a more conceptually simple and computa-
 1516 tionally affordable framework.
- 1517 **ISO** Intra-seasonal Oscillation
- 1518 **ITCZ** Intertropical Convergence Zone. The location where the trade winds of the North-
 1519 ern and Southern Hemispheres converge, coincident with the ascending branch of
 1520 the Hadley circulation. Precipitation and the strength of the overturning circula-
 1521 tion are driven primarily by eddy momentum fluxes and precipitation is located
 1522 with $\sim 10^\circ$ of the Equator.
- 1523 **ITCZ** The zonal and annual mean convergence zone, which is located at 1.7°N if es-
 1524 timated by the precipitation centroid; (Donohoe et al., 2013), or $\sim 6^\circ\text{N}$ if judged
 1525 by the precipitation maximum; e.g., (Gruber et al., 2000).
- 1526 **Monsoon** The rainy summer season of a tropical or subtropical region, in which pre-
 1527 cipitation associated with the convergence zone extends far from the Equator, the
 1528 lower-level prevailing wind changes direction or strength, and the overturning cir-
 1529 culation approaches the angular momentum conserving (eddy-less) limit. Precip-
 1530 itation and the strength of the overturning circulation are primarily controlled by
 1531 the energy budget.
- 1532 **MJO** Madden-Julian Oscillation
- 1533 **MSE** Moist static energy, defined in Eq. 9.
- 1534 **RCE** Radiative-convective equilibrium. Describes the balance between the radiative cool-
 1535 ing of the atmosphere and the heating via latent heat release resulting from con-
 1536 vection.
- 1537 **Sea breeze** A wind that blows from a large body of water onto a landmass due to dif-
 1538 ferences in surface temperature, and consequently air pressure, between the land
 1539 and water.
- 1540 **SACZ** South Atlantic Convergence Zone. The band of convergence observed extend-
 1541 ing across southeast Brazil and over the southwest Atlantic, e.g., Fig. 1e.
- 1542 **SPCZ** South Pacific Convergence Zone. The band convergence observed over the south-
 1543 west Pacific, e.g., Fig. 1e.
- 1544 **SST** Sea Surface Temperature

Acknowledgments

RG was supported by the UK-China Research and Innovation Partnership Fund, through the Met Office Climate Science for Service Partnership (CSSP) China, as part of the Newton Fund. SB and KLH acknowledge support from the Caltech Terrestrial Hazard Observation and Reporting (THOR) center and the Caltech GPS Discovery Fund. DSB was funded by the Tamaki Foundation. Datasets for this research are available in these in-text data citation references: Japan Meteorological Agency/Japan (2013); Mesoscale Atmospheric Processes Branch/Laboratory for Atmospheres/Earth Sciences Division/Science and Exploration Directorate/Goddard Space Flight Center/NASA, and Earth System Science Interdisciplinary Center/University of Maryland (2018); Huffman, G. J. and D. T. Bolvin and R. F. Adler (2016). We thank Dennis Hartmann, John Chiang, Mike Wallace, Fabio Bellacanzone and three anonymous reviewers for their thoughtful and helpful comments on the manuscript.

References

- Adam, O., Bischoff, T., & Schneider, T. (2016a). Seasonal and interannual variations of the energy flux equator and ITCZ. Part II: Zonally varying shifts of the ITCZ. *Journal of Climate*, 29(20), 7281–7293. doi: 10.1175/JCLI-D-15-0710.1
- Adam, O., Bischoff, T., & Schneider, T. (2016b). Seasonal and interannual variations of the energy flux equator and ITCZ. Part I: Zonally averaged ITCZ position. *Journal of Climate*, 29(9), 3219–3230. doi: 10.1175/JCLI-D-15-0512.1
- Adames, Á. F., & Wallace, J. M. (2017). On the tropical atmospheric signature of El Niño. *Journal of the Atmospheric Sciences*, 74(6), 1923–1939.
- Adams, D. K., & Comrie, A. C. (1997). The North American Monsoon. *Bulletin of the American Meteorological Society*, 78(10), 2197–2214. doi: 10.1175/1520-0477(1997)078<2197:TNAM>2.0.CO;2
- An, Z., Guoxiong, W., Jianping, L., Youbin, S., Yimin, L., Weijian, Z., . . . Juan, F. (2015). Global Monsoon Dynamics and Climate Change. *Annual Review of Earth and Planetary Sciences*, 43(1), 29–77. doi: 10.1146/annurev-earth-060313-054623
- Ananthakrishnan, R., & Soman, M. K. (1988). The Onset of the Southwest Monsoon over Kerala: 1901–1980. *Journal of Climatology*, 8, 283–296. doi: 10.1002/joc.3370080305
- Andersen, J. A., & Kuang, Z. (2012). Moist Static Energy Budget of MJO-like Disturbances in the Atmosphere of a Zonally Symmetric Aquaplanet. *Journal of Climate*, 25(8), 2782–2804. Retrieved from <https://doi.org/10.1175/JCLI-D-11-00168.1> doi: 10.1175/JCLI-D-11-00168.1
- Annamalai, H., & Slingo, J. M. (2001). Active/break cycles: Diagnosis of the intraseasonal variability of the Asian Summer Monsoon. *Climate Dynamics*, 18(1), 85–102. Retrieved from <https://doi.org/10.1007/s003820100161> doi: 10.1007/s003820100161
- Arakawa, A., & Schubert, W. H. (1974). Interaction of a Cumulus Cloud Ensemble with the Large-Scale Environment, Part I. *J. Atmos. Sci.*, 31, 674–701. doi: 10.1175/1520-0469(1974)031%3C0674:IOACCE%3E2.0.CO;2
- Arbuszewski, J. A., Demenocal, P. B., Cléroux, C., Bradtmiller, L., & Mix, A. (2013). Meridional shifts of the Atlantic Intertropical Convergence Zone since the Last Glacial Maximum. *Nature Geoscience*, 6(11), 959–962. doi: 10.1038/ngeo1961
- Atwood, A. R., Donohoe, A., Battisti, D. S., Liu, X., & Pausata, F. S. R. (2020). Robust longitudinally-variable responses of the ITCZ to a myriad of climate forcings. *Geophys. Res. Lett.*, in press.
- Baldwin, J. W., Vecchi, G. A., & Bordon, S. (2019). The direct and ocean-mediated influence of Asian orography on tropical precipitation and cyclones. *Climate*

- Dynamics*, 1–20. Retrieved from <http://dx.doi.org/10.1007/s00382-019-04615-5> <http://link.springer.com/10.1007/s00382-019-04615-5> doi: 10.1007/s00382-019-04615-5
- Barlow, M., Nigam, S., & Berbery, E. H. (1998). Evolution of the North American Monsoon System. *Journal of Climate*, 11(9), 2238–2257. doi: 10.1175/1520-0442(1998)011<2238:EOTNAM>2.0.CO;2
- Battisti, D. S., Ding, Q., & Roe, G. H. (2014). Coherent pan-Asian climatic and isotopic response to orbital forcing of tropical insolation. *Journal of Geophysical Research*, 119(21), 11,997–12,020. doi: 10.1002/2014JD021960
- Becker, E., Schmitz, G., & Geprags, R. (1997). The feedback of midlatitude waves onto the Hadley cell in a simple general circulation model. *Tellus A*, 49, 182–199.
- Berger, A. L. (1978). Long-Term Variations of Caloric Insolation Resulting from the Earth’s Orbital Elements. *Quaternary Research*, 9(2), 139–167. doi: 10.1016/0033-5894(78)90064-9
- Biasutti, M., & Voigt, A. (2020). Seasonal and CO₂-Induced Shifts of the ITCZ: Testing Energetic Controls in Idealized Simulations with Comprehensive Models. *Journal of Climate*, 33(7), 2853–2870.
- Biasutti, M., Voigt, A., Boos, W. R., Braconnot, P., Hargreaves, J. C., Harrison, S. P., ... Xie, S.-P. (2018). Global energetics and local physics as drivers of past, present and future monsoons. *Nature Geoscience*, 11(6), 392–400. doi: 10.1038/s41561-018-0137-1
- Bischoff, T., & Schneider, T. (2014). Energetic constraints on the position of the Intertropical Convergence Zone. *Journal of Climate*, 27(13), 4937–4951. doi: 10.1175/JCLI-D-13-00650.1
- Bischoff, T., & Schneider, T. (2016). The equatorial energy balance, ITCZ position, and double-ITCZ bifurcations. *Journal of Climate*, 29(8), 2997–3013. doi: 10.1175/JCLI-D-15-0328.1
- Boos, W. R., & Korty, R. L. (2016). Regional energy budget control of the Intertropical Convergence Zone and application to mid-Holocene rainfall. *Nature Geoscience*, 9(12), 892–897. doi: 10.1038/ngeo2833
- Boos, W. R., & Kuang, Z. (2010). Dominant control of the South Asian monsoon by orographic insulation versus plateau heating. *Nature*, 463(7278), 218–222. doi: 10.1038/nature08707
- Boos, W. R., & Kuang, Z. (2013). Sensitivity of the South Asian monsoon to elevated and non-elevated heating. *Scientific Reports*, 3, 3–6. doi: 10.1038/srep01192
- Bordoni, S., Ciesielski, P. E., Johnson, R. H., McNoldy, B. D., & Stevens, B. (2004). The low-level circulation of the North American Monsoon as revealed by QuikSCAT. *Geophysical Research Letters*, 31, L10109. doi: 10.1029/2004GL020009
- Bordoni, S., & Schneider, T. (2008). Monsoons as eddy-mediated regime transitions of the tropical overturning circulation. *Nature Geoscience*, 1(8), 515–519. doi: 10.1038/ngeo248
- Bordoni, S., & Schneider, T. (2010). Regime Transitions of Steady and Time-Dependent Hadley Circulations: Comparison of Axisymmetric and Eddy-Permitting Simulations. *Journal of the Atmospheric Sciences*, 67(5), 1643–1654. doi: 10.1175/2009JAS3294.1
- Broccoli, A. J., Dahl, K. A., & Stouffer, R. J. (2006). Response of the ITCZ to Northern Hemisphere cooling. *Geophysical Research Letters*, 33(1), 1–4. doi: 10.1029/2005GL024546
- Burpee, R. W. (1972). The origin and structure of easterly waves in the lower troposphere of North Africa. *Journal of the Atmospheric Sciences*, 29(1), 77–90.
- Burpee, R. W. (1974). Characteristics of North African easterly waves during the summers of 1968 and 1969. *Journal of the Atmospheric Sciences*, 31(6), 1556–

- 1570.
- 1653 Byerle, L. A., & Paegle, J. (2002). Description of the Seasonal Cycle of Low-Level
1654 Flows Flanking the Andes and their Interannual Variability. *Meteorologica*, 27,
1655 71–88.
- 1656 Byrne, M. P., & Zanna, L. (2020, in press). Radiative effects of clouds and water va-
1657 por on an axisymmetric monsoon. *Journal of Climate*.
- 1658 Campetella, C. M., & Vera, C. S. (2002). The influence of the Andes mountains on
1659 the South American low-level flow. *Geophysical Research Letters*, 29(17), 7:1–
1660 4. doi: 10.1029/2002gl015451
- 1661 Chadwick, R., Boutle, I., & Martin, G. (2013). Spatial patterns of precipitation
1662 change in CMIP5: Why the rich do not get richer in the tropics. *Journal of*
1663 *Climate*, 26(11), 3803–3822.
- 1664 Chadwick, R., Douville, H., & Skinner, C. B. (2017). Timeslice experiments for
1665 understanding regional climate projections: applications to the tropical hydro-
1666 logical cycle and European winter circulation. *Climate Dynamics*, 49(9-10),
1667 3011–3029.
- 1668 Chang, P., & Philander, S. G. (1994). A coupled ocean–atmosphere instability of
1669 relevance to the seasonal cycle. *Journal of the Atmospheric Sciences*, 51(24),
1670 3627–3648.
- 1671 Charney, J. G., & Drazin, P. G. (1961). Propagation of planetary-scale disturbances
1672 from the lower into the upper atmosphere. *Journal of Geophysical Research*,
1673 66(1), 83–109. Retrieved from [https://agupubs.onlinelibrary.wiley.com/](https://agupubs.onlinelibrary.wiley.com/doi/abs/10.1029/JZ066i001p00083)
1674 [doi/abs/10.1029/JZ066i001p00083](https://agupubs.onlinelibrary.wiley.com/doi/abs/10.1029/JZ066i001p00083) doi: 10.1029/JZ066i001p00083
- 1675 Chen, J., & Bordoni, S. (2014). Orographic Effects of the Tibetan Plateau on the
1676 East Asian Summer Monsoon: An Energetic Perspective. *Journal of Climate*,
1677 27(8), 3052–3072. doi: 10.1175/JCLI-D-13-00479.1
- 1678 Cheng, H., Edwards, R. L., Broecker, W. S., Denton, G. H., Kong, X., Wang, Y., ...
1679 Wang, X. (2009). Ice Age Terminations. *Science*, 326(5950), 248–252. doi:
1680 10.1126/science.1177840
- 1681 Cheng, H., Sinha, A., Cruz, F. W., Wang, X., Edwards, R. L., d’Horta, F. M., ...
1682 Auler, A. S. (2013). Climate change patterns in Amazonia and biodiversity.
1683 *Nature Communications*, 4(1411).
- 1684 Cheng, H., Sinha, A., Wang, X., Cruz, F. W., & Edwards, R. L. (2012). The Global
1685 Paleomonsoon as seen through speleothem records from Asia and the Ameri-
1686 cas. *Climate Dynamics*, 39, 1045–1062. doi: 10.1007/s00382-012-1363-7
- 1687 Cheng, Y.-M., Thorncroft, C. D., & Kiladis, G. N. (2019). Two contrasting African
1688 easterly wave behaviors. *Journal of the Atmospheric Sciences*, 76(6), 1753–
1689 1768.
- 1690 Chiang, J. C. H., & Bitz, C. M. (2005). Influence of high latitude ice cover on the
1691 marine Intertropical Convergence Zone. *Climate Dynamics*, 25(5), 477–496.
1692 doi: 10.1007/s00382-005-0040-5
- 1693 Chiang, J. C. H., Fung, I. Y., Wu, C.-H., Cai, Y., Edman, Jacob, P., Liu, Y., ...
1694 Labrousse, C. A. (2015). Role of seasonal transitions and westerly jets in
1695 East Asian paleoclimate. *Quaternary Science Reviews*, 108, 111–129. doi:
1696 10.1016/j.quascirev.2014.11.009
- 1697 Chiang, J. C. H., Kong, W., Wu, C. H., & Battisti, D. (2020). Origins of East Asian
1698 Summer Monsoon Seasonality. *Journal of Climate*. Retrieved from [https://](https://doi.org/10.1175/JCLI-D-19-0888.1)
1699 doi.org/10.1175/JCLI-D-19-0888.1 doi: 10.1175/JCLI-D-19-0888.1
- 1700 Chiang, J. C. H., Swenson, L. M., & Kong, W. (2017). Role of seasonal transitions
1701 and the westerlies in the interannual variability of the East Asian summer
1702 monsoon precipitation. *Geophysical Research Letters*, 44(8), 3788–3795. doi:
1703 10.1002/2017GL072739
- 1704 Chiang, J. C. H., Zebiak, S. E., & Cane, M. A. (2001). Relative roles of elevated
1705 heating and surface temperature gradients in driving anomalous surface winds
1706 over tropical oceans. *Journal of the Atmospheric Sciences*, 58(11), 1371–1394.
- 1707

- Chou, C., & Neelin, J. D. (2001). Mechanisms limiting the southward extend of the South American summer monsoon. *Geophysical Research Letters*, 28(12), 2433–2436. doi: 10.1029/2000GL012138
- Chou, C., & Neelin, J. D. (2003). Mechanisms limiting the northward extent of the northern summer monsoons over North America, Asia, and Africa. *Journal of Climate*, 16(3), 406–425. doi: 10.1175/1520-0442(2003)016<0406:MLTNEO>2.0.CO;2
- Christensen, J., Krishna Kumar, K., Aldrian, E., An, S.-I., Cavalcanti, I., de Castro, M., ... Zhou, T. (2013). Climate phenomena and their relevance for future regional climate change [Book Section]. In T. Stocker et al. (Eds.), *Climate Change 2013: The Physical Science Basis. Contribution of Working Group I to the Fifth Assessment Report of the Intergovernmental Panel on Climate Change* (pp. 1217–1308). Cambridge, United Kingdom and New York, NY, USA: Cambridge University Press. Retrieved from www.climatechange2013.org doi: 10.1017/CBO9781107415324.028
- Cook, K. H. (2000). The South Indian Convergence Zone and Interannual Rainfall Variability over Southern Africa. *Journal of Climate*, 13(21), 3789–3804. doi: 10.1175/1520-0442(2000)013<3789:TSICZA>2.0.CO;2
- D’Agostino, R., Bader, J., Bordon, S., Ferreira, D., & Jungclauss, J. (2019). Northern Hemisphere Monsoon Response to Mid-Holocene Orbital Forcing and Greenhouse Gas-Induced Global Warming. *Geophysical Research Letters*, 1–11. doi: 10.1029/2018GL081589
- Dansgaard, W., Johnsen, S. J., Clausen, H. B., Dahl-Jensen, D., Gundestrup, N., Hammer, C., ... others (1993). Evidence for general instability of past climate from a 250-kyr ice-core record. *Nature*, 364(6434), 218–220.
- Deplazes, G., Lckge, A., Peterson, L. C., Timmermann, A., Hamann, Y., Huguen, K. A., ... Haug, G. H. (2013). Links between tropical rainfall and North Atlantic climate during the last glacial period. *Nature Geosci*, 6, 213–217. doi: 10.1038/ngeo1712
- Diaz, M., & Boos, W. R. (2019a). Barotropic growth of monsoon depressions. *Quarterly Journal of the Royal Meteorological Society*, 145(719), 824–844.
- Diaz, M., & Boos, W. R. (2019b). Monsoon depression amplification by moist barotropic instability in a vertically sheared environment. *Quarterly Journal of the Royal Meteorological Society*, 145(723), 2666–2684. doi: 10.1002/qj.3585
- Ding, Y., & Chan, J. C. L. (2005). The East Asian summer monsoon: An overview. *Meteorology and Atmospheric Physics*, 89(1), 117–142. doi: 10.1007/s00703-005-0125-z
- Dokken, T. M., Nisancioglu, K. H., Li, C., Battisti, D. S., & Kissel, C. (2013). Dansgaard-Oeschger cycles: Interactions between ocean and sea ice intrinsic to the Nordic seas. *Paleoceanography*, 28(3), 491–502.
- Donohoe, A., Marshall, J., Ferreira, D., & Mcgee, D. (2013). The relationship between ITCZ location and cross-equatorial atmospheric heat transport: From the seasonal cycle to the last glacial maximum. *Journal of Climate*, 26(11), 3597–3618. doi: 10.1175/JCLI-D-12-00467.1
- Duffy, M. L., O’Gorman, P. A., & Back, L. E. (2020). Importance of laplacian of low-level warming for the response of precipitation to climate change over tropical oceans. *Journal of Climate*, 33(10), 4403–4417.
- Egger, J., Weickmann, K., & Hoinka, K.-P. (2007). Angular momentum in the global atmospheric circulation. *Reviews of Geophysics*, 45(4). Retrieved from <https://agupubs.onlinelibrary.wiley.com/doi/abs/10.1029/2006RG000213> doi: 10.1029/2006RG000213
- Ellis, A. W., Saffell, E. M., & Hawkins, T. W. (2004). A method for defining monsoon onset and demise in the Southwestern USA. *International Journal of Climatology*, 24(2), 247–265. doi: 10.1002/joc.996
- Eltahir, E. A., & Gong, C. (1996). Dynamics of Wet and Dry Years in West Africa.

- Journal of Climate*, 9, 1030–1042. doi: 10.1175/1520-0442(1996)009%3C1030:DOWADY%3E2.0.CO;2
- Emanuel, K. A. (1983a). The Lagrangian parcel dynamics of moist symmetric instability. *Journal of the Atmospheric Sciences*, 40, 2368–2376.
- Emanuel, K. A. (1983b). On assessing local conditional symmetric instability from atmospheric soundings. *Monthly weather review*, 111, 2016–2033.
- Emanuel, K. A. (1988). Observational evidence of slantwise convective adjustment. *Monthly weather review*, 116(9), 1805–1816.
- Emanuel, K. A. (1995). On Thermally Direct Circulations in Moist Atmospheres. *Journal of the Atmospheric Sciences*, 52(9), 1529–1534. doi: 10.1175/1520-0469(1995)052<1529:OTDCIM>2.0.CO;2
- Emanuel, K. A., Neelin, J. D., & Bretherton, C. S. (1994). On large-scale circulations in convecting atmospheres. *Quarterly Journal of the Royal Meteorological Society*, 120(519), 1111–1143. doi: 10.1002/qj.49712051902
- Eroglu, D., McRobie, F. H., Ozken, I., Stemler, T., Wyrwoll, K. H., Breitenbach, S. F., ... Kurths, J. (2016). See-saw relationship of the Holocene East Asian-Australian summer monsoon. *Nature Communications*, 7, 1–7. doi: 10.1038/ncomms12929
- Faulk, S., Mitchell, J., & Bordoni, S. (2017). Effects of Rotation Rate and Seasonal Forcing on the ITCZ Extent in Planetary Atmospheres. *Journal of the Atmospheric Sciences*, 74(3), 665–678. doi: 10.1175/JAS-D-16-0014.1
- Frierson, D. M., Hwang, Y. T., Fućkar, N. S., Seager, R., Kang, S. M., Donohoe, A., ... Battisti, D. S. (2013). Contribution of ocean overturning circulation to tropical rainfall peak in the Northern Hemisphere. *Nature Geoscience*, 6(11), 940–944. doi: 10.1038/ngeo1987
- Frierson, D. M. W. (2007). The Dynamics of Idealized Convection Schemes and Their Effect on the Zonally Averaged Tropical Circulation. *Journal of the Atmospheric Sciences*, 64(6), 1959–1976. doi: 10.1175/JAS3935.1
- Frierson, D. M. W., & Hwang, Y. T. (2012). Extratropical influence on ITCZ shifts in slab ocean simulations of global warming. *Journal of Climate*, 25(2), 720–733. doi: 10.1175/JCLI-D-11-00116.1
- Fućkar, N. S., Xie, S.-P., Farneti, R., Maroon, E. A., & Frierson, D. M. (2013). Influence of the extratropical ocean circulation on the intertropical convergence zone in an idealized coupled general circulation model. *Journal of Climate*, 26(13), 4612–4629. doi: 10.1175/JCLI-D-12-00294.1
- Gadgil, S. (2018). The monsoon system: Land-sea breeze or the ITCZ? *Journal of Earth System Science*, 127(1), 1–29. doi: 10.1007/s12040-017-0916-x
- Geen, R., Lambert, F. H., & Vallis, G. K. (2018). Regime Change Behavior During Asian Monsoon Onset. *Journal of Climate*, 31, 3327–3348. Retrieved from <http://journals.ametsoc.org/doi/10.1175/JCLI-D-17-0118.1> doi: 10.1175/JCLI-D-17-0118.1
- Geen, R., Lambert, F. H., & Vallis, G. K. (2019). Processes and Timescales in Onset and Withdrawal of ‘Aquaplanet Monsoons’. *J. Atmos. Sci.*, 76, 2357–2373. doi: 10.1175/JAS-D-18-0214.1
- Godbole, R. V. (1977). The composite structure of the monsoon depression. *Tellus*, 29(1), 25–40.
- Goswami, B. N., & Ajaya Mohan, R. S. (2001). Intraseasonal Oscillations and Interannual Variability of the Indian Summer Monsoon. *Journal of Climate*, 14, 1180–1198. doi: 10.1175/1520-0442(2001)014<1180:IOAIVO>2.0.CO;2
- Green, B., & Marshall, J. (2017). Coupling of Trade Winds with Ocean Circulation Damps ITCZ Shifts. *Journal of Climate*, 30(12), 4395–4411. Retrieved from <https://doi.org/10.1175/JCLI-D-16-0818.1> doi: 10.1175/JCLI-D-16-0818.1
- Gruber, A., Su, X., Kanamitsu, M., & Schemm, J. (2000). The Comparison of Two Merged Rain Gauge-Satellite Precipitation Datasets. *Bul-*

- 1818 *letin of the American Meteorological Society*, 81(11), 2631–2644. doi:
 1819 10.1175/1520-0477(2000)081<2631:TCOTMR>2.3.CO;2
- 1820 Hagos, S. M., & Cook, K. H. (2007). Dynamics of the West African monsoon jump.
 1821 *Journal of Climate*, 20(21), 5264–5284. doi: 10.1175/2007JCLI1533.1
- 1822 Halley, E. (1686). An Historical Account of the Trade Winds, and Monsoons,
 1823 Observable in the Seas between and Near the Tropicks, with an Attempt to
 1824 Assign the Phisical Cause of the Said Winds, By E. Halley. *Philosophical*
 1825 *Transactions of the Royal Society of London*, 16(179–191), 153–168. doi:
 1826 10.1098/rstl.1686.0026
- 1827 Harrop, B. E., Lu, J., & Leung, L. R. (2019). Sub-cloud moist entropy curvature as
 1828 a predictor for changes in the seasonal cycle of tropical precipitation. *Climate*
 1829 *Dynamics*, 53(5–6), 3463–3479.
- 1830 Hartmann, D. L., & Michelsen, M. L. (1989). Intraseasonal periodicities in Indian
 1831 rainfall. *Journal of the Atmospheric Sciences*, 46(18), 2838–2862.
- 1832 Hawcroft, M., Haywood, J. M., Collins, M., Jones, A., Jones, A. C., & Stephens, G.
 1833 (2017). Southern Ocean albedo, inter-hemispheric energy transports and the
 1834 double ITCZ: Global impacts of biases in a coupled model. *Climate Dynamics*,
 1835 48(7–8), 2279–2295.
- 1836 Heinrich, H. (1988). Origin and consequences of cyclic ice rafting in the north-
 1837 east Atlantic Ocean during the past 130,000 years. *Quaternary research*, 29(2),
 1838 142–152.
- 1839 Held, I. M. (2005). The gap between simulation and understanding in climate
 1840 modeling. *Bulletin of the American Meteorological Society*, 86(11), 1609–
 1841 1614. Retrieved from <https://doi.org/10.1175/BAMS-86-11-1609> doi:
 1842 10.1175/BAMS-86-11-1609
- 1843 Hemming, S. R. (2004). Heinrich events: Massive late Pleistocene detritus layers
 1844 of the North Atlantic and their global climate imprint. *Reviews of Geophysics*,
 1845 42(1).
- 1846 Hendon, H. H., & Liebmann, B. (1990). A Composite Study of Onset of the Aus-
 1847 tralian Summer Monsoon. *Journal of Atmospheric Sciences*, 47(18), 2227–
 1848 2240. doi: 10.1175/1520-0469(1990)047<2227:ACS000>2.0.CO;2
- 1849 Hide, R. (1969). Dynamics of the Atmospheres of the Major Planets with an Ap-
 1850 pendix on the Viscous Boundary Layer at the Rigid Bounding Surface of an
 1851 Electrically-Conducting Rotation Fluid in the Presence of a Magnetic Field.
 1852 *J. Atmos. Sci.*, 26, 841–853. doi: 10.1175/1520-0469(1969)026%3C0841:
 1853 DOTAOT%3E2.0.CO;2
- 1854 Hilgenbrink, C. C., & Hartmann, D. L. (2018). The response of Hadley circulation
 1855 extent to an idealized representation of poleward ocean heat transport in an
 1856 aquaplanet GCM. *Journal of Climate*, 31, 9753–9770.
- 1857 Hill, S. A. (2019). Theories for Past and Future Monsoon Rainfall Changes. *Current*
 1858 *Climate Change Reports*, 5, 160–171.
- 1859 Hill, S. A., Bordoni, S., & Mitchell, J. L. (2019). Hadley cell emergence and extent
 1860 in axisymmetric, nearly inviscid, planetary atmospheres. *J. Atmos. Sci.*
- 1861 Hill, S. A., Ming, Y., & Held, I. M. (2015). Mechanisms of forced tropical meridional
 1862 energy flux change. *Journal of Climate*, 28, 1725–1742. doi: 10.1175/JCLI-D
 1863 -14-00165.1
- 1864 Hill, S. A., Ming, Y., Held, I. M., & Zhao, M. (2017). A moist static energy budget-
 1865 based analysis of the Sahel rainfall response to uniform oceanic warming. *Jour-
 1866 nal of Climate*, 30(15), 5637–5660. doi: 10.1175/JCLI-D-16-0785.1
- 1867 Hill, S. A., Ming, Y., & Zhao, M. (2018). Robust Responses of the Hydrological Cy-
 1868 cle to Global Warming. *Journal of Climate*, 1931, 9793–9814. doi: 10.1175/
 1869 JCLI-D-18-0238.1
- 1870 Holton, J. R., Wallace, J. M., & Young, J. (1971). On boundary layer dynamics and
 1871 the ITCZ. *Journal of the Atmospheric Sciences*, 28(2), 275–280.
- 1872 Houze Jr, R. A. (2018). 100 years of research on mesoscale convective systems. *Me-*

- 1873 *teorological Monographs*, 59, 17–1.
- 1874 Huffman, G. J., Adler, R. F., Morrissey, M. M., Bolvin, D. T., Curtis, S., Joyce, R.,
1875 ... Susskind, J. (2001). Global Precipitation at One-Degree Daily Resolution
1876 from Multisatellite Observations. *Journal of Hydrometeorology*, 2, 36–50.
- 1877 Huffman, G. J. and D. T. Bolvin and R. F. Adler. (2016). *GPCP Version 1.2 One-*
1878 *Degree Daily Precipitation Data Set*. Boulder CO: Research Data Archive
1879 at the National Center for Atmospheric Research, Computational and Infor-
1880 mation Systems Laboratory. Retrieved from [https://doi.org/10.5065/](https://doi.org/10.5065/D6D50K46)
1881 [D6D50K46](https://doi.org/10.5065/D6D50K46)
- 1882 Hui, K., & Bordoni, S. (submitted.). Influence of Continental Geometry on the On-
1883 set and Spatial Distribution of Monsoonal Precipitation. *J. Atmos. Sci.*
- 1884 Hunt, K. M., Turner, A. G., Inness, P. M., Parker, D. E., & Levine, R. C. (2016).
1885 On the structure and dynamics of Indian monsoon depressions. *Monthly*
1886 *Weather Review*, 144(9), 3391–3416.
- 1887 Hurley, J. V., & Boos, W. R. (2013). Interannual variability of monsoon precipita-
1888 tion and local subcloud equivalent potential temperature. *Journal of Climate*,
1889 26(23), 9507–9527. doi: 10.1175/JCLI-D-12-00229.1
- 1890 Hurley, J. V., & Boos, W. R. (2015). A global climatology of monsoon low-pressure
1891 systems. *Quarterly Journal of the Royal Meteorological Society*, 141(689),
1892 1049–1064. doi: 10.1002/qj.2447
- 1893 Japan Meteorological Agency/Japan. (2013). *JRA-55: Japanese 55-year Reanalysis,*
1894 *Monthly Means and Variances*. Boulder CO: Research Data Archive at the
1895 National Center for Atmospheric Research, Computational and Information
1896 Systems Laboratory. Retrieved from <https://doi.org/10.5065/D60G3H5B>
- 1897 Jeevanjee, N., Hassanzadeh, P., Hill, S., & Sheshadri, A. (2017). A perspective
1898 on climate model hierarchies. *Journal of Advances in Modeling Earth Systems*,
1899 9(4), 1760–1771. doi: 10.1002/2017MS001038
- 1900 Jiang, X., Adames, . F., Zhao, M., Waliser, D., & Maloney, E. (2018). A unified
1901 moisture mode framework for seasonality of the Madden-Julian oscillation.
1902 *Journal of Climate*, 31(11), 4215–4224. Retrieved from [https://doi.org/](https://doi.org/10.1175/JCLI-D-17-0671.1)
1903 [10.1175/JCLI-D-17-0671.1](https://doi.org/10.1175/JCLI-D-17-0671.1) doi: 10.1175/JCLI-D-17-0671.1
- 1904 Jourdain, N. C., Gupta, A. S., Taschetto, A. S., Ummenhofer, C. C., Moise, A. F., &
1905 Ashok, K. (2013). The Indo-Australian monsoon and its relationship to ENSO
1906 and IOD in reanalysis data and the CMIP3/CMIP5 simulations. *Climate*
1907 *Dynamics*, 41(11), 3073–3102. Retrieved from [https://doi.org/10.1007/](https://doi.org/10.1007/s00382-013-1676-1)
1908 [s00382-013-1676-1](https://doi.org/10.1007/s00382-013-1676-1) doi: 10.1007/s00382-013-1676-1
- 1909 Jouzel, J., Masson-Delmotte, V., Cattani, O., Dreyfus, G., Falourd, S., Hoffmann,
1910 G., ... Wolff, E. W. (2007). Orbital and Millennial Antarctic Climate
1911 Variability over the Past 800,000 Years. *Science*, 317(5839), 793–796. doi:
1912 [10.1126/science.1141038](https://doi.org/10.1126/science.1141038)
- 1913 Kang, S. M. (2020). Extratropical Influence on the Tropical Rainfall Distribution.
1914 *Current Climate Change Reports*, 6, 24–36.
- 1915 Kang, S. M., Frierson, D. M. W., & Held, I. M. (2009). The Tropical Response
1916 to Extratropical Thermal Forcing in an Idealized GCM: The Importance of
1917 Radiative Feedbacks and Convective Parameterization. *Journal of the Atmo-*
1918 *spheric Sciences*, 66(9), 2812–2827. doi: 10.1175/2009jas2924.1
- 1919 Kang, S. M., & Held, I. M. (2012). Tropical precipitation, SSTs and the surface
1920 energy budget: A zonally symmetric perspective. *Climate Dynamics*, 38(9-10),
1921 1917–1924. doi: 10.1007/s00382-011-1048-7
- 1922 Kang, S. M., Held, I. M., Frierson, D. M., & Zhao, M. (2008). The response of the
1923 ITCZ to extratropical thermal forcing: Idealized slab-ocean experiments with a
1924 GCM. *Journal of Climate*, 21(14), 3521–3532. doi: 10.1175/2007JCLI2146.1
- 1925 Kang, S. M., Shin, Y., & Xie, S.-P. (2018). Extratropical forcing and tropical rainfall
1926 distribution: Energetics framework and ocean Ekman advection. *npj Climate*
1927 *and Atmospheric Science*, 1(1), 1–10.

- Kanner, L. C., Burns, S. J., Cheng, H., & Edwards, R. L. (2012). High-Latitude Forcing of the South American Summer Monsoon During the Last Glacial. *Science*, 335(6068), 570–573. doi: 10.1126/science.1213397
- Kay, J. E., Wall, C., Yettella, V., Medeiros, B., Hannay, C., Caldwell, P., & Bitz, C. (2016). Global climate impacts of fixing the Southern Ocean shortwave radiation bias in the Community Earth System Model (CESM). *Journal of Climate*, 29(12), 4617–4636.
- Kerns, B., & Chen, S. S. (2020). A 20-year climatology of Madden-Julian Oscillation convection: Large-scale precipitation tracking from TRMM-GPM rainfall. *In press, J. Geophys. Res. Atmos.*
- Kiladis, G. N., Thorncroft, C. D., & Hall, N. M. J. (2006). Three-Dimensional Structure and Dynamics of African Easterly Waves. Part I: Observations. *Journal of the Atmospheric Sciences*, 63(9), 2212–2230. doi: 10.1175/JAS3741.1
- Kiladis, G. N., Wheeler, M. C., Haertel, P. T., Straub, K. H., & Roundy, P. E. (2009). Convectively coupled equatorial waves. *Reviews of Geophysics*, 47(RG2003).
- Kobayashi, S., Ota, Y., Harada, Y., Ebata, A., Moriya, M., Onoda, H., ... Takahashi, K. (2015). The JRA-55 Reanalysis: General Specifications and Basic Characteristics. *J. Meteorol. Soc. Jpn.*, 93(1), 5–48. doi: 10.2151/jmsj.2015-001
- Kodama, Y. (1992). Large-Scale Common Features of Subtropical Precipitation Zones (the Baiu Frontal Zone, the SPCZ, and the SACZ). Part I: Characteristics of Subtropical Frontal Zones. *Journal of the Meteorological Society of Japan*, 70(4), 813–836. doi: 10.2151/jmsj1965.70.4.813
- Kong, W., & Chiang, J. C. H. (2020). Interaction of the Westerlies with the Tibetan Plateau in Determining the Mei-Yu Termination. *Journal of Climate*, 33(1), 339–363. doi: 10.1175/JCLI-D-19-0319.1
- Kong, W., Swenson, L. M., & Chiang, J. C. H. (2017). Seasonal transitions and the westerly jet in the Holocene East Asian summer monsoon. *Journal of Climate*, 30(9), 3343–3365. doi: 10.1175/JCLI-D-16-0087.1
- Kothawale, D., & Kumar, K. R. (2002). Tropospheric temperature variation over India and links with the Indian summer monsoon: 1971–2000. *Mausam*, 53, 289–308.
- Lea, D. W., Pak, D. K., Peterson, L. C., & Hughen, K. A. (2003). Temperatures over the Last Glacial Termination Synchronicity of Tropical and High-Latitude Atlantic Temperatures over the Last Glacial Termination. *Science*, 301, 1361–1364. doi: 10.1126/science.1088470
- Lebel, T. (2003). Seasonal cycle and interannual variability of the Sahelian rainfall at hydrological scales. *Journal of Geophysical Research*, 108(D8), 8389. doi: 10.1029/2001JD001580
- Lee, J.-Y., Wang, B., Wheeler, M. C., Fu, X., Waliser, D. E., & Kang, I.-S. (2013). Real-time multivariate indices for the boreal summer intraseasonal oscillation over the Asian summer monsoon region. *Climate Dynamics*, 40(1), 493–509. Retrieved from <https://doi.org/10.1007/s00382-012-1544-4> doi: 10.1007/s00382-012-1544-4
- Lenters, J. D., & Cook, K. H. (1997). On the Origin of the Bolivian High and Related Circulation Features of the South American Climate. *Journal of the Atmospheric Sciences*, 54, 656–678. doi: 10.1175/1520-0469(1997)054%3C0656:OTOOTB%3E2.0.CO;2
- Levine, X. J., & Schneider, T. (2011). Response of the Hadley Circulation to Climate Change in an Aquaplanet GCM Coupled to a Simple Representation of Ocean Heat Transport. *Journal of the Atmospheric Sciences*, 68(4), 769–783. Retrieved from <https://doi.org/10.1175/2010JAS3553.1> doi: 10.1175/2010JAS3553.1
- Levins, R. (1966). The strategy of model building in population biology. *American*

- 1983 *Scientist*, 54(4), 421–431.
- 1984 Levy, G., & Battisti, D. S. (1995). The symmetric stability and the low level equato-
1985 rial flow. *Global Atmosphere-Ocean System*, 3(4), 341–354.
- 1986 Liebmann, B., & Hendon, H. H. (1990). Synoptic-scale disturbances near the equa-
1987 tor. *Journal of the Atmospheric Sciences*, 47(12), 1463–1479.
- 1988 Lindzen, R. S., & Hou, A. Y. (1988). Hadley Circulations for Zonally Averaged
1989 Heating Centred off the Equator. *J. Atmos. Sci.*, 45(17), 2416–2427.
- 1990 Lindzen, R. S., & Nigam, S. (1987). On the role of sea surface temperature gradients
1991 in forcing low-level winds and convergence in the tropics. *Journal of the Atmo-
1992 spheric Sciences*, 44(17), 2418–2436.
- 1993 Linho, L. H., Huang, X., & Lau, N. C. (2008). Winter-to-spring transition in east
1994 Asia: A planetary-scale perspective of the south China spring rain onset. *Jour-
1995 nal of Climate*, 21(13), 3081–3096. doi: 10.1175/2007JCLI1611.1
- 1996 Liu, X., & Battisti, D. S. (2015). The influence of orbital forcing of tropical in-
1997 solation on the climate and isotopic composition of precipitation in South
1998 America. *Journal of Climate*, 28(12), 4841–4862.
- 1999 Liu, X., Battisti, D. S., & Donohoe, A. (2017). Tropical precipitation and cross-
2000 equatorial ocean heat transport during the mid-Holocene. *Journal of Climate*,
2001 30(10), 3529–3547. doi: 10.1175/JCLI-D-16-0502.1
- 2002 Madden, R. A., & Julian, P. R. (1971). Detection of a 40–50 day oscillation in the
2003 zonal wind in the tropical Pacific. *Journal of the Atmospheric Sciences*, 28(5),
2004 702–708.
- 2005 Madden, R. A., & Julian, P. R. (1972). Description of global-scale circulation cells
2006 in the tropics with a 40–50 day period. *Journal of the Atmospheric Sciences*,
2007 29(6), 1109–1123.
- 2008 Maher, P., Gerber, E. P., Medeiros, B., Merlis, T. M., Sherwood, S., Sheshadri, A.,
2009 ... ZuritaGotor, P. (2019). Model Hierarchies for Understanding Atmo-
2010 spheric Circulation. *Reviews of Geophysics*, 2018RG000607. Retrieved from
2011 <https://onlinelibrary.wiley.com/doi/abs/10.1029/2018RG000607> doi:
2012 10.1029/2018RG000607
- 2013 Mao, J., & Wu, G. (2007). Interannual variability in the onset of the summer mon-
2014 soon over the Eastern Bay of Bengal. *Theoretical and Applied Climatology*,
2015 89(3-4), 155–170. doi: 10.1007/s00704-006-0265-1
- 2016 Marengo, J. A., Liebmann, B., Grimm, A. M., Misra, V., Silva Dias, P. L., Cav-
2017 alcanti, I. F., ... Alves, L. M. (2012). Recent developments on the South
2018 American monsoon system. *International Journal of Climatology*, 32(1), 1–21.
2019 doi: 10.1002/joc.2254
- 2020 Maroon, E. A., Frierson, D. M., & Battisti, D. S. (2015). The tropical precipitation
2021 response to Andes topography and ocean heat fluxes in an aquaplanet model.
2022 *Journal of Climate*, 28(1), 381–398. doi: 10.1175/JCLI-D-14-00188.1
- 2023 Marshall, J., Donohoe, A., Ferreira, D., & McGee, D. (2014). The ocean’s role in
2024 setting the mean position of the Inter-Tropical Convergence Zone. *Climate Dy-
2025 namics*, 42(7-8), 1967–1979. doi: 10.1007/s00382-013-1767-z
- 2026 Martin, G. M., Chevuturi, A., Comer, R. E., Dunstone, N. J., Scaife, A. A., &
2027 Zhang, D. (2019). Predictability of South China Sea Summer Mon-
2028 soon Onset. *Advances in Atmospheric Sciences*, 36(3), 253–260. doi:
2029 10.1007/s00376-018-8100-z
- 2030 Matsuno, T. (1966). Quasi-Geostrophic Motions in the Equatorial Area. *J. Meteor.
2031 Soc. Japan*, 44(1), 25–43. doi: 10.2151/jmsj1965.44.1.25
- 2032 McGee, D., Donohoe, A., Marshall, J., & Ferreira, D. (2014). Changes in ITCZ
2033 location and cross-equatorial heat transport at the Last Glacial Maximum,
2034 Heinrich Stadial 1, and the mid-Holocene. *Earth and Planetary Science Let-
2035 ters*, 390, 69–79. doi: 10.1016/j.epsl.2013.12.043
- 2036 Merlis, T. M., Schneider, T., Bordoni, S., & Eisenman, I. (2013). Hadley circu-
2037 lation response to orbital precession. Part I: Aquaplanets. *Journal of Climate*,

- 26, 740–753. doi: 10.1175/JCLI-D-11-00716.1
- Mesoscale Atmospheric Processes Branch/Laboratory for Atmospheres/Earth Sciences Division/Science and Exploration Directorate/Goddard Space Flight Center/NASA, and Earth System Science Interdisciplinary Center/University of Maryland. (2018). *GPCP Version 2.3 Monthly Analysis Product*. Boulder CO: Research Data Archive at the National Center for Atmospheric Research, Computational and Information Systems Laboratory. Retrieved from <https://doi.org/10.5065/D6SN07QX>
- Mitchell, T. P., & Wallace, J. M. (1992). The Annual Cycle in Equatorial Convection and Sea Surface Temperature. *Journal of Climate*, 5(10), 1140–1156. doi: 10.1175/1520-0442(1992)005<1140:TACIEC>2.0.CO;2
- Molnar, P., Boos, W. R., & Battisti, D. S. (2010). Orographic controls on climate and paleoclimate of Asia: thermal and mechanical roles for the Tibetan Plateau. *Annual Review of Earth and Planetary Sciences*, 38(1), 77–102. doi: 10.1146/annurev-earth-040809-152456
- Mooley, D. A. (1973). Some aspects of Indian monsoon depression and associated rainfall. *Monthly Weather Review*, 101, 271–280.
- Mulitza, S., Prange, M., Stuut, J.-B., Zabel, M., von Döbenek, T., Itambi, A. C., ... Wefer, G. (2008). Sahel megadroughts triggered by glacial slowdowns of Atlantic meridional overturning. *Paleoceanography*, 23(4). doi: 10.1029/2008PA001637
- Nicholson, S. E. (2009). On the factors modulating the intensity of the tropical rainbelt over West Africa. *International Journal of Climatology*, 29(5), 673–689.
- Nicholson, S. E., Barillon, A. I., Challa, M., & Baum, J. (2007). Wave Activity on the Tropical Easterly Jet. *Journal of the Atmospheric Sciences*, 64(7), 2756–2763. doi: 10.1175/JAS3946.1
- Nie, J., Boos, W. R., & Kuang, Z. (2010). Observational evaluation of a convective quasi-equilibrium view of monsoons. *Journal of Climate*, 23(16), 4416–4428. doi: 10.1175/2010JCLI3505.1
- Parthasarathy, B., Munot, A. A., & Kothawale, D. R. (1994). All-India monthly and seasonal rainfall series: 1871–1993. *Theoretical and Applied Climatology*, 49(4), 217–224. doi: 10.1007/BF00867461
- Pausata, F. S., Battisti, D. S., Nisancioglu, K. H., & Bitz, C. M. (2011). Chinese stalagmite $\delta^{18}\text{O}$ controlled by changes in the Indian monsoon during a simulated Heinrich event. *Nature Geoscience*, 4(7), 474.
- Philander, S., Gu, D., Lambert, G., Li, T., Halpern, D., Lau, N., & Pacanowski, R. (1996). Why the ITCZ is Mostly North of the Equator. *Journal of Climate*, 9(12), 2958–2972.
- Plumb, R. A., & Hou, A. Y. (1992). The response of a zonally symmetric atmosphere to subtropical thermal forcing - Threshold behavior. *Journal of the Atmospheric Sciences*, 49(19), 1790–1799. doi: 10.1175/1520-0469(1992)049<1790:TROAZS>2.0.CO;2
- Privé, N. C., & Plumb, R. A. (2007a). Monsoon Dynamics with Interactive Forcing. Part I: Axisymmetric Studies. *Journal of the Atmospheric Sciences*, 64(5), 1417–1430. doi: 10.1175/JAS3916.1
- Privé, N. C., & Plumb, R. A. (2007b). Monsoon Dynamics with Interactive Forcing. Part II: Impact of Eddies and Asymmetric Geometries. *Journal of the Atmospheric Sciences*, 64(5), 1431–1442. doi: 10.1175/JAS3917.1
- Rao, V. B., Cavalcanti, I. F. A., & Hada, K. (1996). Annual variation of rainfall over Brazil and water vapor characteristics over South America. *Journal of Geophysical Research: Atmospheres*, 101(D21), 26539–26551. doi: 10.1029/96JD01936
- Reed, R. J., Norquist, D. C., & Recker, E. E. (1977). The structure and properties of African wave disturbances as observed during Phase III of GATE. *Monthly Weather Review*, 105(3), 317–333.

- Roberts, W. H., Valdes, P. J., & Singarayer, J. S. (2017). Can energy fluxes be used to interpret glacial/interglacial precipitation changes in the tropics? *Geophysical Research Letters*, 44(12), 6373–6382. doi: 10.1002/2017GL073103
- Rodwell, M. J., & Hoskins, B. J. (2001). Subtropical anticyclones and summer monsoons. *Journal of Climate*, 14(15), 3192–3211. doi: 10.1175/1520-0442(2001)014<3192:SAASM>2.0.CO;2
- Roehrig, R., Bouniol, D., Guichard, F., Hourdin, F., & Redelsperger, J.-L. (2013). The Present and Future of the West African Monsoon: A Process-Oriented Assessment of CMIP5 Simulations along the AMMA Transect. *Journal of Climate*, 26(17), 6471–6505. Retrieved from <https://doi.org/10.1175/JCLI-D-12-00505.1> doi: 10.1175/JCLI-D-12-00505.1
- Roundy, P. E., & Frank, W. M. (2004). A climatology of waves in the equatorial region. *Journal of the Atmospheric Sciences*, 61(17), 2105–2132.
- Sampe, T., & Xie, S.-P. (2010). Large-scale dynamics of the Meiyu-Baiu rainband: Environmental forcing by the westerly jet. *Journal of Climate*, 23(1), 113–134. doi: 10.1175/2009JCLI3128.1
- Schneider, T. (2017). Feedback of Atmosphere-Ocean Coupling on Shifts of the Intertropical Convergence Zone. *Geophysical Research Letters*, 44(22), 11,644–11,653. Retrieved from <https://agupubs.onlinelibrary.wiley.com/doi/abs/10.1002/2017GL075817> doi: 10.1002/2017GL075817
- Schneider, T., Bischoff, T., & Haug, G. H. (2014). Migrations and dynamics of the Intertropical Convergence Zone. *Nature*, 513(7516), 45–53. doi: 10.1038/nature13636
- Schneider, T., & Bordoni, S. (2008). Eddy-Mediated Regime Transitions in the Seasonal Cycle of a Hadley Circulation and Implications for Monsoon Dynamics. *Journal of the Atmospheric Sciences*, 65(1), 915–934. doi: 10.1175/2007JAS2415.1
- Schneider, T., O’Gorman, P., & Levine, X. (2010). Water vapor and the dynamics of climate changes. *Reviews of Geophysics*(48), 1–22. doi: 10.1029/2009RG000302
1. INTRODUCTION
- Schumacher, C., & Houze Jr, R. A. (2003). Stratiform rain in the tropics as seen by the TRMM precipitation radar. *Journal of Climate*, 16(11), 1739–1756.
- Schwendike, J., Govekar, P., Reeder, M. J., Wardle, R., Berry, G. J., & Jakob, C. (2014). Local partitioning of the overturning circulation in the tropics and the connection to the Hadley and Walker circulations. *Journal of Geophysical Research*, 119(3), 1322–1339. doi: 10.1002/2013JD020742
- Seo, J., Kang, S. M., & Merlis, T. M. (2017). A model intercomparison of the tropical precipitation response to a CO₂ doubling in aquaplanet simulations. *Geophysical Research Letters*, 44(2), 993–1000. Retrieved from <https://agupubs.onlinelibrary.wiley.com/doi/abs/10.1002/2016GL072347> doi: 10.1002/2016GL072347
- Seth, A., Giannini, A., Rojas, M., Rauscher, S. A., Bordoni, S., Singh, D., & Camargo, S. J. (2019, Jun 01). Monsoon responses to climate changes—connecting past, present and future. *Current Climate Change Reports*, 5(2), 63–79. Retrieved from <https://doi.org/10.1007/s40641-019-00125-y> doi: 10.1007/s40641-019-00125-y
- Shaw, T. A. (2014). On the Role of Planetary-Scale Waves in the Abrupt Seasonal Transition of the Northern Hemisphere General Circulation. *Journal of the Atmospheric Sciences*, 71(5), 1724–1746. doi: 10.1175/JAS-D-13-0137.1
- Shaw, T. A., & Voigt, A. (2015). Tug of war on summertime circulation between radiative forcing and sea surface warming. *Nature Geoscience*, 8(7), 560–566. doi: 10.1038/ngeo2449
- Shekhar, R., & Boos, W. R. (2016). Improving energy-based estimates of monsoon location in the presence of proximal deserts. *Journal of Climate*, 29(13), 4741–4761. doi: 10.1175/JCLI-D-15-0747.1

- 2148 Shekhar, R., & Boos, W. R. (2017). Weakening and shifting of the Saharan shallow
2149 meridional circulation during wet years of the West African monsoon. *Journal*
2150 *of Climate*, 30(18), 7399–7422.
- 2151 Shi, X., Lohmann, G., Sidorenko, D., & Yang, H. (2020). Early-Holocene simu-
2152 lations using different forcings and resolutions in AWI-ESM. *The Holocene*,
2153 30(7), 996–1015. doi: 10.1177/0959683620908634
- 2154 Sikka, D. (1978). Some aspects of the life history, structure and movement of mon-
2155 soon depressions. In *Monsoon dynamics* (pp. 1501–1529). Springer.
- 2156 Sikka, D. R., & Gadgil, S. (1980). On the Maximum Cloud Zone and the
2157 ITCZ over Indian, Longitudes during the Southwest Monsoon. *Monthly*
2158 *Weather Review*, 108(11), 1840–1853. Retrieved from [https://doi.org/](https://doi.org/10.1175/1520-0493(1980)108<1840:OTMCZA>2.0.CO;2)
2159 10.1175/1520-0493(1980)108<1840:OTMCZA>2.0.CO;2 doi: 10.1175/
2160 1520-0493(1980)108(1840:OTMCZA)2.0.CO;2
- 2161 Simpson, G. (1921). The South-West monsoon. *Quarterly Journal of the Royal Me-*
2162 *teorological Society*, 47(199), 151–171.
- 2163 Singh, M. S. (2019). Limits on the extent of the solstitial Hadley Cell: The role of
2164 planetary rotation. *Journal of Atmospheric Sciences*.
- 2165 Smyth, J. E., Hill, S. A., & Ming, Y. (2018). Simulated Responses of the West
2166 African Monsoon and Zonal-Mean Tropical Precipitation to Early Holocene
2167 Orbital Forcing. *Geophysical Research Letters*(Figure 1), 49–57. doi:
2168 10.1029/2018GL080494
- 2169 Sobel, A., & Maloney, E. (2013). Moisture Modes and the Eastward Propagation
2170 of the MJO. *Journal of the Atmospheric Sciences*, 70(1), 187–192. Retrieved
2171 from <https://doi.org/10.1175/JAS-D-12-0189.1> doi: 10.1175/JAS-D-12-
2172 -0189.1
- 2173 Sperber, K. R., Annamalai, H., Kang, I.-S., Kitoh, A., Moise, A., Turner, A., ...
2174 Zhou, T. (2013). The Asian summer monsoon: An intercomparison of CMIP5
2175 vs. CMIP3 simulations of the late 20th century. *Climate Dynamics*, 41(9),
2176 2711–2744. Retrieved from <https://doi.org/10.1007/s00382-012-1607-6>
2177 doi: 10.1007/s00382-012-1607-6
- 2178 Stevens, D. E. (1983). On symmetric stability and instability of zonal mean flows
2179 near the equator. *Journal of the Atmospheric Sciences*, 40(4), 882–893.
- 2180 Sultan, B., & Janicot, S. (2003). The West African monsoon dynamics. Part II: The
2181 preonset and onset of the summer monsoon. *Journal of climate*, 16(21), 3407–
2182 3427. doi: 10.1175/1520-0442(2003)016<3407:TWAMDP>2.0.CO;2
- 2183 Svensson, A., Andersen, K. K., Bigler, M., Clausen, H. B., Dahl-Jensen, D., Davies,
2184 S. M., ... Vinther, B. M. (2008). A 60 000 year Greenland stratigraphic ice
2185 core chronology. *Climate of the Past*, 4(1), 47–57. doi: 10.5194/cp-4-47-2008
- 2186 Takahashi, K. (2005). The annual cycle of heat content in the Peru current region.
2187 *Journal of Climate*, 18(23), 4937–4954. doi: 10.1175/JCLI3572.1
- 2188 Takahashi, K., & Battisti, D. S. (2007). Processes Controlling the Mean Tropical
2189 Pacific Precipitation Pattern. Part I: The Andes and the Eastern Pacific ITCZ.
2190 *Journal of Climate*, 20(14), 3434–3451. doi: 10.1175/jcli4198.1
- 2191 Tomas, R. A., & Webster, P. J. (1997). The role of inertial instability in determin-
2192 ing the location and strength of near-equatorial convection. *Quarterly Journal*
2193 *of the Royal Meteorological Society*, 123(542), 1445–1482.
- 2194 Trenberth, K. E., Stepaniak, D. P., & Caron, J. M. (2000). The global mon-
2195 soon as seen through the divergent atmospheric circulation. *Journal of*
2196 *Climate*, 13(22), 3969–3993. doi: 10.1175/1520-0442(2000)013<3969:
2197 TGMAS>2.0.CO;2
- 2198 Uppala, S. M., Kållberg, P., Simmons, A., Andrae, U., Bechtold, V. D. C., Fiorino,
2199 M., ... others (2005). The ERA-40 re-analysis. *Q. J. R. Meteorol. Soc.*, 131,
2200 2961–3012.
- 2201 Vallis, G., Colyer, G., Geen, R., Gerber, E., Jucker, M., Maher, P., ... Thomson, S.
2202 (2018). Isca, v1.0: A framework for the global modelling of the atmospheres

- of Earth and other planets at varying levels of complexity. *Geoscientific Model Development*, 11, 843–859. doi: 10.5194/gmd-11-843-2018
- Voigt, A., Biasutti, M., Scheff, J., Bader, J., Bordoni, S., Codron, F., . . . Zeppetello, L. R. V. (2016). The Tropical Rain belts with an Annual Cycle and Continent Model Intercomparison Project: TRACMIP. *JAMES*, 8(4), 1868–1891.
- Walker, C. C., & Schneider, T. (2006). Eddy Influences on Hadley Circulations: Simulations with an Idealized GCM. *Journal of the Atmospheric Sciences*, 63(12), 3333–3350. Retrieved from <http://journals.ametsoc.org/doi/abs/10.1175/JAS3821.1> doi: 10.1175/JAS3821.1
- Walker, J. M., & Bordoni, S. (2016). Onset and withdrawal of the large-scale South Asian monsoon: A dynamical definition using change point detection. *Geophysical Research Letters*, 43(22), 11,815–11,822. doi: 10.1002/2016GL071026
- Walker, J. M., Bordoni, S., & Schneider, T. (2015). Interannual variability in the large-scale dynamics of the South Asian summer monsoon. *Journal of Climate*, 28(9), 3731–3750. doi: 10.1175/JCLI-D-14-00612.1
- Wang, B., & Ding, Q. (2008). Global monsoon: Dominant mode of annual variation in the tropics. *Dynamics of Atmospheres and Oceans*, 44(3), 165 - 183. doi: <https://doi.org/10.1016/j.dynatmoce.2007.05.002>
- Wang, B., Ding, Q., & Joseph, P. V. (2009). Objective definition of the Indian summer monsoon onset. *Journal of Climate*, 22(12), 3303–3316. doi: 10.1175/2008JCLI2675.1
- Wang, B., & LinHo. (2002). Rainy Season of the Asian-Pacific Summer Monsoon. *Journal of Climate*, 15, 386–398. doi: 10.1175/1520-0442(2002)015%3C0386:RSOTAP%3E2.0.CO;2
- Wang, B., LinHo, Zhang, Y., & Lu, M. M. (2004). Definition of South China Sea monsoon onset and commencement of the East Asian summer monsoon. *Journal of Climate*, 17(4), 699–710. doi: 10.1175/2932.1
- Wang, B., Liu, J., Kim, H. J., Webster, P. J., & Yim, S. Y. (2012). Recent change of the global monsoon precipitation (1979–2008). *Climate Dynamics*, 39(5), 1123–1135. doi: 10.1007/s00382-011-1266-z
- Wang, B., & Wang, Y. (1999). Dynamics of the ITCZ–Equatorial Cold Tongue Complex and Causes of the Latitudinal Climate Asymmetry. *Journal of Climate*, 12(6), 1830–1847.
- Wang, B., & Xie, X. (1997). A model for the boreal summer intraseasonal oscillation. *Journal of the Atmospheric Sciences*, 54(1), 72–86. doi: 10.1175/1520-0469(1997)054<0072:AMFTBS>2.0.CO;2
- Wang, P. X., Wang, B., Cheng, H., Fasullo, J., Guo, Z. T., Kiefer, T., & Liu, Z. Y. (2014). The global monsoon across timescales: Coherent variability of regional monsoons. *Climate of the Past*, 10(6), 2007–2052. doi: 10.5194/cp-10-2007-2014
- Wang, X., Auler, A. S., Edwards, R. L., Cheng, H., Cristalli, P. S., Smart, P. L., . . . Shen, C.-C. (2004). Wet periods in northeastern Brazil over the past 210 kyr linked to distant climate anomalies. *Nature*, 432, 740 - 743.
- Wang, X., Auler, A. S., Edwards, R. L., Cheng, H., Ito, E., & Solheid, M. (2006). Interhemispheric anti-phasing of rainfall during the last glacial period. *Quaternary Science Reviews*, 25(23), 3391 - 3403. (Critical Quaternary Stratigraphy) doi: <https://doi.org/10.1016/j.quascirev.2006.02.009>
- Wang, X., Auler, A. S., Edwards, R. L., Cheng, H., Ito, E., Wang, Y., . . . Solheid, M. (2007). Millennial-scale precipitation changes in southern Brazil over the past 90,000 years. *Geophysical Research Letters*, 34(23). doi: 10.1029/2007GL031149
- Webb, M. J., Andrews, T., Bodas-Salcedo, A., Bony, S., Bretherton, C. S., Chadwick, R., . . . others (2017). The cloud feedback model intercomparison project (CFMIP) contribution to CMIP6. *Geoscientific Model Development*, 2017, 359–384.

- Webster, P. J., Magaña, V. O., Palmer, T. N., Shukla, J., Tomas, R. A., Yanai, M., & Yasunari, T. (1998). Monsoons: Processes, predictability, and the prospects for prediction. *Journal of Geophysical Research: Oceans*, 103(C7), 14451–14510. Retrieved from <http://doi.wiley.com/10.1029/97JC02719> doi: 10.1029/97JC02719
- Wei, H.-H., & Bordoni, S. (2016). On the Role of the African Topography in the South Asian Monsoon. *Journal of the Atmospheric Sciences*, 73(8), 3197–3212. Retrieved from <http://journals.ametsoc.org/doi/10.1175/JAS-D-15-0182.1> doi: 10.1175/JAS-D-15-0182.1
- Wei, H.-H., & Bordoni, S. (2018). Energetic Constraints on the ITCZ Position in Idealized Simulations With a Seasonal Cycle. *Journal of Advances in Modeling Earth Systems*, 10(7), 1708–1725. doi: 10.1029/2018MS001313
- Wei, H.-H., & Bordoni, S. (2020). Energetic Constraints on the ITCZ position in the Observed Seasonal Cycle from MERRA-2 Reanalysis. Retrieved from <https://resolver.caltech.edu/CaltechAUTHORS:20200625-123438067>
- Weldeab, S. (2012). Bipolar modulation of millennial-scale West African monsoon variability during the last glacial (75,000–25,000 years ago). *Quaternary Science Reviews*, 40, 21–29. doi: <https://doi.org/10.1016/j.quascirev.2012.02.014>
- Wheeler, M., & Kiladis, G. N. (1999). Convectively coupled equatorial waves: Analysis of clouds and temperature in the wavenumber-frequency domain. *Journal of the Atmospheric Sciences*, 56(3), 374–399. doi: 10.1175/1520-0469(1999)056<0374:CCEWAO>2.0.CO;2
- White, R., Battisti, D., & Skok, G. (2017). Tracking precipitation events in time and space in gridded observational data. *Geophysical Research Letters*, 44(16), 8637–8646.
- Wu, M.-L. C., Reale, O., Schubert, S. D., Suarez, M. J., & Thorncroft, C. D. (2012). African easterly jet: Barotropic instability, waves, and cyclogenesis. *Journal of Climate*, 25(5), 1489–1510.
- Wu, R., & Wang, B. (2001). Multi-stage onset of the summer monsoon over the western North Pacific. *Climate Dynamics*, 17(4), 277–289. doi: 10.1007/s003820000118
- Xiang, B., Zhao, M., Ming, Y., Yu, W., & Kang, S. M. (2018). Contrasting impacts of radiative forcing in the Southern Ocean versus southern tropics on ITCZ position and energy transport in one GFDL climate model. *Journal of Climate*, 31(14), 5609–5628. doi: 10.1175/JCLI-D-17-0566.1
- Xie, S.-P., & Philander, S. G. H. (1994). A coupled ocean-atmosphere model of relevance to the ITCZ in the eastern Pacific. *Tellus*, 46A, 340–350. doi: 10.3402/tellusa.v46i4.15484
- Yang, G.-Y., Methven, J., Woolnough, S., Hodges, K., & Hoskins, B. (2018). Linking African easterly wave activity with equatorial waves and the influence of Rossby waves from the Southern Hemisphere. *Journal of the Atmospheric Sciences*, 75(6), 1783–1809.
- Yim, S.-Y., Wang, B., Liu, J., & Wu, Z. (2014). A comparison of regional monsoon variability using monsoon indices. *Climate Dynamics*, 43, 1423–1437.
- Zhai, J., & Boos, W. R. (2017). The drying tendency of shallow meridional circulations in monsoons. *Quarterly Journal of the Royal Meteorological Society*, 143(708), 2655–2664. doi: 10.1002/qj.3091
- Zhang, C. (2005). Madden-Julian oscillation. *Reviews of Geophysics*, 43(2).
- Zhang, C., Nolan, D. S., Thorncroft, C. D., & Nguyen, H. (2008). Shallow meridional circulations in the tropical atmosphere. *Journal of Climate*, 21(14), 3453–3470. doi: 10.1175/2007JCLI1870.1
- Zhang, G., & Wang, Z. (2013). Interannual variability of the Atlantic Hadley circulation in boreal summer and its impacts on tropical cyclone activity. *Journal of Climate*, 26(21), 8529–8544. doi: 10.1175/JCLI-D-12-00802.1

- 2313 Zhang, R., & Delworth, T. L. (2005). Simulated tropical response to a substan-
 2314 tial weakening of the Atlantic thermohaline circulation. *Journal of Climate*,
 2315 18(12), 1853–1860. doi: 10.1175/JCLI3460.1
- 2316 Zhang, S., & Wang, B. (2008). Global summer monsoon rainy seasons. *International*
 2317 *Journal of Climatology*, 28, 1563–1578. doi: 10.1002/joc.1659
- 2318 Zhou, T., Turner, A. G., Kinter, J. L., Wang, B., Qian, Y., Chen, X., ... He, B.
 2319 (2016). GMMIP (v1.0) contribution to CMIP6: Global Monsoons Model Inter-
 2320 comparisonProject. *Geoscientific Model Development*, 9(10), 3589–3604. doi:
 2321 10.5194/gmd-9-3589-2016
- 2322 Zhou, W., & Xie, S.-P. (2018). A Hierarchy of Idealized Monsoons in an Interme-
 2323 diate GCM. *Journal of Climate*, 31, 9021–9036. Retrieved from [http://](http://journals.ametsoc.org/doi/10.1175/JCLI-D-18-0084.1)
 2324 journals.ametsoc.org/doi/10.1175/JCLI-D-18-0084.1 doi: 10.1175/JCLI-
 2325 -D-18-0084.1
- 2326 Ziegler, M., Simon, M. H., Hall, I. R., Barker, S., Stringer, C., & Zahn, R. (2014).
 2327 Development of Middle Stone Age innovation linked to rapid climate change.
 2328 *Nature Communications*, 4(1905).